

**COMPARISON OF**

**THREE DIMENSIONAL VELOCITY MODELS**

**FOR FLANGED RECTANGUALR HOODS**

**by**

**Marie Louise Fitzgerald**

**University of North Carolina**

**Chapel Hill, NC**

**May 1988**

## ABSTRACT

Marie Louise Fitzgerald. Comparison of Three-Dimensional Velocity Models for Flanged Rectangular Hoods. (Under the direction of Dr. Michael R. Flynn)

The purpose of a local exhaust hood is to capture an airborne contaminant as close to the point of generation as possible and prevent it from entering the worker's breathing zone. Presently, local exhaust hood designs are based on capture velocity and practical experience. This process involves several deficiencies, the most significant being the inability to determine the contaminant concentration in the worker's breathing zone as well as the inability to incorporate crossdrafts and source momentum characteristics.

Three-dimensional velocity field models which predict the magnitude and direction of the velocity vector at any point in the field of flanged, rectangular exhaust hoods have been developed recently. This is a first step in determining the contaminant concentration in the worker's breathing zone and can, by vector addition, predict how crossdrafts and source momentum will effect contaminant capture.

The purpose is to determine which of the available velocity field equations is the most accurate predictor of the velocity vector. This should help to determine optimal hood size, position and flow, resulting in more efficient and economical exhaust designs for industry. The theoretical basis for models in potential theory is presented and the limitations for industrial settings are discussed.

The accuracy of the models was evaluated by measuring two-dimensional velocity vectors in the x-z and y-z planes of local exhaust hoods having aspect ratios of 1, 2, and 5. Measurements were made from 5% to 80% of the maximum hoodface velocity with an anemometer modified to permit rotation about its axis. The X, Y, and Z velocity components of each point were statistically compared to calculated data. The ability to implement the models in computer programs is also discussed.

Much work remains. The analysis can be expanded over a larger range of hood aspect ratios, and known crossdraft and source momentum vectors can be included.

## CONTENTS

INTRODUCTION.....	1
LITERATURE REVIEW.....	4
INADEQUACIES OF PAST AND PRESENT DESIGN METHODS.....	10
POTENTIAL THEORY.....	11
THEORY OF THREE DIMENSIONAL EQUATIONS.....	14
OBJECTIVE.....	18
EXPERIMENTAL METHODS AND INSTRUMENTATION.....	19
RESULTS.....	22
STATISTICAL ANALYSIS.....	23
DISCUSSION .....	27
CONCLUSIONS AND FURTHER WORK.....	28

## REFERENCES

## APPENDICES

- APPENDIX A: EXPERIMENTAL SET-UP
- APPENDIX B: CALIBRATION GRAPHS
- APPENDIX C: RESULTS TABLE
- APPENDIX D: BASICA PROGRAMS
- APPENDIX E: PERFORMANCE INDEX VALUES  
T-TESTS RESULTS
- APPENDIX F: LEAST-SQUARES REGRESSION
- APPENDIX G: ANALYSIS OF VARIANCE RESULTS
- APPENDIX H: QUANTILE - QUANTILE PLOTS
- APPENDIX I: GRAPHS OF PREDICTED VELOCITIES VERSUS  
MEASURED VELOCITIES

**FIGURES**

- FIGURE 1: CONTOUR LINES
- FIGURE 2: GARRISON'S NOMOGRAM
- FIGURE 3: CENTERLINE AGREEMENT WITH GARRISON

**TABLE 1: GARRISON'S CENTERLINE EQUATION**

## INTRODUCTION:

Various methods can be used to prevent worker overexposure to airborne contaminants(9):

1. Eliminate the source
2. Prevent dispersion at the source by
  - a: segregating the process
  - b: enclosing the process
  - c: wetting contaminant if in dust form
  - d: LOCAL EXHAUST VENTILATION
3. Provide personal protective equipment

Eliminating the source by replacement is often not possible because another, less toxic option may not exist. The first three divisions under category two may not be feasible for a given process. The third category, providing personal protection, is always a last resort solution because respirators and protective clothing are often cumbersome, uncomfortable, and may not work properly. Local exhaust ventilation however, has been called the "most important single method of preventing industrial atmospheric pollution(4)".

Enclosing or confining hoods are preferred over exterior hoods, because they prevent crossdrafts and other air motions from easily affecting the hood capturing ability. Exterior hoods capture the contaminated air and bring it into the hood(17). The source momentum can also be ignored with an enclosure hood since all the contaminant is captured regardless of its initial trajectory however there must be sufficient flow to carry away the captured contaminant. However, such hood configurations are not always feasible due to the type of equipment or process used in a workplace. Examples of such processes are: exhaust of abrasive grinding wheels, woodworking machinery, electric-arc welding, conveyor transfer points, downdraft grilles, work benches, stone cutting and

finishing, portable grinding and sanding, tool room and cast iron machinery(1).

Local exhaust ventilation has been developed to capture airborne contaminants that cannot be handled adequately by the methods listed above or by dilution ventilation. The purpose of a local exhaust hood (LEH) is to capture an airborne contaminant as close to the point of generation and as completely as possible via a certain airflow, Q, pulled through the hood(17). Such ventilation involves the use of a hood to exhaust air specifically from a particular source. To determine the proper hood configuration to be used, several aspects of the particular operation must be considered. First, one must determine what type of equipment will be used and the type of environment it will be used in. This will affect where and how close the hood can be placed to the source. The volume of the contaminant source should influence the shape and size of the hood. Next, the volume of air that must be exhausted can be estimated based on the rate and amount of contaminant generation. Another consideration for design is ambient air movement.(2) Causes of air movement are(9,10):

1. Thermal currents
2. Machinery movement
3. Material movement
4. Room air currents
5. Operator movement
6. "Spot cooling and heating equipment"

If a hood is not properly designed, the worker could be exposed to toxic levels of the airborne contaminant. Alice Hamilton said "...the air of the factory is of chief importance and to keep it free from dangerous dust, fumes and gases is the first measure of protection, all others are secondary. If the worker is breathing contaminated air, he cannot be saved from poisoning or silicosis by the best of washing facilities, working clothes, good lunchrooms and so forth. It is the air that must be made clean and kept so(4)."

Local exhaust hoods should be specifically designed for each individual process however, very little detailed work has been done to optimize the design and use of local exhaust hoods. The ability to predict accurately the three-dimensional flow field is now possible through mathematical models that can easily be used on personal computers.

## LITERATURE REVIEW:

Past research on local exhaust ventilation (LEV) has relied mainly on the studies by DallaValle(6,7,8) and Silverman(27,28). Fletcher(12-16) and Garrison(20,21) expanded these works. Fletcher(13) experimentally measured the variation in velocity between hoods with different width to length ratios. Garrison(20) tried to determine the effect that flanges, aspect ratio (hood length / hood width) and face velocity has on the accuracy of centerline velocity equations. All these studies were based on capture velocity, defined as the speed at which the air must move to overcome the contaminant's natural movement and pull it into the hood(10). Ellenbecker(10) and others(18,19) have recently continued LEV research to include the concepts of capture efficiency and potential flow theory. Capture efficiency is the percent of the total generated airborne contaminant that is captured by a local exhaust hood(10).

In 1931, Dallavalle(8) experimentally mapped the velocity contours for round, square and rectangular hoods. Velocity contours are lines that define points of equal velocity in front of a hood, as illustrated in Figure 1. He did this for several combinations of airflows, hood shapes, hood areas and the shapes of the transition piece from the hood to the duct. The velocity entering the hood was measured by a modified pitot tube over a grid placed in front of the hood openings. The contour lines were not appreciably affected by rate of airflow or shape of the transition piece. The geometric shape of the hood caused a variation in the contour lines. The amount of change was proportional to the ratio of the width of the hood to the length. He also observed a slight shift of the contours outward from the centerline axis and closer inward toward the hood face when he increased the area of the hood opening. He concluded that a general pattern of velocity contour lines for exhaust hoods exists that could be used in conjunction with centerline velocity equations for design purposes. Based on the centerline velocity equation he developed, the percentage of face velocity for a given X

FIGURE 1  
Reference 8

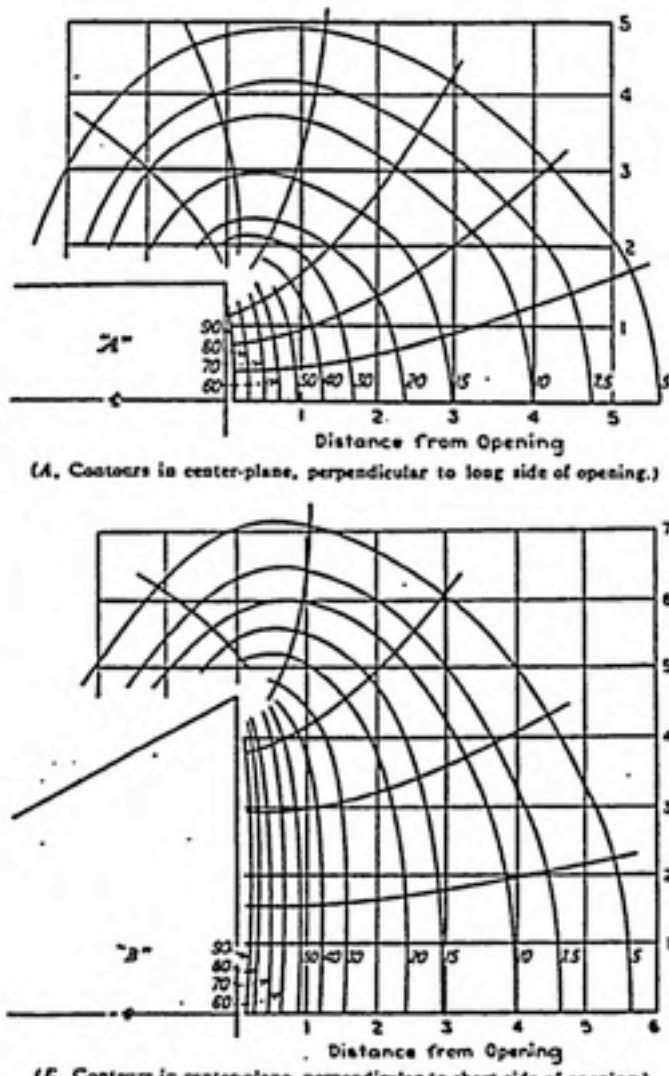


FIG. 1 VELOCITY CONTOURS FOR 3-INCH BY 9-INCH OPENING

(distance from hood opening) could be calculated and the expected contour lines could be drawn freehand. He felt his work "should serve as a starting point for more elaborate studies and the collection of detailed information on the design of local exhaust hoods"(8). He proposed a revised form of these centerline velocity equations in 1952 (6). These formulas were accepted by the ACGIH as the recommended equations for calculation of centerline velocities and have not been replaced. The general form of his equation is  $f(Y) = bAx^{-2}$  (8).

For flanged, rectangular hoods, the 1952 form of his equation(6) is:

$$\% \text{ Face Velocity} = \frac{4}{3(1 + 10X^2/A)} \quad (1)$$

valid when hood Length/Width  $\leq 5$

where A = area of the hood opening

X = distance from hood face

In 1942, Silverman(28,29) expanded DallaValle's work by performing similar experiments on circular and rectangular hoods except the aspect ratio of the rectangular hoods were greater than or equal to 5 and he was able to use a heated anemometer for his measurements. He then published his own version of centerline velocity equations for plain and flanged circular hoods(28). He further expanded his work to include narrow exhaust slots(29). He found that the velocity varied inversely with the distance from the hood and with the slot length. The slot width was determined to have less of an effect on velocity when the hood was flanged and also, that the advantage of flanging was reduced

as the slot width decreased. By extrapolating from DallaValle's work, he developed centerline equations for plain and flanged rectangular hoods. These equations are also recommended by the ACGIH.

His equation for a flanged rectangular hood is:

$$\% \text{ Face Velocity} = \frac{B}{(2.8 X)} \quad (2)$$

Valid for hood Length/Width  $\geq 5$

where B = Hood Width

X = distance from hood face

The most obvious problem with DallaValle and Silverman's equations for flanged rectangular hoods is that at L/W = 5, the solutions for the two are different. Specifically, each formula has certain innate errors. DallaValle and Silverman did not take into account the effect of aspect ratio, flanging or the vena contracta. The vena contracta is the name given to the smaller flow area created by the convergence of the streamlines inside the hood opening. When the streamlines converge into the hood inertia causes them to continue to converge inside the hood opening creating a flow area which is smaller than the area of the hood opening(27). Furthermore, Silverman's equations go to infinity at the center of the hood face opening(3).

Drinker and Hatch(9) felt the best approach to determine the necessary flow for optimal hood performance was to set up experiments to measure the contaminant capture ability under actual working conditions. These experiments initially would consist of isolating the specific work area to prevent interaction with other processes. The total air flow would be varied through several possible hood configurations which would be selected based on experience. The amount of contaminant not captured by the hood

would then be measured. To obtain which hood and flow configuration worked best for the lowest flow, the hood parameters would be plotted versus the contaminant level in the work area. However, this set of experiments would have to be repeated for each separate process involving large amounts of time and money. As an alternative, Drinker and Hatch suggested using a small "probe" hood. This hood would be placed at several strategic points around the source to measure the velocity needed for contaminant capture. Based on these findings, an effective hood could be designed.

In 1977, Fletcher(13) developed a set of centerline velocity equations for plain rectangular hoods and slots. He found that for a given face area and air volume the velocity decreased as the aspect ratio of the hood increased. He constructed a nomogram, for the ranges over which his equation applied, for easy determination of expected velocities. This is shown in Figure 2. In 1978, Fletcher(15) did compare the velocities of flanged and unflanged hoods, however, he did not develop equations for flanged rectangular hoods.

In 1983, Garrison(20) published work on the centerline velocity of plain and flanged; circular, rectangular and narrow slots for high velocity/low volume airflow conditions. Little effect was found for the use of flanging or varied hood opening size. This was a function of the small size hoods he employed. He developed general equations for both plain and flanged hoods. These are:

$$\begin{aligned} Y(\text{near}) &= [a(b)] X_{DW} \\ Y(\text{far}) &= [a(X_{DW})]^b \end{aligned} \quad (3)$$

where a and b are empirical constants

$X_{DW}$  = distance from hood face

Garrison(21) also did work on graphical design methods. By adding or superimposing the airflow patterns of two or more hoods, one could determine the airflow patterns for a larger hood configuration. This is an especially useful technique

FIGURE 2  
Reference 13  
FLETCHER'S NOMOGRAM

$X$  = distance from the hood face along the centerline axis

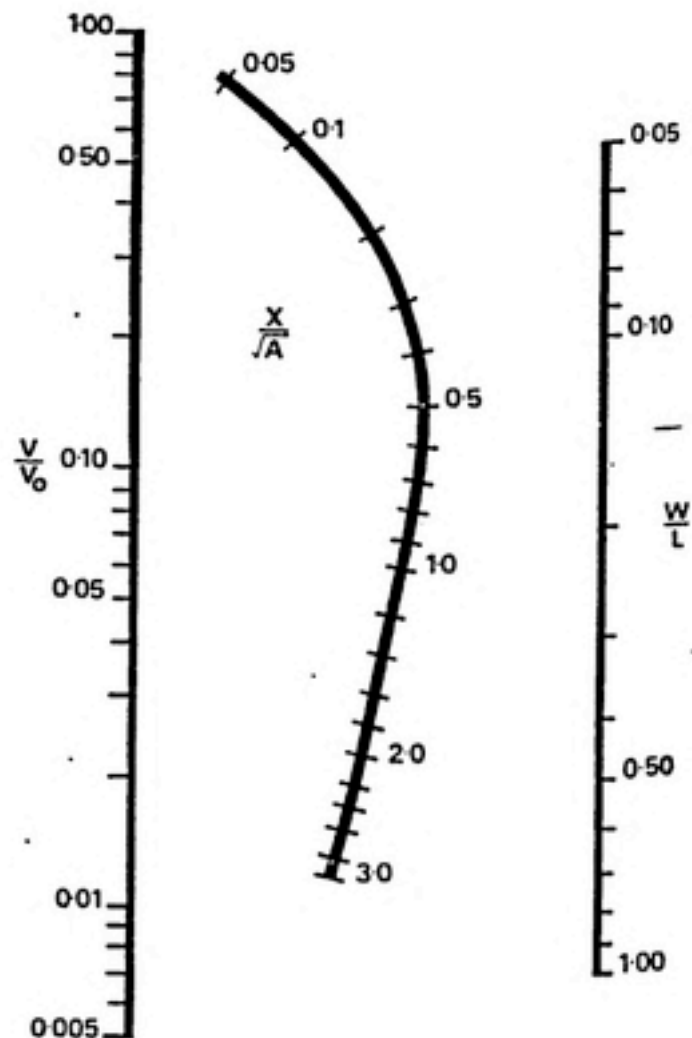
$A$  = area of the hood face opening

$V$  = air velocity at point  $X$

$V_0$  = air velocity at the hood face

$W$  = hood face width

$L$  = hood face length



when there are boundary planes at or near the hood face. The contour lines are still based on the centerline velocity predictions.

In 1983, Ellenbecker, Gempel, and Burgess(10) developed a method to quantitatively evaluate the performance of LEV based on capture efficiency which is the percent of the total generated airborne contaminant that is actually captured by a local exhaust hood(10). This approach allowed for the addition of crossdrafts but was only useful as a performance estimate after the hood was in place.

This research was continued by Flynn and Ellenbecker in 1985 (19). A mathematical model was derived to predict the three-dimensional velocity field into flanged, circular hoods, with potential theory as its basis. Flynn and Ellenbecker assumed that the equipotential lines were coincident with the velocity contours mapped by DallaValle. By assuming that the gradient of the potential was constant along a given equipotential surface, they developed an approximate solution for the three-dimensional velocity. Potential theory will be discussed in detail later in the paper. The equations they developed are:

$$\vec{v}_z = \frac{\partial \Phi}{\partial z} \vec{k} = - \frac{Qz}{\pi \gamma_1 \gamma_2 \sqrt{(\gamma_1 + \gamma_2)^2 - 4a^2}} \vec{k} \quad (4)$$

$$\vec{v}_r = \frac{\partial \Phi}{\partial r} \vec{r} = - \left( \frac{Q}{\pi} \right) \left( \frac{(a+r)\gamma_2 + (r-a)\gamma_1}{(\gamma_1 + \gamma_2)\gamma_1 \gamma_2 \sqrt{(\gamma_1 + \gamma_2)^2 - 4a^2}} \right) \vec{r}$$

$$\gamma_1 = \sqrt{z^2 + (a+r)^2}$$

$$\gamma_2 = \sqrt{z^2 + (a-r)^2}$$

where  $Q$  = flowrate through the hood

$a$  = radius

$r$  = radial distance perpendicular to the Z axis

$z$  = axial distance from hood

The predicted velocities from this equation were compared to values measured by DallaValle in 1930 and found to be in good agreement. Based on this, Flynn and

Ellenbecker(19) expanded the equation to include crossdrafts in order to calculate the predicted capture efficiency of flanged circular hoods. They later tested this equation by comparing predicted velocities to experimental and found good agreement(18).

#### INADEQUACIES OF PRESENT DESIGN METHODS:

The present design concepts are still based on research done by DallaValle and Silverman in the 1930's and 1940's. One of the major deficiencies is the use of the concept of capture velocity as a design parameter where capture velocity is the speed at which the air must move to overcome the contaminant's natural movement and pull it into the hood(10). This approach does not consider the area of the hood opening, in that, a small hood will need a higher velocity to capture the same quantity of air as a larger hood at the same velocity(12). Also, it does not consider that the velocity required to capture a contaminant increases as the distance between the hood and source increase. The source momentum that may be imparted to the contaminant from the process is not incorporated(12). Furthermore, the variations in the flow field velocity that occur away from the centerline cannot be determined. This method can not easily assess how a change in size or position of the hood will affect the capture ability(12). However, the most serious drawback is its inability to predict contamination concentration in the worker's breathing zone. These deficiencies result in a lack of specific, quantitative information that is needed to support judgements on system design and flow(10).

It is important that these deficiencies be overcome for many reasons. It is a waste of time, energy and money to design and install a hood that will not control adequately but, more importantly, if the exhaust hood is not designed and operated correctly, the worker can be overexposed to the contaminant. It is possible to address some of these deficiencies now by the use of velocity models which determine the three-dimensional flow field.

## POTENTIAL THEORY

Potential flow theory has been referred to by DallaValle(6,7,8), Silverman(27,28), Garrison(20,21), and Flynn and Ellenbecker(18). Due to its importance a brief overview of potential theory will be given. Fluid flow is defined by the laws of mechanics(24). These laws describe the interaction between a quantity of mass, called the "system", relative to boundary conditions, termed the "surroundings". There are four basic laws of mechanics.

### 1. Conservation of Mass:

Mass( $m$ ) of a system does not change

$$m \text{ (system)} = \text{constant}$$

$$t = \text{time}$$

$$\frac{dm}{dt} = 0$$

### 2. Conservation of Linear Momentum: Newton's Second Law

A mass accelerates when a force  $F$  is applied to it.

$$F = ma = \frac{d(mV)}{dt} = m \frac{dV}{dt}$$

$$a = \text{acceleration}$$

$$V = \text{velocity vector}$$

### 3. Conservation of Angular Momentum:

Rotation will result if the surroundings exert a net moment( $M$ ) on the system.

$$M = \frac{dH}{dt}$$

$$H = \text{sum } (r \times V)dm$$

$$r = \text{radius}$$

4. 2nd Law of Thermodynamics:

$$dS \geq dQ/dt$$

$S$  = entropy change

$dQ/dt$  = heat added to the system(24)

To use potential theory one must solve Laplace's equation. First, certain boundary conditions must be defined and several assumptions must be made about the flow characteristics. These assumptions are that the flow is inviscid, incompressible and irrotational(3,4). Inviscid means the flow poses no internal resistance to movement, i.e. negligible friction.

The second condition, incompressibility, also exists when the divergence is zero. The divergence is zero when the exact same volume that enters a space also leaves that space i.e. density = constant(5). Additionally, the ratio of the speed of the flow to the speed of sound must be less than 0.3 and the density changes must be negligible. This is stated by the Continuity equation:  $\frac{\partial \rho}{\partial t} + \nabla \cdot (\rho \vec{v}) = 0$  (5)

where  $\rho$  = density

$\vec{v}$  = velocity vector

The last condition, irrotationality, means the flow does not have a spinning

motion around itself. It is defined mathematically by the equation:

$$\nabla \times \mathbf{V}(\text{vector}) = 0 \quad (6)$$

By assuming the flow is incompressible, irrotational and inviscid, the Continuity equation is simplified to Laplace's equation:

$$\nabla^2 \Phi = 0 \quad (7)$$

where

$\Phi$  = Scalar potential function of position

### THEORY OF THREE DIMENSIONAL VELOCITY MODELS:

Three models are presently available which predict the three-dimensional velocity flow field in front of flanged rectangular local exhaust hoods. The first two are based on potential theory, but differ in their approach to a mathematical solution(29,5). The third is based on a combination of potential theory and isokinetic velocity contour lines(11). A brief description of each model will be given. For a complete derivation, see References (29,5,11).

The first equations, which will be referred to as Model A, were developed by Tyaglo and Shepelev(30). They developed an analytical solution to Laplace's equation, by assuming constant velocity across the face of the hood. They were able to solve this equation and integrate over the entire hood opening region of a flanged rectangular exhaust hood. These equations are:

$$VZ = C(T_1 - T_2 - T_3 + T_4)$$

$$VX = C \ln \left[ \frac{\sqrt{R_3} + D}{\sqrt{R_2} + D} \times \frac{\sqrt{R_1} + E}{\sqrt{R_4} + E} \right] \quad (9)$$

$$VY = C \ln \left[ \frac{\sqrt{R_1} + F}{\sqrt{R_2} + F} \times \frac{\sqrt{R_3} + G}{\sqrt{R_4} + G} \right]$$

where

$$T_1 = \arctan \left[ \frac{DF}{Z\sqrt{Z^2 + D^2 + F^2}} \right] \quad R_1 = (Z^2 + E^2 + F^2) \quad C = -\frac{Q}{8ILAB}$$

$$T_2 = \arctan \left[ \frac{EF}{Z\sqrt{Z^2 + E^2 + F^2}} \right] \quad R_2 = (Z^2 + D^2 + F^2) \quad D = Y + B$$

$$T_3 = \arctan \left[ \frac{DG}{Z\sqrt{Z^2 + D^2 + G^2}} \right] \quad R_3 = (Z^2 + G^2 + D^2) \quad E = Y - B$$

$$T_4 = \arctan \left[ \frac{EG}{Z\sqrt{Z^2 + E^2 + G^2}} \right] \quad R_4 = (Z^2 + G^2 + E^2) \quad F = X + A$$

$$G = X - A$$

A second was developed by Conroy, Flynn and Ellenbecker(5). These equations will be referred to as Model B. They actually developed four models but determined that their exact inscribed ellipse solution was best. It will be the only one described. They modeled the hood opening as an elliptical aperture in order to use Lamb's analytical solution to Laplace's Equation. At the time of their study, no previously defined analytical solution was commonly known for rectangular openings. Their equations for rectangular hoods were based on the work they had done modeling the three-dimensional flow field into circular hoods. The assumptions made were the same as those stated for potential theory. Also, the flange was considered infinite. Due to the inscribed ellipse method, the model assumes there is a flange in the corners, and thus zero velocity, where in reality there is flow. The assumption of flanging in the corners was considered insignificant due to the vena contracta. The exact solution does not take into account conditions where potential flow theory no longer holds, such as near the hood face, where the flow becomes viscous and turbulent. Flynn and Ellenbecker felt the elliptical assumption would not present a vast error in flow field calculations. There are three problems with this set of equations. One is that the hood face area used for the model is smaller than the actual hood face area by a factor of  $\pi/4$ . This causes the average face velocity to be larger than the actual average face velocity by a factor of  $\pi/4$ . Also, the velocities at the edges of the hood go to infinity. Lastly, the predicted velocity at the center of the hood face is 64% of the actual face velocity.

The potential function for flow through an elliptical space was found to be:

$$\phi = \frac{\pi Q}{4\pi} \int_0^{\lambda} \frac{d\lambda}{((a^2+\lambda)(b^2+\lambda)\lambda)^{1/2}} \quad (10)$$

The solution for each velocity component is

$$V_z = \frac{dz}{dt} = \frac{\partial \phi}{\partial z} = \frac{Qz(a^2+\lambda)^{3/2}(b^2+\lambda)^{3/2}\lambda^{1/2}}{2\pi E}$$

$$V_x = \frac{dx}{dt} = \frac{\partial \phi}{\partial x} = \frac{Qx(a^2+\lambda)^{1/2}(b^2+\lambda)^{3/2}\lambda^{3/2}}{2\pi E}$$

$$V_y = \frac{dy}{dt} = \frac{\partial \phi}{\partial y} = \frac{Qy(a^2+\lambda)^{3/2}(b^2+\lambda)^{1/2}\lambda^{3/2}}{2\pi E}$$

where

$$E = x^2\lambda^2(b^2+\lambda)^2 + y^2\lambda^2(a^2+\lambda)^2 + z^2(a^2+\lambda)^2(b^2+\lambda)^2$$

$x$  = distance from hood center along the hood length

$y$  = distance from hood center along the hood width

$a$  = hood length

$b$  = hood width

= a coordinate in Lame's elliptic coordinate system

$$\frac{x^2}{a^2+\lambda} + \frac{y^2}{b^2+\lambda} + \frac{z^2}{\lambda} = 1$$

Esmen, Weyel and McGuigan(11) also developed a three-dimensional model which will be referred to as Model C. They experimentally determined isokinetic contour lines for three hood configurations all having the same hood area. The equations they developed included the existence of two flanking planes at the hood, however the position of these flanges was arbitrary and could be ignored by defining their distance from the hood as infinity. The theoretical basis for their model was the equations of motion of an ideal fluid "expressed as potential flow to a mesh of sinks by the method of

imposition(11)". They assumed the airflow was at constant density, its viscosity was insignificant and that turbulent flow could be ignored. They included the theory of continuity in their analysis. Continuity exists when the flowrate, Q, equals the area of any contour surface multiplied by the velocity along that surface.

The major drawback of this approach is that "velocity contours generated by multiple openings are not additive in the simple sense(11)". Also, the velocity predicted by the model went to infinity at the center of the hood face opening when Z=0. The equations are:

$$\begin{aligned}
 V(X, Y, Z) &= \frac{Q}{4ab[F(R)]} \\
 V(X) &= V(X, Y, Z) \cos \left[ \frac{(2X(K_X + 1) - 2aK_X)}{D} \right] \\
 V(Y) &= V(X, Y, Z) \cos \left[ \frac{(2Y(K_Y + 1) - 2aK_Y)}{D} \right] \\
 V(Z) &= V(X, Y, Z) \cos \left[ \frac{4Z}{D} \right]
 \end{aligned} \tag{11}$$

$$D = \sqrt{16(Z^2) + [2X(K_X + 1) - 2aK_X]^2 + [2Y(K_Y + 1) - 2aK_Y]^2}$$

$$F(R) = \left( \frac{\pi}{8} \right) \left( \frac{R}{a} + \frac{R}{b} \right) + \left( \frac{R^2}{2ab} + \left( \sqrt{1 + \frac{(|ZX| + |YZ|)}{(a^2 + b^2)}} \right) \right)$$

$$R = \sqrt{Z^2 + K_X(|X| - a)^2 + K_Y(|Y| - b)^2}$$

$$K_X = 0 \text{ if } X \leq a \text{ ELSE } K_X = 1$$

$$K_Y = 0 \text{ if } Y \leq b \text{ ELSE } K_Y = 1$$

**OBJECTIVE:**

Mathematical models have been developed recently to predict the three-dimensional flow field entering a flanged rectangular exhaust hood. The objective is to determine if any of these equations gives an accurate prediction of the velocity flow field in front of flanged, rectangular hoods and if so, which is best. These equations have the potential for overcoming some of the previously listed deficiencies and improving local exhaust hood design. If an accurate model is determined, it be used in industry to determine optimal hood size, positioning and flowrate. Eventually, such a model should be incorporated into hood design manuals.

## EXPERIMENTAL METHODS AND INSTRUMENTATION:

A set of velocity measurements were taken separately in front of three flanged rectangular exhaust hoods. The coordinate system designation is illustrated in Appendix A. The magnitude and direction of the velocity vector was determined at specified points over a stationary grid. This was done in both the XZ and YZ planes. The coordinate system is illustrated in Appendix A. The hoods used had aspect ratios, (length/width), of 1, 2, and 5. The dimensions were as follows:

Aspect Ratio	Length(in)	Width(in)
1	3.5	3.5
2	5.0	2.5
5	8.0	1.625

Measurements were made over three flowrates, 142.89, 131.24 and 112.06 cfm, which were maintained by a baffle placed upstream of the hood. The flow was measured via the pressure drop, which was measured on an inclined manometer, across a four inch, sharp-edged orifice. This orifice was calibrated by the specified method given in the ACGIH Ventilation Manual(2). The calibration graph is shown in Appendix A. The velocities were measured from 80% to 5% of the hood face velocity.

The grid, which was placed in front of each hood, was subdivided into one inch increments. For hoods with aspect ratio 1 and 2 the area of the grid began at (0, 0, 0.5) inches and ended at (4, 4, 5.5) inches. For the hood with aspect ratio 5, the grid began at (0, 0, 0.5) inches but ended at (5, 3, 5.5) inches. This difference in grid size for aspect ratio 5 was due to the velocity reaching the 5% level at different points than the other two hoods.

The fan used to generate the flow was connected to a six inch diameter flexible duct. The flexible duct led to a six inch diameter solid duct in which a four inch sharp-

edged orifice was positioned. The orifice had three feet of solid aluminum duct before and after it to control turbulence and allow accurate measurement of the pressure drop. The velocity measurements were made with a TSI hot wire thermoanemometer and a voltmeter. The voltmeter allowed a more precise reading to be taken by measuring the bridge voltage across the thermoanemometer. The anemometer was positioned in a holder which allowed horizontal movement and rotation about its axis. The base of the holder was marked in 5 degree intervals to measure the degrees of rotation. This angle was used to calculate the X, Y, and Z components of the velocity. The velocity direction of rotation was determined by use of smoke tubes. The angle can be considered accurate within +/- 5 degrees.

The voltmeter was calibrated based on King's Law (31), where the relationship between the effective cooling velocity( $U_{eff}$ ) and the bridge voltage( $E_b$ ) is given by:

$$(E_b)^2 = k_1 + k_2 (U_{eff})^{k_3}$$

where (12)

$k_1$ ,  $k_2$  are constants to be determined experimentally

$$k_3 = 1/2$$

The calibration was determined by plotting the least-squares regression line of the square root of the effective cooling velocity versus the squared bridge voltage. This graph is shown in Appendix B. The calibration was conducted by three methods. The voltmeter was calibrated based on the centerline velocity within ductwork or within a windtunnel, depending on the magnitude of the velocity range being calibrated. For the range of 47 fpm to 332 fpm, the calibration was carried out in the wind tunnel. For the range from 367 fpm to 1000 fpm, a micromanometer was used in conjunction with a pitot tube to determine the velocity within an eight inch duct. The range from 1080 fpm to 1550 fpm was done similarly to above but with a plain inclined manometer. Various size

ducts and orifices were used to achieve the desired velocity ranges. Calibrations of the six and eight inch sharp-edged orifices used were conducted the same as the calibration for the four inch orifice(2).

Similiar experimental measurements of the velocity vectors in front of flanged, rectangular hoods have been done by DallaValle(8) and Fletcher(13), however none of their raw data was published. DallaValle plotted contour lines which were to be used in conjunction with his centerline velocity equation. Fletcher plotted velocity profiles of various hoods for comparison with the centerline velocities his nomogram predicts.

## RESULTS:

A total of 534 velocity vectors were measured. The position, voltmeter reading and displacement angle were entered into LOTUS 123<sup>R</sup> for data management purposes. The velocity vector value was determined via the voltmeter calibration equation. A table of the results is given in Appendix C.

To calculate the predicted velocities, a BASIC computer program was written for each mathematical model. A printout of each program is given in Appendix D. The variables flowrate (Q), hood length (L), and hood width (W), are needed as input, but the grid points were written within the program. These points can easily be altered for other grid sizes. Lotus 123<sup>R</sup> spreadsheets were used for data management.

To prove that this experimental set-up was reliable, the experimental centerline velocities were plotted versus the predicted centerline velocities determined from Garrison's centerline equation(3) which is shown in Table 1. Garrison's equations were chosen for comparison because they have been shown to be fairly accurate(3). The experimental readings agreed well with predicted as can be seen from Figure 3.

TABLE 1

## Centerline Velocity Equations

$$\begin{array}{ll} 1.07 (K_{04})^{X/B} & 0 \leq X/B < 0.5 \\ K_{07} (X/B)^{-0.4} & 0.5 \leq X/B < 1 \\ K_{07} (X/B)^{-0.6} & 1 \leq X/B \leq K_{010} \end{array}$$

X = distance from the hood face along the centerline

B = hood width

A = hood length

## Constants for the Centerline Velocity Equations

A/B	1	2	4	10
K <sub>01</sub>	0.09	0.14	0.18	0.19
K <sub>02</sub>	0.10	0.18	0.23	0.24
K <sub>03</sub>	1.7	1.2	1.0	1.0
K <sub>04</sub>	1.7	1.7	1.5	1.2
K <sub>05</sub>	1.5	2.0	2.5	3.5
K <sub>06</sub>	0.11	0.17	0.22	0.22
K <sub>07</sub>	0.12	0.21	0.27	0.29
K <sub>08</sub>	1.6	1.1	0.9	0.8
K <sub>09</sub>	1.6	1.6	1.4	1.1
K <sub>010</sub>	1.5	2.0	3.0	4.0

## CENTERLINE AGREEMENT WITH GARRISON

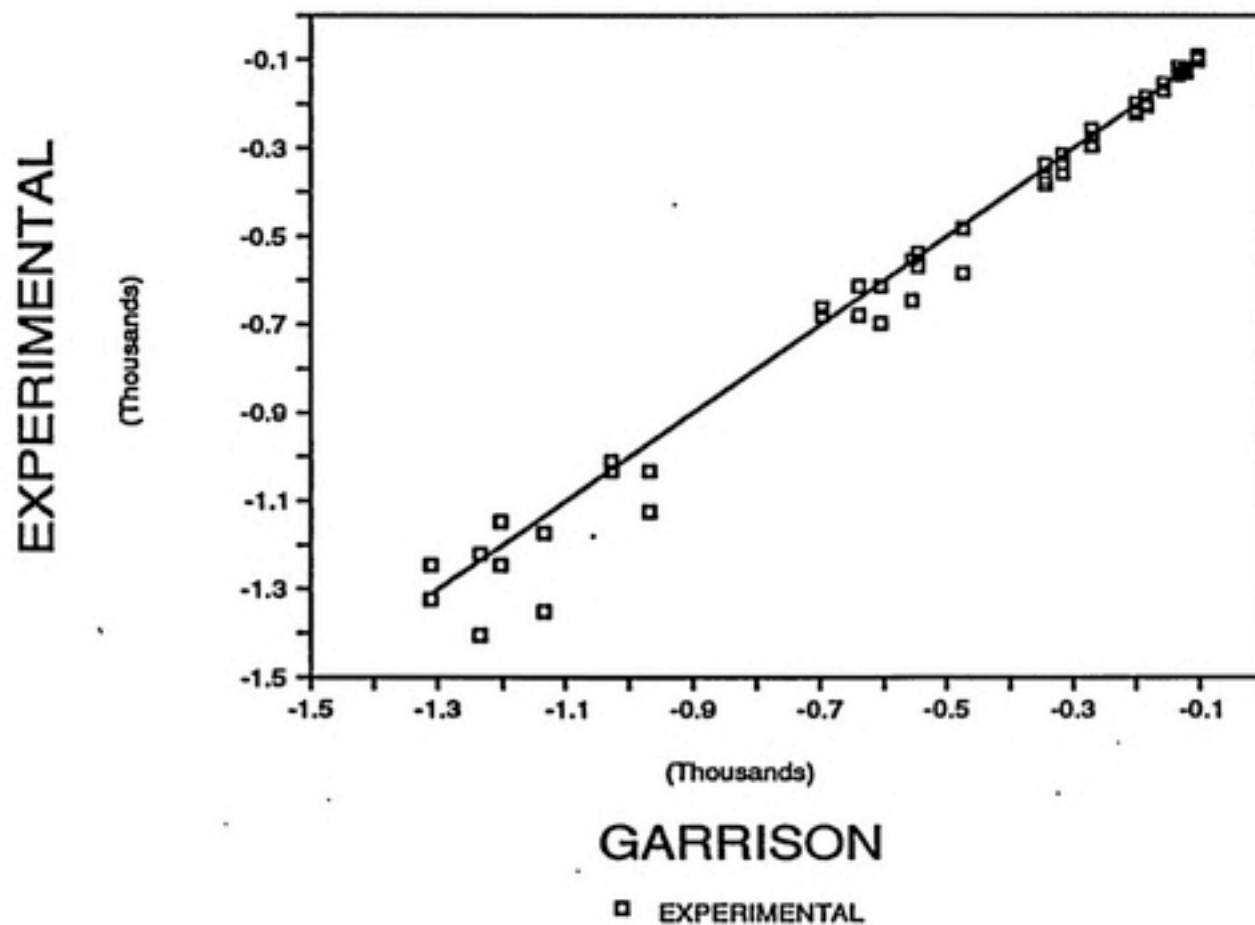


FIGURE 3

#### STATISTICAL ANALYSIS:

The statistical analysis involved several steps. SYSTAT was used for ANOVA and T-Test analyses as well as for quantile-quantile plots. LOTUS 123<sup>R</sup> was used for Performance Index and Least-Squares calculations.

Initially a Performance Index (PI) and Bias Index were calculated for each point(5,23). The Performance Index gives a measure of how well the predicted velocities match the experimental velocities. A large value indicates a large deviation, which means the theory does a poor job in predicting the velocity. The Bias value is the mean difference between the theoretical and the measured value. The formulas are:

$$\text{PI} = \Sigma(P-M)/N \quad \text{BIAS} = \Sigma(P-M)^2/N$$

(13)

where P = Predicted Velocity

M = Measured Velocity

N = Number of Points

A PI and Bias were calculated separately for each velocity component and for the total velocity per plane over each aspect ratio, resulting in 18 categories of analysis.

These categories are shown below, where AR = Aspect Ratio.

VELOCITIES	AR 1	AR 2	AR 5
------------	------	------	------

XZ plane

X component	1	2	3
Z component	4	5	6
XZ total	7	8	9

YZ plane

Y component	10	11	12
Z component	13	14	15
YZ total	16	17	18

Results are given in Appendix E. To test whether the differences between PI values for each model was significant, a one-tailed paired T-Test at the 95% level was performed on the PI values. Pairing was chosen because the Performance Index values represent differences in observations from two populations. This was done for each model over all eighteen categories.

In eight of the eighteen categories, Model A had the lowest Performance Index of the three Models and was significantly different from Models B and C. In ten cases, the difference between Performance Index values for Models A and B was not significant. In seventeen of the eighteen cases, Model C had the greatest PI value and was significantly different from Models A and B. The T-test results are in Appendix D. A summary of the findings is given here.

The categories where no significant difference was found for PI values between Model A and Model B are:

ASPECT RATIO = 1 X, Y, YZ TOTAL

ASPECT RATIO = 2 X, Y, Z(YZ plane)

ASPECT RATIO = 5 X, Y, Z(YZ plane), YZ TOTAL

The categories where Model A was significantly best are:

ASPECT RATIO = 1 Z(XZ plane), Z(YZ plane), XZ TOTAL

ASPECT RATIO = 2 Z(XZ plane), XZ TOTAL, YZ TOTAL

ASPECT RATIO = 5 Z(XZ plane), XZ TOTAL

The next step was to determine how well these models actually fit the data, irrespective of how they related to each other. This was accomplished by performing a least-squares regression on the velocity values. Such a regression minimizes the sum of squares of the y axis deviations and gives an equation for the best straight line fit. The regression line was:

$$Y = M(x) + b$$

where

Y = Measured Velocity X = Predicted Velocity

M = Slope of Line b = Y intercept

$R^2$  = deviation of the Y data from the line / deviation

from the line caused by the X and Y data

The best agreement between Predicted and Measured exists when M=1.00, b=0.0 and  $R^2 = 1$ .

A table with the Least-Squares fit for each model is given in Appendix F.

Since the experimental data were taken over different hood sizes and planes, the

data - both predicted and measured - were tested to determine if there was any effect caused by the various hood configurations and if there was any interaction(26). This was done using a two-way Analysis of Variance (ANOVA) test with hood aspect ratio as one factor and plane as the other. It was assumed that the data were normal and that the row, column and interaction effects were independent (25). No interaction or main effects were found at the 95% level. Results are shown in Appendix G.

Quantile-Quantile plots were generated to illustrate the fit of the predicted velocity to the measured. The straighter the line, the more accurate the model. From these plots, it can be seen that Model A forms a straighter line than Model B. Both Model A and B were found to be more accurate than Model C. The plots are shown in Appendix H.

#### DISCUSSION:

Because no difference was found in each models' predicting ability for varied flowrate, the analysis was confined to the variables of hood aspect ratio, measurement plane and velocity component. Graphs of the measured X, Y, and Z velocity components and of the total velocities versus predicted values are shown in Appendix I. The graphical trend was for the X velocity component to be underestimated by the models. This may have been caused by human error in measuring the angle of displacement rather than model error. However, Models A and B showed relatively good agreement with the experimental values. Their  $R^2$  values from the least-squares analysis were 0.880 and 0.943 respectively.

The predicted Y velocity components of Models A and B matched well at magnitudes from 0 to -500 fpm, but then began to overestimated. A problem with the Y-component was encountered with the hood having an aspect ratio of five. Model C predicted Y-component velocity vectors pointing away from this hood. This occurred because of the constant  $K_y$  in Model C's equation. The hood half width and the Y coordinate determine the value of this constant. The small width caused this anomaly to occur and could be corrected by modifying the equation. Again, Models A and B show good agreement with experimental with their  $R^2$  values at 0.876 and 0.895 respectively.

For the Z velocity components, both Models A and B fit the experimental values well, but Model B becomes less precise at approximately -500 fpm, while Model A fits well until -1000 fpm. The agreement begins to break-up near the hood face as expected from potential flow theory. Here the  $R^2$  values for Model A and Model B were 0.983 and 0.955.

### CONCLUSIONS:

In general, Model A is the most rigorous mathematically, and incorporates the most detail. Model B does not consider the flow in the corners of the hood and underestimates the area of the hood opening. Since measurements were not made in the corners of the hood, it is not possible to determine what the effect of assuming an inscribed ellipse was. Model C was initially developed for use with hoods that have flanking planes. It is possible, that with the addition of such planes, this model would be more accurate.

No significant difference was found between the performance index values of Model A and B over the X and Y velocity components. However, Model A was significantly better for four of the Z component categories and for three of the total velocity cases. The Z component of an airflow into a local exhaust hood is one of the most vital parameters for purposes of optimal design. The quantile-quantile plots reveal that Model A is the most accurate. Based on these findings, Model A should be chosen over any other presently known method for use in the design of local exhaust hoods.

Future work is still to be done. These equations should be tested for a larger range of hood sizes and shapes. However, the most useful research would be on how well the models can predict the velocity flow field when there are other air movement forces in effect such as crossdrafts, source momentum and obstructions to the flow.

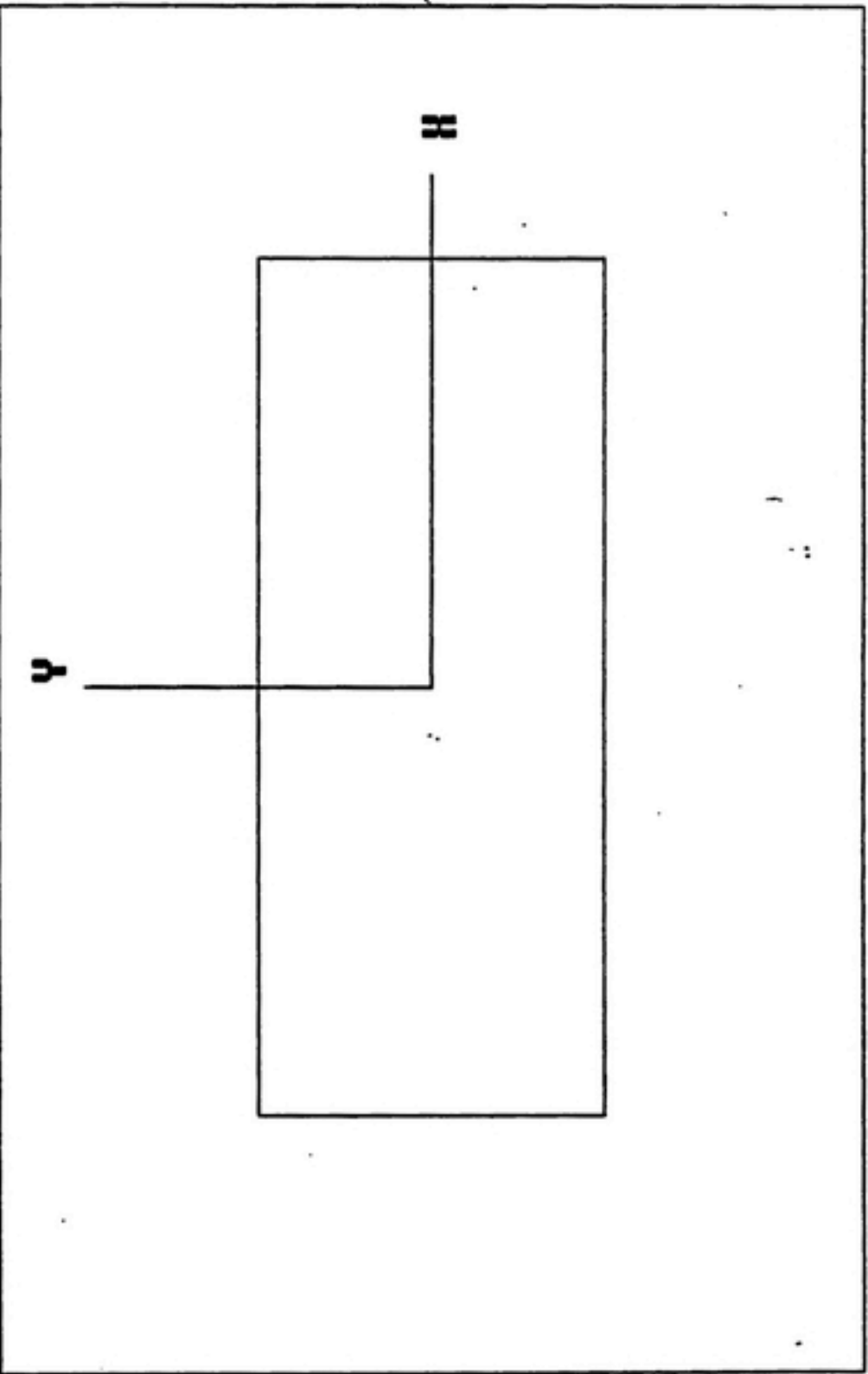
## REFERENCES

1. Alden, J. L., Kane, J. M., Design Of Industrial Ventilation Systems, 5th ed., Industrial Press Inc., New York, (1982).
2. American Conference of Governmental Industrial Hygienists, Industrial Ventilation Manual, 19th ed., ACGIH Inc., Cincinnati, (1987).
3. Braconnier, R., "Bibliographic Review of Velocity Fields in the Vicinity of Local Exhaust Openings", American Industrial Hygiene Association Journal, Vol 49(4), pp.185-198, (April 1988).
4. Brandt, A. D., Industrial Health Engineering, John Wiley and Sons, Inc., New York, (1947).
5. Conroy, L. M., Ellenbecker, M. J., Flynn, M. R., "Prediction and Measurement of Velocity into Flanged Slot Hoods", (1986).
6. DallaValle, J. M., Exhaust Hoods, 2nd ed., The Industrial Press, New York, (1952).
7. DallaValle, J. M., The Industrial Environment and Its Control, Pitman Publishing Corporation, New York, (1948).
8. DallaValle, J. M., Hatch, T., "Studies in the Design of Local Exhaust Hoods.", Paper presented at the Sixth Annual Wood-Industries Meeting, Winston Salem, NC, of The American Society of Mechanical Engineers, (1931).
9. Drinker, P., Hatch, T., Industrial Dust - Hygienic Measurement and Control, 1st ed., McGraw Hill Book Co., Inc., New York, (1936).
10. Ellenbecker, M.J., Gempel, R. F. , Burgess, W. A., "Capture Efficiency of Local Exhaust Ventilation Systems", American Industrial Hygiene Association Journal, Vol 44(10), pp.752-755, (1983).
11. Esmen, N. A., Weyel, D. A., "Aerodynamics of Multiple Orifice Hoods", Ventilation '85, Goodfellow - Editor, pp.735-741, (1986).
12. Fletcher, B., Johnson, A. E., "Capture of Local Exhaust - Ventilation Hoods and the Role of Capture Velocity", Ventilation '85, Goodfellow - Editor, pp.369-390, (1986).

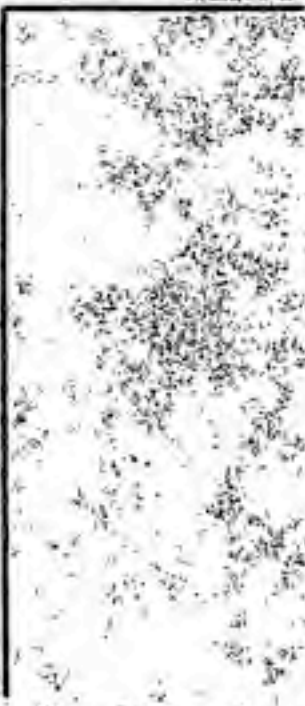
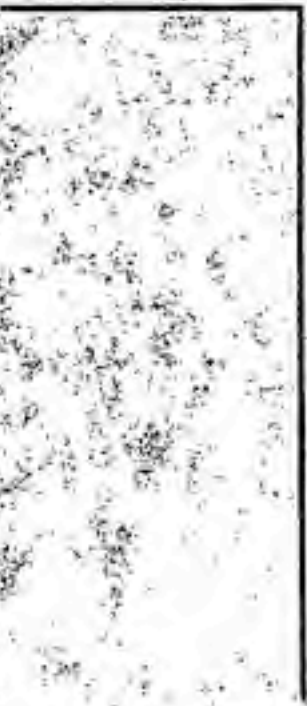
13. Fletcher, B., "Centerline Velocity Characteristics of Rectangular Hoods and Slots Under Suction", Annals of Occupational Hygiene, Vol 20, pp. 141-146, (1977).
14. Fletcher, B., "Comments...Centerline Velocity Characteristics of Local Exhaust Ventilation Hoods", American Industrial Hygiene Association Journal, Vol 43(8), August, (1982).
15. Fletcher, b, "Effect of Flanges on the Velocity in Front of Exhaust Ventilation Hoods", Annals of Occupation Hygiene, Vol 21, pp.265-269, (1978).
16. Fletcher, B., Johnson, A. E., "Velocity Profiles Around Hoods and Slots and The Effects of an Adjacent Plane", Annals of Occupational Hygiene, Vol 25, NO. 4, pp. 365 -372, (1982).
17. Flynn, M. R., Dissertation - Introduction, Harvard Graduate School.
18. Flynn, M. R., Ellenbecker, M. J., "Empirical Validation of Theoretical Velocity Fields into Flanged Circular Hoods", American Industrial Hygiene Association Journal, Vol 48(4), pp.380-389, (April 1987).
19. Flynn, M. R., Ellenbecker, M. J., "The Potential Flow Solution for Air Flow into a Flanged Circular Hood", American Industrial Hygiene Association Journal, Vol 46(6), pp.318-322, (1985).
20. Garrison, R. P., "Velocity Calculation for Local Exhaust Inlets - Empirical Design Equations", American Industrial Hygiene Association Journal, Vol 44(12), pp.937-940, (1983).
21. Garrison, R. P., "Velocity Calculation for Local Exhaust Inlets - Graphical Design Concepts", American Industrial Hygiene Association Journal, Vol 44(12), pp.941-947, (1983).
22. Goodfellow, H. D., Smith, J. W., "Industrial Ventilation - A Review and Update", American Industrial Hygiene Association Journal, Vol 43(3),pp.175-184, (1982).
23. Koehler, J. L. M., Feldman H. A. and Ellenbecker, M. J., "Venturi Scrubber Performance Model Incorporating the Effects of Droplet Size Distribution and Gas-Borne Liquid Flow Rate", In Press.

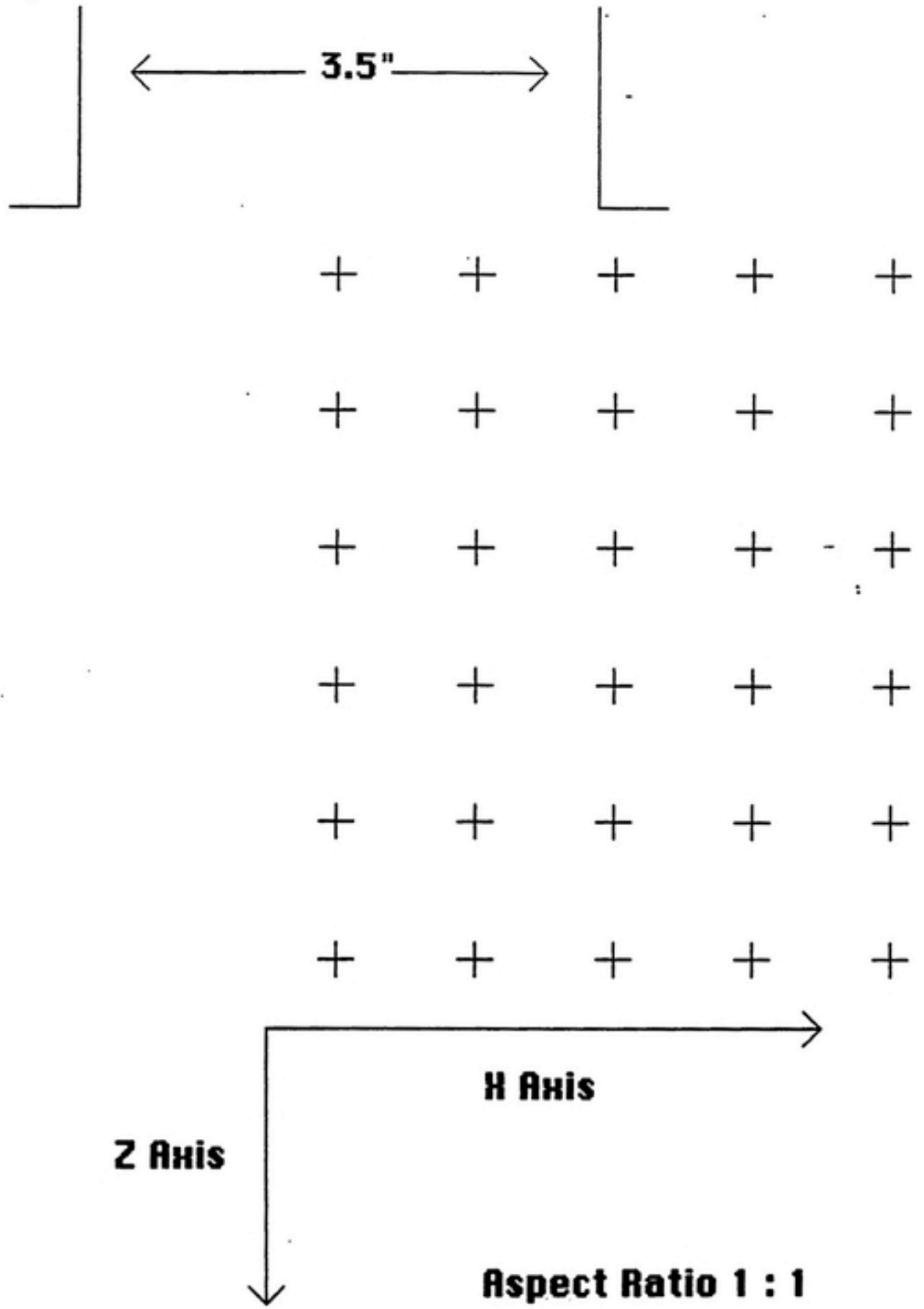
24. Lamb, H, Hydrodynamics, 6th ed., Dover Publications, New York, (1932).
25. Legget, R. W., Williams, L. R., "A Reliability Index for Models", Ecological Modeling, Vol 13, pp. 303-312, (1981).
26. Remington, R. D., Schork, M. A., Statistics with Applications to the Biological and Health Sciences, 2nd ed., Prentice-Hall, Inc., Englewood Cliffs, New Jersey, (1985).
27. Roberson, J. A., Clayton, T. C., Engineering Fluid Mechanics, 2nd ed., Houghton Mifflin Company, New York, (1980).
28. Silverman, L., "Centerline Velocity Characteristics of Round Openings Under Suction", The Journal of Industrial Hygiene and Toxicology, Vol 24, No. 9, pp. 259-266, November, (1942).
29. Silverman, L., "Velocity Characteristics of Narrow Exhaust Slots", The Journal of Industrial Hygiene and Toxicology, Vol 24, No. 9, pp. 267-276, November, (1942).
30. Tyaglo, I. G., Shepelev, I. A., Dvizhenie Vozdushnogo Potoha k Vytazhnomyer Otversityu [Air Flow Near an Exhaust Opening], Vodosnabzhenie i Sanitarnaya Teknika, № 5, pp.24-25, (1970 - in Russian).
31. White, F., Fluid Mechanics, McGraw - Hill, New York, (1982).

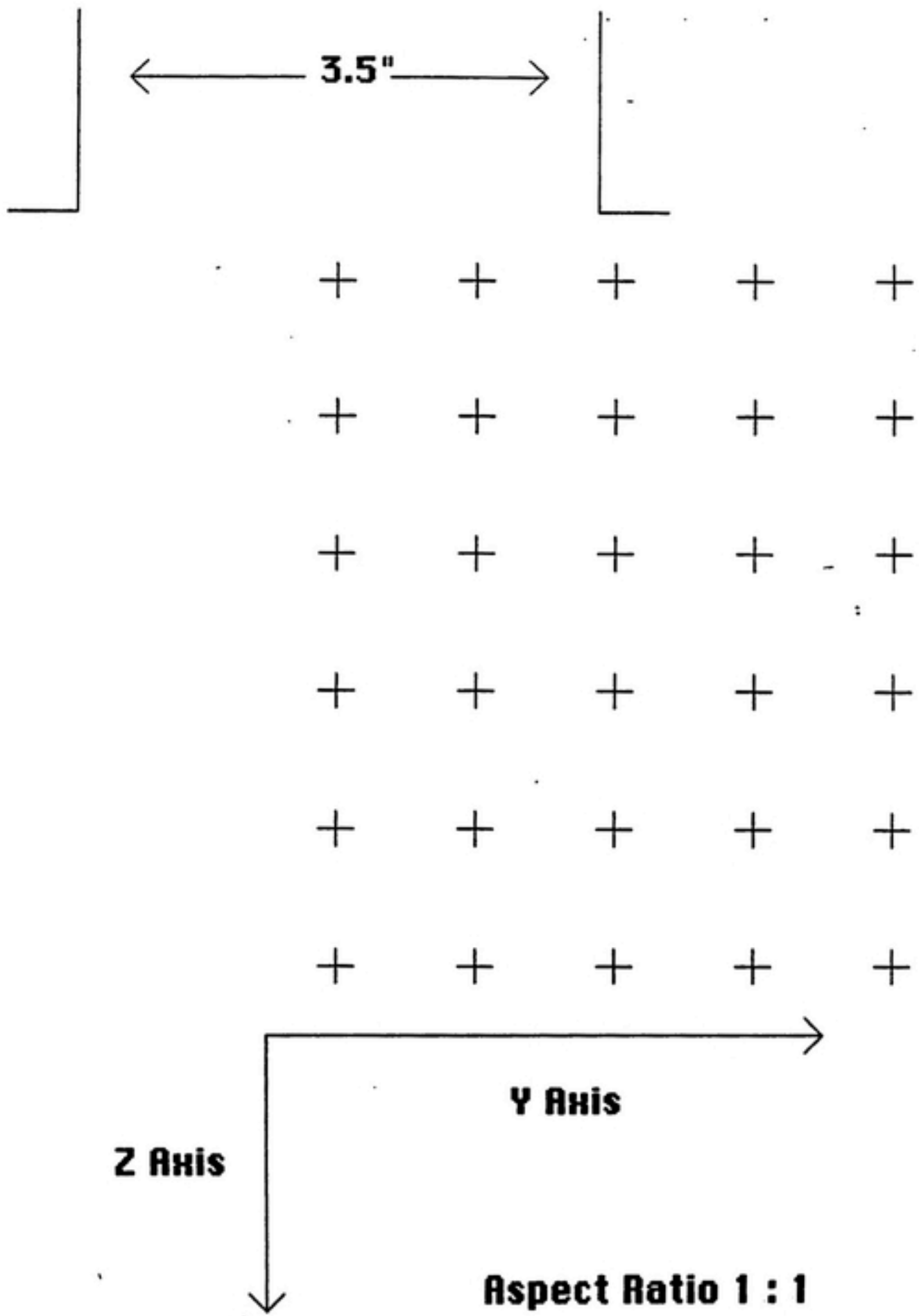
**APPENDIX A**

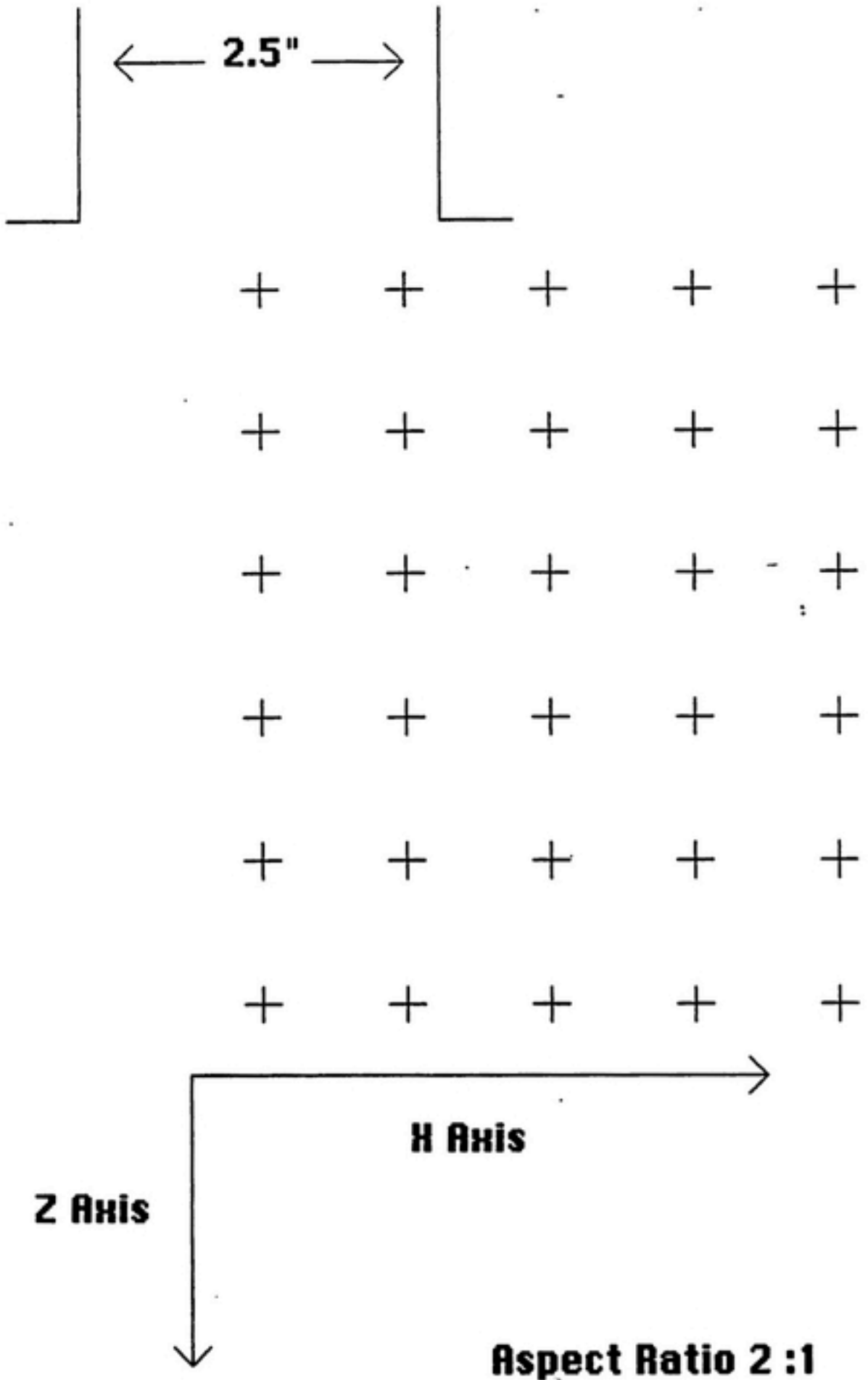


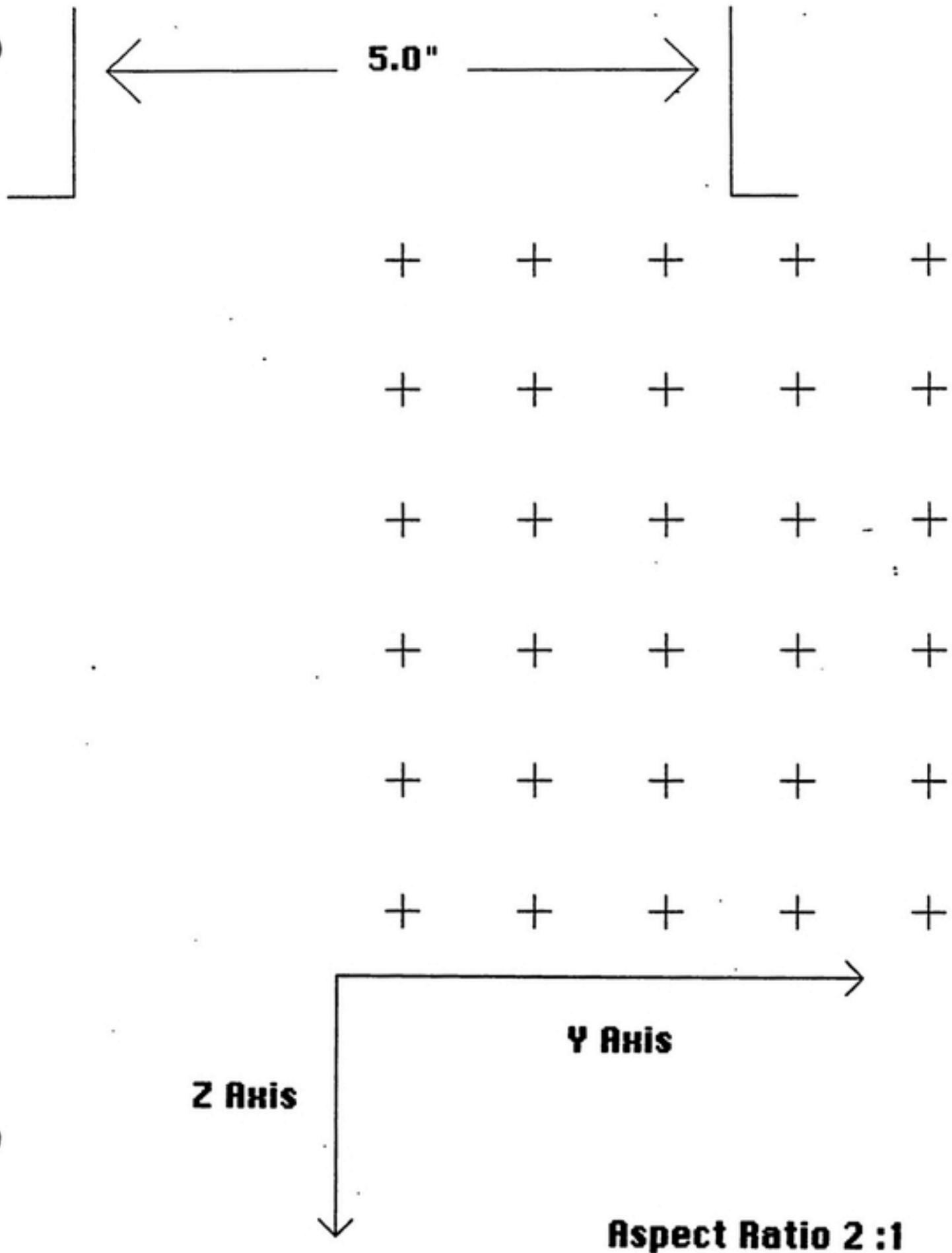
N

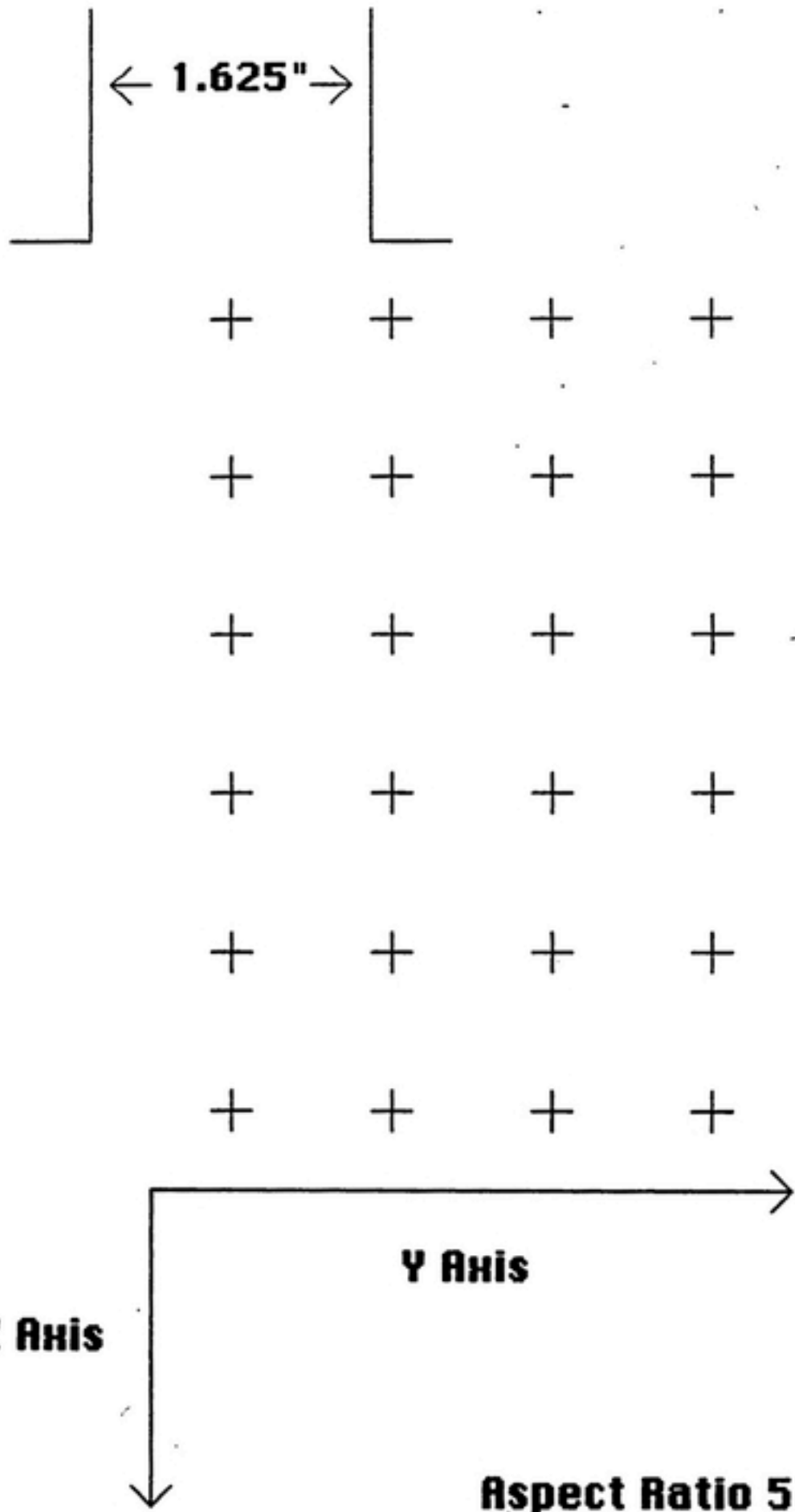


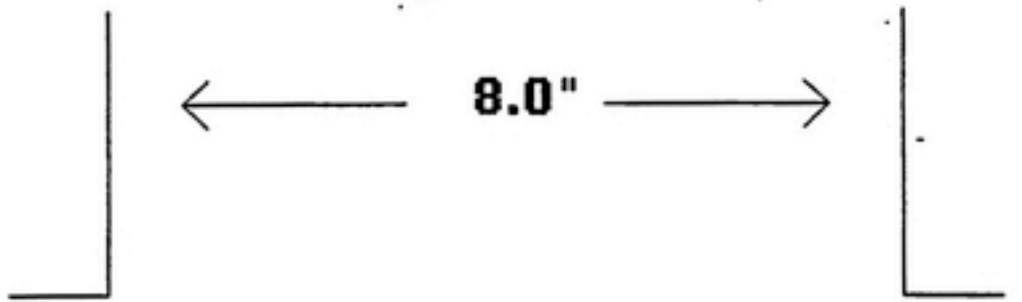




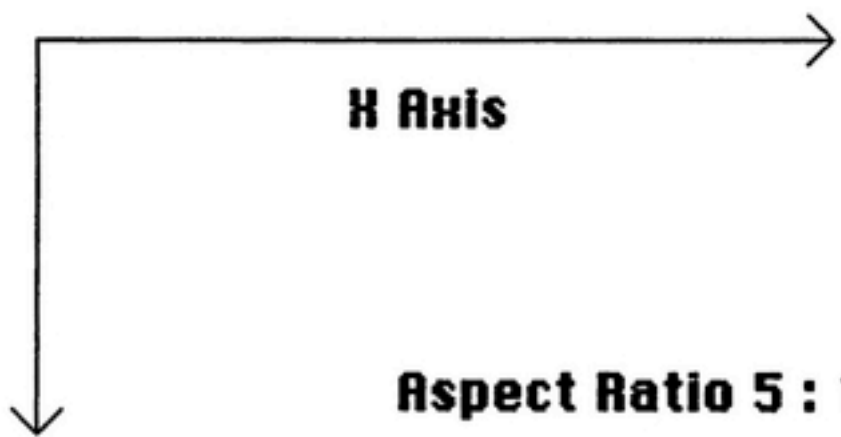






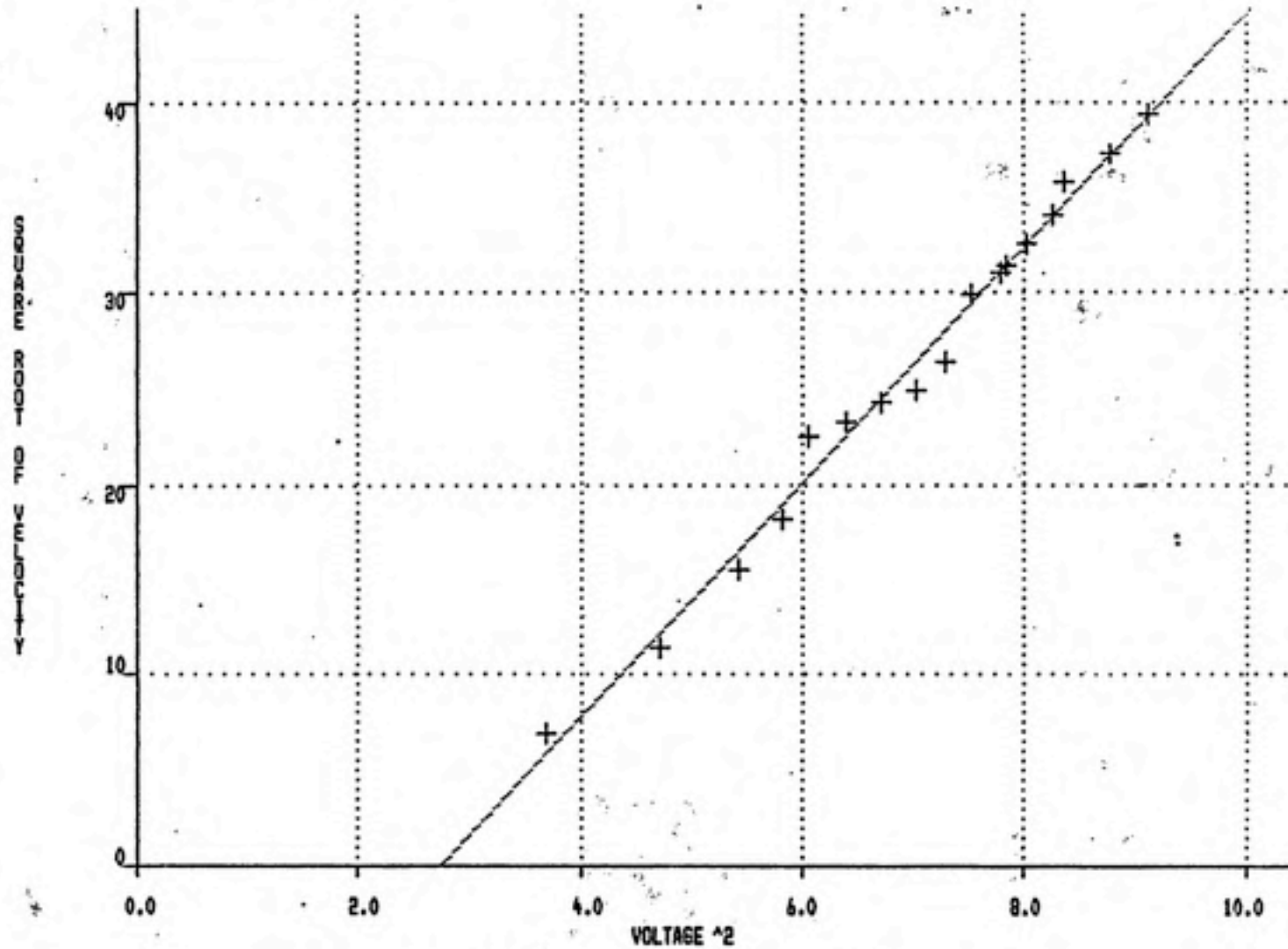


+	+	+	+	+	+
+	+	+	+	+	+
+	+	+	+	+	+
+	+	+	+	+	+
+	+	+	+	+	+
+	+	+	+	+	+



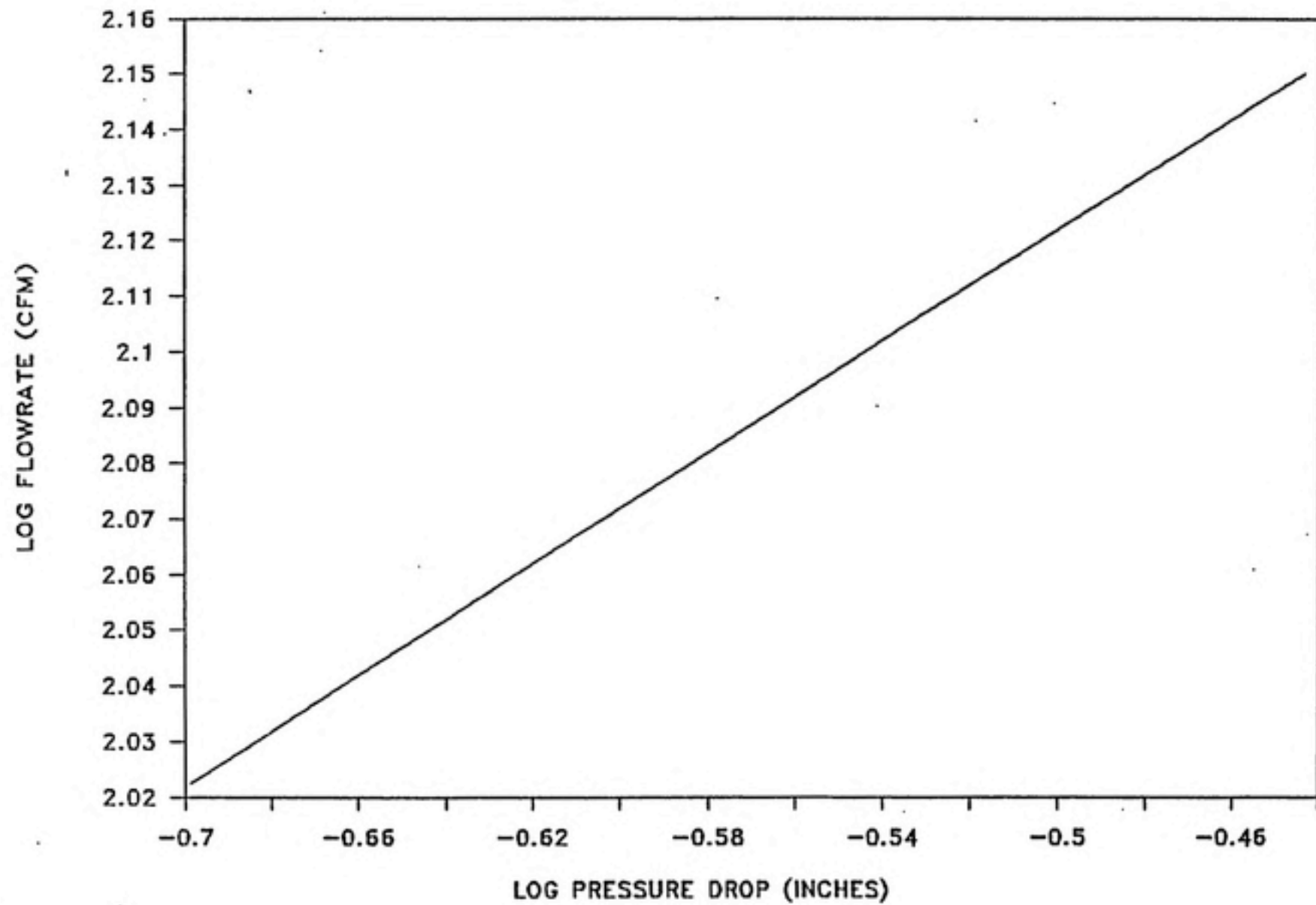
**APPENDIX B**

$y = Ax + B$   
A= 5.156912574, B=-16.63212000  
Correlation=0.9945510



CALIBRATION OF VOLTMETER

## 4" ORIFICE CALIBRATION



**APPENDIX C**

## COMPOSITE OF 24 PLANES

The coordinates Z and I are given in inches  
 The voltmeter reading is given under VOLT column  
 The displacement angle is given under the THETA column in degrees  
 T stands for Tsvaglo's predicted values  
 E stands for Esseen's predicted values  
 F stands for Flynn's predicted values

COMPOSITE OF 12 PLANES  
AR=1 24 PLANE CH=0 945

Z	Z(FT)	I	VOLT	THETA	VEL	XVEL	ZVEL	TVZ	EVZ	FNZ	TVI	EVI	FVI
0.5	0.041666	0	2.91	0	-1246.45	0	-1246.45	-1251.56	-932.402	-988.572	0	0	0
1.5	0.125	0	2.63	0	-663.300	0	-663.300	-657.154	-402.454	-616.417	0	0	0
2.5	0.208333	0	2.42	0	-369.609	0	-369.609	-358.479	-221.843	-351.657	0	0	0
3.5	0.291666	0	2.26	0	-213.595	0	-213.595	-215.433	-140.030	-213.668	0	0	0
4.5	0.375	0	2.14	0	-129.142	0	-129.142	-140.966	-96.2870	-140.478	0	0	0
5.5	0.458333	0	2.04	0	-77.2726	0	-77.2726	-98.5082	-70.2217	-98.3091	0	0	0
0.5	0.041666	1	2.91	0	-1246.45	0	-1246.45	-1159.27	-658.690	-1093.07	-441.441	-658.658	-225.212
1.5	0.125	1	2.6	8	-614.474	-65.5179	-608.494	-575.502	-381.328	-566.920	-202.492	-127.107	-177.792
2.5	0.208333	1	2.38	10	-325.553	-56.5314	-320.607	-322.963	-217.287	-320.289	-92.6817	-43.4570	-88.9055
3.5	0.291666	1	2.24	8	-197.705	-27.5152	-195.782	-195.960	-138.483	-199.071	-46.8475	-19.7832	-46.0741
4.5	0.375	1	2.12	6	-117.494	-12.2814	-116.851	-133.621	-95.6131	-133.276	-26.0711	-10.6236	-25.8671
5.5	0.458333	1	2.04	5	-77.2726	-6.73471	-76.9785	-94.694	-69.8781	-94.5332	-15.7169	-6.35252	-15.6501
0.5	0.041666	2	2.76	60	-904.131	-782.997	-452.069	-438.413	-356.001	-602.583	-754.905	-800.938	-844.233
1.5	0.125	2	2.49	32	-455.453	-241.352	-396.246	-351.626	-316.640	-370.321	-301.274	-237.469	-298.060
2.5	0.208333	2	2.32	24	-265.913	-108.156	-242.923	-235.568	-200.556	-237.660	-144.777	-90.2464	-142.856
3.5	0.291666	2	2.2	21	-168.151	-60.2598	-156.983	-161.139	-132.561	-161.266	-77.6746	-42.6073	-77.0247
4.5	0.375	2	2.09	15	-101.241	-26.2031	-97.7918	-114.525	-93.0276	-114.439	-45.2903	-23.2560	-45.0622
5.5	0.458333	2	2.01	15	-64.6805	-16.7404	-62.4766	-84.4692	-69.5761	-84.3867	-28.2349	-14.0264	-28.1450
0.5	0.041666	3	2.44	80	-392.977	-367.007	-68.2427	-91.2700	-102.672	-101.392	-385.101	-436.329	-409.519
1.5	0.125	3	2.34	49	-284.956	-215.058	-186.949	-161.630	-172.987	-168.756	-246.955	-245.058	-251.522
2.5	0.208333	3	2.24	30	-197.706	-98.8525	-171.218	-146.013	-145.506	-148.001	-144.743	-123.676	-144.947
3.5	0.291666	3	2.14	29	-129.142	-62.6090	-112.950	-116.273	-109.403	-116.715	-86.9816	-56.4220	-86.7894
4.5	0.375	3	2.06	29	-86.4035	-41.8690	-75.5703	-90.4721	-82.0072	-90.5369	-54.5100	-38.7247	-54.4776
5.5	0.458333	3	1.98	26	-53.3694	-23.3954	-47.9681	-70.7610	-62.7589	-70.7415	-35.8213	-24.2472	-35.7491
0.5	0.041666	4	2.25	85	-205.556	-204.774	-17.9170	-32.6588	-38.8305	-33.8236	-214.998	-242.676	-219.761
1.5	0.125	4	2.2	58	-168.151	-142.600	-89.1076	-75.6673	-86.4121	-77.3306	-170.38	-180.020	-172.422
2.5	0.208333	4	2.15	42	-135.215	-90.4762	-100.484	-85.6499	-92.3334	-86.5160	-119.68	-115.414	-120.151
3.5	0.291666	4	2.07	30	-91.1954	-45.5975	-78.9777	-79.0384	-80.6868	-79.3528	-81.2956	-72.0404	-81.3245
4.5	0.375	4	2.01	30	-64.6805	-32.3401	-56.0150	-67.7624	-66.2765	-67.8490	-55.5000	-46.0246	-55.4525
5.5	0.458333	4	1.94	25	-40.1960	-15.9874	-36.4300	-56.6320	-53.7208	-56.6397	-39.6249	-30.5227	-38.5805

AR=1 ZX FLANE DH = 0.29

Z	Z(FT)	I	VOLT	THETA VEL	XVEL	ZVEL	TVZ	EVZ	FVZ	TXI	EVX	FVI
0.5	0.041666	0	2.87	0 -1147.97	0 -1147.97	-1158.75	-355.429	-508.012	0	0	0	0
1.5	0.125	0	2.6	- 0 -614.474	0 -614.474	-603.601	-369.658	-566.184	0	0	0	0
2.5	0.208333	0	2.39	0 -336.237	0 -336.237	-329.266	-203.764	-323.000	0	0	0	0
3.5	0.291666	0	2.24	0 -197.706	0 -197.706	-197.877	-126.619	-196.440	0	0	0	0
4.5	0.375	0	2.13	0 -123.236	0 -123.236	-129.475	-86.4404	-129.030	0	0	0	0
5.5	0.458333	0	2.03	0 -72.9298	0 -72.9298	-90.4806	-64.4992	-90.2977	0	0	0	0
0.5	0.041666	1	2.85	10 -1100.73 -191.140	-1084.01	-1064.8	-605.012	-1003.97	-405.467	-604.983	-207.769	
1.5	0.125	1	2.56	4 -553.087 -38.5812	-551.740	-528.603	-350.253	-510.712	-185.990	-116.749	-163.293	
2.5	0.208333	1	2.36	3 -304.831 -15.9535	-304.413	-296.644	-199.580	-294.184	-65.1290	-39.9156	-81.6558	
3.5	0.291666	1	2.22	0 -182.563	0 -182.563	-183.665	-127.198	-182.846	-43.0298	-18.1710	-42.3172	
4.5	0.375	1	2.11	0 -111.916	0 -111.916	-122.732	-87.8215	-122.413	-23.9465	-9.75789	-23.758	
5.5	0.458333	1	2.03	0 -72.9298	0 -72.9298	-86.9772	-64.1836	-86.8288	-14.4361	-5.83485	-14.3740	
0.5	0.041666	2	2.73	52 -844.177 -665.218	-519.730	-402.686	-326.59	-553.512	-693.387	-735.668	-775.404	
1.5	0.125	2	2.47	28 -429.757 -201.757	-379.453	-322.972	-290.837	-340.145	-276.723	-218.117	-273.762	
2.5	0.208333	2	2.31	22 -256.697 -96.1600	-238.005	-216.371	-184.212	-218.293	-132.978	-82.8921	-131.211	
3.5	0.291666	2	2.19	15 -161.214 -41.7252	-155.721	-148.008	-121.758	-148.124	-71.3448	-39.1352	-70.7458	
4.5	0.375	2	2.09	12 -101.241 -21.0491	-99.0292	-105.192	-85.4465	-105.113	-41.5995	-21.3808	-41.3887	
5.5	0.458333	2	2	9 -60.7702 -9.50651	-60.0220	-77.5857	-62.9878	-77.5096	-25.9340	-12.8834	-25.8507	
0.5	0.041666	3	2.42	74 -369.609 -355.250	-101.880	-83.8323	-94.3055	-93.1401	-353.719	-400.772	-376.153	
1.5	0.125	3	2.33	46 -275.332 -158.056	-191.262	-148.458	-158.890	-155.018	-226.831	-225.088	-231.024	
2.5	0.208333	3	2.22	31 -182.563 -94.0266	-156.487	-134.114	-133.648	-135.941	-132.947	-113.598	-133.133	
3.5	0.291666	3	2.12	25 -117.494 -49.6552	-106.486	-106.798	-100.488	-107.204	-79.8933	-61.0092	-79.7154	
4.5	0.375	3	2.05	16 -81.7632 -22.5368	-78.5959	-83.0994	-75.3243	-83.1590	-50.1597	-35.5690	-50.0373	
5.5	0.458333	3	1.98	10 -53.3694 -9.26745	-52.5586	-64.9946	-57.6446	-64.9766	-32.9022	-22.2713	-32.8352	
0.5	0.041666	4	2.23	71 -190.042 -179.688	-61.8729	-29.5974	-35.6661	-31.0703	-197.477	-222.900	-201.855	
1.5	0.125	4	2.2	56 -168.151 -139.403	-94.0299	-69.5011	-73.3703	-71.0315	-156.495	-165.350	-158.372	
2.5	0.208333	4	2.14	45 -129.142 -91.3169	-91.3176	-78.6702	-84.8050	-79.4673	-109.927	-106.009	-110.36	
3.5	0.291666	4	2.07	35 -91.1954 -52.3073	-74.7031	-72.5975	-74.1115	-72.8870	-74.6707	-66.1638	-74.6966	
4.5	0.375	4	2	21 -60.7702 -21.7780	-56.7339	-62.2404	-60.8755	-62.3202	-50.9773	-42.274	-50.9330	
5.5	0.458333	4	1.95	21 -46.5161 -16.6698	-43.4265	-52.0170	-49.3431	-52.0242	-35.4773	-28.0354	-35.4361	

AR=1 ZX PLANE

DH= 0.21

Z	Z(FT)	I	VOLT	THETA	VEL	XVEL	ZVEL	TVZ	EVZ	FVZ	TVX	EVX	FVX
0.5	0.041666	0	2.81	0	-1010.16	0	-1010.18	-989.412	-731.261	-775.314	0	0	0
1.5	0.125	0	2.55	0	-538.388	0	-538.388	-515.390	-315.655	-463.441	0	0	0
2.5	0.208333	0	2.33	0	-275.332	0	-275.332	-281.145	-173.596	-275.796	0	0	0
3.5	0.291666	0	2.2	0	-168.151	0	-168.151	-168.355	-109.822	-167.732	0	0	0
4.5	0.375	0	2.09	0	-101.241	0	-101.241	-110.556	-75.5156	-110.173	0	0	0
5.5	0.458333	0	2	0	-60.7702	0	-60.7702	-77.2576	-55.0722	-77.1615	0	0	0
0.5	0.041666	1	2.8	3	-988.352	-51.7260	-966.997	-909.188	-516.555	-657.250	-346.211	-516.570	-177.405
1.5	0.125	1	2.52	3	-495.807	-25.9484	-495.127	-451.352	-299.066	-444.615	-158.609	-99.6873	-139.429
2.5	0.208333	1	2.33	0	-275.332	0	-275.332	-253.292	-170.413	-251.191	-72.6881	-34.0823	-69.7225
3.5	0.291666	1	2.18	0	-154.454	0	-154.454	-156.824	-108.609	-155.125	-36.7414	-15.5155	-36.1325
4.5	0.375	1	2.08	0	-96.1408	0	-96.1408	-104.796	-74.9871	-104.524	-20.4469	-8.33185	-20.2859
5.5	0.458333	1	2	0	-60.7702	0	-60.7702	-74.2662	-54.8037	-74.1395	-12.3264	-4.98213	-12.2734
0.5	0.041666	2	2.66	54	-714.585	-578.109	-420.025	-343.837	-279.203	-472.621	-592.054	-628.157	-662.085
1.5	0.125	2	2.42	33	-369.609	-201.302	-309.980	-275.772	-248.333	-290.436	-236.282	-186.241	-233.754
2.5	0.208333	2	2.27	23	-221.826	-86.6739	-204.192	-184.751	-157.291	-186.391	-113.545	-70.7782	-112.035
3.5	0.291666	2	2.15	13	-135.215	-30.4166	-131.749	-126.378	-103.964	-126.477	-60.9184	-33.4159	-60.4069
4.5	0.375	2	2.04	5	-77.2726	-6.73471	-76.9785	-89.8195	-72.9593	-89.7518	-35.5201	-18.2391	-35.3401
5.5	0.458333	2	1.97	4	-49.8752	-3.47910	-49.7537	-66.2472	-53.7826	-66.1822	-22.1440	-11.0006	-22.0728
0.5	0.041666	3	2.37	74	-315.005	-302.878	-86.8513	-71.5809	-80.5235	-79.5285	-302.026	-342.202	-321.181
1.5	0.125	3	2.29	49	-238.867	-180.274	-155.712	-126.762	-135.670	-132.363	-193.681	-192.193	-197.262
2.5	0.208333	3	2.19	32	-154.454	-81.8482	-130.985	-114.514	-114.117	-116.075	-113.519	-96.9968	-113.677
3.5	0.291666	3	2.09	26	-101.241	-44.3811	-90.9954	-91.1905	-85.8027	-91.5372	-63.2176	-52.0932	-68.0657
4.5	0.375	3	2	19	-60.7702	-19.7847	-57.4594	-70.9552	-64.3163	-71.0060	-42.8293	-30.3709	-42.7247
5.5	0.458333	3	1.95	16	-43.2903	-11.9323	-41.6133	-55.4962	-49.2203	-55.4808	-28.0938	-19.0165	-28.0366
0.5	0.041666	4	2.19	62	-161.214	-159.645	-22.4379	-25.6136	-30.4538	-25.5296	-168.617	-190.325	-172.356
1.5	0.125	4	2.16	56	-141.456	-117.272	-79.1023	-59.3441	-67.7710	-60.6508	-133.625	-141.185	-135.227
2.5	0.208333	4	2.1	40	-105.459	-68.4562	-81.5836	-67.1732	-72.4149	-67.8538	-93.8621	-90.5167	-94.2317
3.5	0.291666	4	2.03	37	-72.9298	-43.8900	-58.2445	-61.998	-63.2807	-62.2352	-63.7582	-56.4996	-63.7603
4.5	0.375	4	1.98	27	-53.3654	-24.2290	-47.5525	-53.1445	-51.9791	-53.2126	-43.5274	-36.0960	-43.4896

Composite of all a  
z=2 ZX PLANE DH=0.345

Z	Z(FT)	I	VOLT	THETA	VEL	IVEL	ZVEL	TVZ	EVZ	FHZ	TVI	EVI	F
0.5	0.041666	0	2.9	0	-1221.32	0	-1221.32	-1199.20	-898.221	-954.082	0	0	
1.5	0.125	0	2.6	0	-614.474	0	-614.474	-609.115	-387.170	-575.273	0	0	
2.5	0.208333	0	2.39	0	-336.236	0	-336.236	-337.313	-214.451	-331.394	0	0	
3.5	0.291666	0	2.24	0	-197.705	0	-197.705	-206.298	-135.981	-204.870	0	0	
4.5	0.375	0	2.12	0	-117.494	0	-117.494	-136.677	-93.8480	-136.216	0	0	
5.5	0.458333	0	2.04	0	-77.2724	0	-77.2724	-96.2998	-68.6446	-96.1082	0	0	
0.5	0.041666	1	2.9	0	-1221.32	0	-1221.32	-1175.54	-634.576	-1012.12	-198.329	-634.499	-91.25
1.5	0.125	1	2.58	0	-583.258	0	-583.258	-575.947	-366.855	-558.692	-124.128	-122.280	-107.5
2.5	0.208333	1	2.38	0	-325.552	0	-325.552	-316.956	-210.051	-313.666	-68.0769	-42.0092	-65.23
3.5	0.291666	1	2.23	0	-190.042	0	-190.042	-195.551	-134.480	-194.616	-39.1087	-19.2111	-37.47
4.5	0.375	1	2.12	0	-117.494	0	-117.494	-130.968	-93.1916	-130.621	-22.5501	-10.3544	-22.37
5.5	0.458333	1	2.04	0	-77.2724	0	-77.2724	-93.1224	-68.3088	-92.9629	-14.1325	-6.20982	-14.07
0.5	0.041666	2	2.88	29	-1172.08	-558.236	-1025.13	-991.439	-400.977	-1174.19	-556.042	-801.857	-411.8
1.5	0.125	2	2.53	20	-509.750	-174.343	-479.008	-449.066	-321.366	-464.055	-243.494	-214.235	-232.0
2.5	0.208333	2	2.34	19	-284.956	-92.7723	-269.431	-256.622	-198.668	-257.865	-121.595	-79.4655	-119.2
3.5	0.291666	2	2.2	12	-168.151	-34.9604	-164.477	-165.833	-130.490	-165.806	-67.6319	-37.2824	-66.97
4.5	0.375	2	2.1	8	-106.499	-14.8217	-105.462	-115.328	-91.4528	-115.212	-40.6312	-20.3225	-40.41
5.5	0.458333	2	2.02	5	-68.7329	-5.99044	-68.4714	-84.3474	-67.4319	-84.2586	-25.9212	-12.2602	-25.83
0.5	0.041666	3	2.65	60	-697.212	-603.801	-348.609	-243.641	-200.475	-313.966	-582.245	-701.556	-670.2
1.5	0.125	3	2.42	44	-369.608	-256.750	-265.875	-242.261	-237.681	-256.09	-266.168	-277.273	-270.6
2.5	0.208333	3	2.26	30	-213.595	-106.797	-184.979	-173.832	-170.766	-176.194	-139.994	-119.529	-139.8
3.5	0.291666	3	2.16	29	-141.456	-68.5792	-123.721	-125.911	-119.537	-126.334	-81.7734	-59.7654	-81.56
4.5	0.375	3	2.07	22	-91.1953	-34.1621	-84.5548	-93.9077	-86.4298	-93.9557	-51.2096	-33.6100	-51.06
5.5	0.458333	3	2	19	-60.7701	-19.7847	-57.4593	-71.9882	-64.8365	-71.9624	-33.7773	-20.6288	-33.76
0.5	0.041666	4	2.35	65	-294.788	-269.302	-119.903	-55.3184	-65.4680	-58.9987	-280.453	-360.023	-292.1
1.5	0.125	4	2.26	54	-213.595	-172.801	-125.549	-106.923	-125.498	-110.316	-195.741	-230.066	-199.0
2.5	0.208333	4	2.18	39	-154.454	-97.2010	-120.034	-104.064	-117.45	-105.303	-124.813	-129.189	-125.3
3.5	0.291666	4	2.09	36	-101.241	-59.5079	-81.9062	-87.9759	-94.3512	-88.3429	-80.8019	-74.1302	-80.80
4.5	0.375	4	2.02	26	-68.7329	-30.1304	-61.7768	-71.9093	-73.6337	-71.9986	-54.0553	-44.9968	-53.95
5.5	0.458333	4	1.95	24	-43.2902	-17.6076	-39.5476	-58.5477	-57.8100	-58.5533	-37.3620	-28.9040	-37.31

AR=2 ZX PLANE OH=0.29

Z	Z(FT)	X	VOLT	THETA	VEL	XVEL	ZVEL	TVZ	EVZ	FNVZ	TVX	EVX	FV1
0.5	0.041666	0	2.88	0	-1172.08	0	-1172.08	-1101.47	-825.024	-876.333	0	0	0
1.5	0.125	0	2.56	0	-553.087	0	-553.087	-559.477	-355.619	-528.393	0	0	0
2.5	0.208333	0	2.37	0	-315.085	0	-315.085	-309.825	-196.975	-304.389	0	0	0
3.5	0.291666	0	2.22	0	-182.563	0	-182.563	-189.486	-124.900	-188.175	0	0	0
4.5	0.375	0	2.12	0	-117.494	0	-117.494	-125.539	-86.2002	-125.115	0	0	0
5.5	0.458333	0	2.03	0	-72.9298	0	-72.9298	-88.4522	-63.0506	-88.2762	0	0	0
0.5	0.041666	1	2.87	0	-1147.97	0	-1147.97	-1079.74	-582.863	-929.643	-182.167	-582.793	-83.8207
1.5	0.125	1	2.55	8	-538.388	-74.9288	-533.148	-529.013	-336.960	-513.164	-114.013	-112.315	-98.8196
2.5	0.208333	1	2.35	12	-294.789	-61.2898	-288.347	-291.127	-192.933	-288.105	-62.5292	-38.5858	-59.9193
3.5	0.291666	1	2.21	3	-175.267	-9.17273	-175.027	-179.615	-123.521	-178.756	-35.0032	-17.6456	-34.4242
4.5	0.375	1	2.1	0	-106.499	0	-106.499	-120.296	-85.5973	-119.977	-20.7125	-9.51068	-20.5506
5.5	0.458333	1	2.02	0	-69.7331	0	-69.7331	-85.5338	-62.7422	-85.3873	-12.9809	-5.70377	-12.9256
0.5	0.041666	2	2.84	17	-1077.61	-315.062	-1030.53	-910.645	-368.300	-1078.51	-510.729	-736.513	-378.261
1.5	0.125	2	2.5	23	-468.661	-183.119	-431.405	-412.471	-295.177	-426.239	-223.652	-196.777	-213.102
2.5	0.208333	2	2.32	21	-265.913	-95.2942	-248.251	-235.710	-182.478	-236.851	-111.686	-72.9898	-109.524
3.5	0.291666	2	2.18	12	-154.454	-32.1128	-151.079	-152.319	-119.856	-152.294	-62.1205	-34.2442	-61.5211
4.5	0.375	2	2.09	9	-101.241	-15.8375	-99.9951	-105.930	-84.0002	-105.824	-37.3201	-18.6654	-37.1201
5.5	0.458333	2	2	8	-60.7702	-8.45754	-60.1788	-77.4738	-61.9368	-77.3923	-23.8088	-11.2611	-23.7309
0.5	0.041666	3	2.61	58	-630.480	-534.676	-334.106	-223.787	-184.138	-288.380	-534.798	-644.385	-615.586
1.5	0.125	3	2.38	38	-325.553	-200.429	-256.540	-222.518	-218.312	-235.220	-244.477	-254.678	-248.632
2.5	0.208333	3	2.25	31	-205.556	-105.868	-176.196	-159.666	-156.850	-161.836	-128.586	-109.789	-128.415
3.5	0.291666	3	2.13	20	-123.236	-42.1490	-115.804	-115.650	-109.795	-116.038	-75.1095	-54.8950	-74.8641
4.5	0.375	3	2.05	15	-81.7632	-21.1617	-78.9772	-86.2551	-79.3865	-86.2991	-47.0364	-30.8710	-46.9051
5.5	0.458333	3	1.99	15	-57.0004	-14.7527	-55.0582	-66.1218	-59.5529	-66.0981	-31.0247	-18.9478	-30.9581
0.5	0.041666	4	2.32	69	-265.913	-248.250	-95.2963	-50.8104	-60.1329	-54.1908	-257.599	-330.684	-268.321
1.5	0.125	4	2.24	45	-197.706	-139.798	-139.799	-98.2101	-115.271	-101.326	-179.790	-211.318	-182.808
2.5	0.208333	4	2.16	37	-141.456	-85.1305	-112.972	-95.5838	-107.878	-96.7218	-114.642	-118.661	-115.113
3.5	0.291666	4	2.07	29	-91.1954	-44.2122	-79.7614	-80.8067	-86.6624	-81.1437	-74.2173	-69.0892	-74.2196
4.5	0.375	4	2	24	-60.7702	-24.7173	-55.5164	-66.0493	-67.6332	-66.1313	-49.6503	-41.3299	-49.5975
5.5	0.458333	4	1.94	24	-40.1960	-16.3491	-36.7209	-53.7765	-53.0990	-53.7817	-34.3173	-26.5486	-34.2745

## AR=2 ZX PLANE OH=0.21

Z	Z(FT)	I	VOLT	THETA	VEL	XVEL	ZVEL	TVZ	EVZ	FNZ	TVX	EVX	FVX	
0.5	0.041666	0	2.82		0 -1032.34	0 -1032.34	-940.507	-704.454	-748.264	0	0	0	0	
1.5	0.125	0	2.51		0 -482.111	0 -482.111	-477.714	-303.649	-451.173	0	0	0	0	
2.5	0.208333	0	2.31		0 -256.697	0 -256.697	-264.547	-168.169	-259.905	0	0	0	0	
3.5	0.291666	0	2.18		0 -154.454	0 -154.454	-161.794	-106.647	-160.674	0	0	0	0	
4.5	0.375	0	2.07		0 -91.1954	0 -91.1954	-107.192	-73.6028	-106.831	0	0	0	0	
5.5	0.458333	0	1.99		0 -57.0004	0 -57.0004	-75.5256	-53.8363	-75.3754	0	0	0	0	
0.5	0.041666	1	2.81		0 -1010.18	0 -1010.18	-921.949	-497.683	-793.784	-155.545	-497.623	-71.5710		
1.5	0.125	1	2.51		11 -482.111	11 -482.111	-91.9907	-473.254	-451.702	-287.716	-438.169	-97.3510	-95.9016	-84.378
2.5	0.208333	1	2.31		5 -256.697	5 -256.697	-22.3725	-255.720	-248.581	-164.738	-246.001	-53.3911	-32.9468	-51.1626
3.5	0.291666	1	2.18		5 -154.454	5 -154.454	-13.4615	-153.867	-153.366	-105.47	-152.632	-29.8878	-15.0668	-29.3934
4.5	0.375	1	2.07		2 -91.1954	2 -91.1954	-3.18265	-91.1399	-102.715	-73.0880	-102.443	-17.6855	-8.12078	-17.5473
5.5	0.458333	1	1.99		0 -57.0004	0 -57.0004	-73.0337	-53.5729	-72.9086	-11.0838	-4.87021	-11.0366		
0.5	0.041666	2	2.78		26 -945.621	26 -945.621	-414.531	-849.919	-777.562	-314.476	-920.896	-436.091	-628.878	-322.982
1.5	0.125	2	2.46		15 -417.264	15 -417.264	-107.995	-403.046	-352.192	-252.04	-363.947	-190.967	-168.019	-181.959
2.5	0.208333	2	2.27		16 -221.826	16 -221.826	-61.1432	-213.233	-201.263	-155.811	-202.237	-95.3648	-62.3229	-93.5183
3.5	0.291666	2	2.13		6 -123.236	6 -123.236	-12.8816	-122.560	-130.059	-102.340	-130.038	-53.0421	-29.2397	-52.5303
4.5	0.375	2	2.04		4 -77.2726	4 -77.2726	-5.39023	-77.0843	-90.4495	-71.7243	-90.3588	-31.8661	-15.9385	-31.6954
5.5	0.458333	2	1.96		5 -46.5161	5 -46.5161	-4.05412	-46.3391	-66.1517	-52.8853	-66.0821	-20.3294	-9.61540	-20.2628
0.5	0.041666	3	2.57		66 -568.043	66 -568.043	-518.932	-231.047	-191.082	-157.228	-246.236	-456.641	-560.214	-525.624
1.5	0.125	3	2.36		31 -304.831	31 -304.831	-156.998	-261.291	-189.999	-186.407	-200.845	-208.749	-217.459	-212.297
2.5	0.208333	3	2.21		24 -175.267	24 -175.267	-71.2872	-160.114	-136.332	-133.928	-138.185	-109.794	-93.7443	-109.648
3.5	0.291666	3	2.1		24 -106.499	24 -106.499	-43.3170	-97.2922	-98.7491	-93.7500	-99.0807	-64.1329	-46.8726	-63.9233
4.5	0.375	3	2.02		11 -68.7331	11 -68.7331	-13.1148	-67.4703	-73.6496	-67.7849	-73.6872	-40.1625	-26.3595	-40.0503
5.5	0.458333	3	1.95		10 -43.2903	10 -43.2903	-7.51724	-42.6326	-56.4587	-50.8497	-56.4384	-26.4907	-16.1787	-26.4339
0.5	0.041666	4	2.28		68 -230.249	68 -230.249	-213.482	-86.2542	-43.3849	-51.3450	-46.2713	-219.953	-282.357	-229.108
1.5	0.125	4	2.21		46 -175.267	46 -175.267	-126.076	-121.751	-83.8575	-98.4255	-86.5185	-153.515	-180.435	-156.092
2.5	0.208333	4	2.12		39 -117.494	39 -117.494	-73.9415	-91.3109	-81.6150	-92.1133	-82.5868	-97.8880	-101.32	-98.2909
3.5	0.291666	4	2.04		30 -77.2726	30 -77.2726	-38.6361	-66.9201	-68.9974	-73.9974	-69.2853	-63.3710	-58.1386	-63.3730
4.5	0.375	4	1.97		24 -49.8752	24 -49.8752	-20.2859	-45.5633	-56.3968	-57.7492	-56.4668	-42.3943	-35.2899	-42.3492

AR=5 ZX PLANE DH=0.345

Z	Z(FT)	I	VOLT	THETA	VEL	IVEL	ZVEL	TVZ	EVZ	FNZ	TVX	EVX	FVI
0.5	0.041666	0	2.83	0	-1054.61	0	-1054.61	-1014.36	-794.125	-851.516	0	0	0
1.5	0.125	0	2.49	0	-455.453	0	-455.453	-465.883	-336.464	-449.364	0.000033	0	0
2.5	0.208333	0	2.3	0	-247.682	0	-247.682	-267.325	-168.835	-254.110	0	0	0
3.5	0.291666	0	2.19	0	-161.214	0	-161.214	-172.397	-121.509	-171.484	0.000033	0	0
4.5	0.375	0	2.08	0	-96.1408	0	-96.1408	-119.287	-84.9279	-118.951	-0.00002	0	0
5.5	0.458333	0	2	0	-60.7702	0	-60.7702	-85.7694	-62.7736	-86.6159	0	0	0
0.5	0.041666	1	2.81	0	-1010.18	0	-1010.18	-1011.91	-561.056	-869.752	-51.9049	-561.029	-28.4866
1.5	0.125	1	2.48	3	-442.486	-23.1578	-441.879	-460.495	-318.845	-447.237	-42.763	-106.290	-38.5960
2.5	0.208333	1	2.31	0	-256.697	0	-256.697	-262.006	-184.978	-259.468	-31.1060	-36.9952	-30.1128
3.5	0.291666	1	2.18	0	-154.454	0	-154.454	-168.370	-120.176	-167.631	-21.4739	-17.1680	-21.1857
4.5	0.375	1	2.08	0	-96.1408	0	-96.1408	-116.534	-84.3383	-116.25	-14.7033	-9.37087	-14.6056
5.5	0.458333	1	2	0	-60.7702	0	-60.7702	-84.9440	-62.4689	-84.8079	-10.1980	-5.67897	-10.1599
0.5	0.041666	2	2.82	5	-1032.34	-89.9742	-1028.41	-1000.54	-354.540	-930.539	-125.887	-709.047	-75.4589
1.5	0.125	2	2.48	7	-442.486	-53.9251	-439.187	-439.078	-279.341	-435.372	-94.9517	-186.224	-87.9130
2.5	0.208333	2	2.28	4	-230.249	-16.0613	-229.688	-243.778	-174.970	-243.011	-63.7049	-69.9876	-62.2111
3.5	0.291666	2	2.16	4	-141.456	-9.86748	-141.112	-155.774	-116.619	-155.467	-42.0785	-33.3195	-41.6534
4.5	0.375	2	2.06	0	-86.4035	0	-86.4035	-108.312	-82.7688	-108.154	-28.2868	-18.3929	-28.1385
5.5	0.458333	2	1.99	0	-57.0004	0	-57.0004	-79.6032	-61.6693	-79.5106	-19.5210	-11.2125	-19.4603
0.5	0.041666	3	2.81	9	-1010.18	-158.027	-997.752	-947.814	-250.482	-1043.16	-281.284	-751.411	-207.277
1.5	0.125	3	2.45	9	-405.005	-63.3564	-400.019	-378.989	-237.136	-388.007	-162.897	-237.132	-157.598
2.5	0.208333	3	2.26	10	-213.595	-37.0903	-210.351	-206.902	-161.430	-208.013	-94.8528	-96.8574	-93.7948
3.5	0.291666	3	2.13	10	-123.236	-21.3996	-121.363	-134.016	-111.378	-134.147	-59.3455	-47.7334	-59.0091
4.5	0.375	3	2.05	5	-81.7632	-7.12609	-81.4521	-95.0735	-80.3721	-95.0498	-39.2469	-26.7905	-39.1131
5.5	0.458333	3	1.96	7	-46.5161	-5.66885	-46.1694	-71.2445	-60.4281	-71.2005	-27.0632	-16.4803	-27.0016
0.5	0.041666	4	2.7	44	-786.901	-546.625	-566.051	-513.233	-191.945	-714.072	-584.889	-767.746	-670.617
1.5	0.125	4	2.36	25	-304.831	-128.826	-276.271	-245.750	-200.999	-256.788	-210.900	-267.995	-213.092
2.5	0.208333	4	2.2	22	-168.151	-62.9904	-155.907	-151.023	-146.858	-152.639	-112.260	-117.485	-112.211
3.5	0.291666	4	2.08	17	-95.1408	-28.1087	-91.9399	-105.224	-105.116	-105.543	-69.1476	-60.0663	-69.0240
4.5	0.375	4	2	12	-60.7702	-12.6347	-59.4422	-78.3989	-77.3564	-78.4525	-45.9607	-34.3804	-45.8812
5.5	0.458333	4	1.93	9	-37.2314	-5.82425	-36.7731	-60.8658	-58.8223	-60.8565	-32.0587	-21.3898	-32.0115
0.5	0.041666	5	2.35	62	-294.789	-260.282	-138.396	-76.1312	-73.0412	-82.4312	-294.891	-438.214	-310.345
1.5	0.125	5	2.24	42	-197.706	-132.290	-146.924	-111.886	-123.299	-115.117	-175.354	-246.589	-178.022
2.5	0.208333	5	2.13	38	-123.236	-75.8713	-97.1116	-94.5039	-109.625	-95.4188	-106.111	-131.545	-106.484
3.5	0.291666	5	2.03	24	-72.9298	-29.6631	-66.6248	-75.7386	-87.0056	-75.9962	-69.243	-74.5737	-69.2635
4.5	0.375	5	1.96	20	-45.5161	-15.9093	-43.7108	-61.0381	-67.9317	-61.1031	-47.7366	-45.2863	-47.7064
5.5	0.458333	5	1.93	20	-37.2314	-12.7338	-34.9861	-49.8575	-53.5549	-49.8629	-34.2190	-29.2108	-34.1891

## AR=5 ZX PLANE DH=0.29

Z	Z(FT)	I	VOLT	THETA	VEL	XVEL	ZVEL	TVZ	EVZ	FNZ	TVI	EVX	FVX
0.5	0.041666	0	2.78	0	-945.621	0	-945.621	-931.717	-729.411	-782.125	0	0	0
1.5	0.125	0	2.46	0	-417.254	0	-417.254	-427.918	-309.045	-412.745	0.000031	0	0
2.5	0.208333	0	2.29	0	-238.867	0	-238.867	-245.540	-173.447	-242.587	0	0	0
3.5	0.291666	0	2.17	0	-147.869	0	-147.869	-158.348	-111.607	-157.509	0.000031	0	0
4.5	0.375	0	2.07	0	-91.1954	0	-91.1954	-109.567	-78.0070	-109.257	-0.00001	0	0
5.5	0.458333	0	1.98	0	-53.3694	0	-53.3694	-79.6984	-57.6580	-79.5574	0	0	0
0.5	0.041666	1	2.77	0	-924.722	0	-924.722	-929.455	-515.335	-798.912	-47.6751	-515.310	-26.1652
1.5	0.125	1	2.45	2	-405.005	-14.1344	-404.758	-422.969	-292.863	-410.791	-39.2781	-97.6195	-35.4526
2.5	0.208333	1	2.29	2	-238.867	-8.33631	-238.722	-240.655	-169.904	-238.323	-28.5712	-33.9804	-27.6588
3.5	0.291666	1	2.16	0	-141.456	0	-141.456	-154.649	-110.383	-153.971	-19.7240	-15.7689	-19.4593
4.5	0.375	1	2.06	0	-86.4035	0	-86.4035	-107.038	-77.4654	-106.776	-13.5051	-8.60722	-13.4153
5.5	0.458333	1	1.98	0	-53.3694	0	-53.3694	-78.0218	-57.3782	-77.8967	-9.36700	-5.21618	-9.33195
0.5	0.041666	2	2.81	0	-1010.18	0	-1010.18	-919.007	-325.648	-854.708	-115.628	-651.266	-69.3096
1.5	0.125	2	2.45	2	-405.005	-14.1344	-404.758	-403.297	-256.577	-399.893	-87.2139	-171.048	-80.7488
2.5	0.208333	2	2.26	5	-213.595	-18.5160	-212.783	-223.912	-160.712	-223.208	-58.5135	-64.2842	-57.1414
3.5	0.291666	2	2.14	7	-129.142	-15.7383	-128.179	-143.08	-107.115	-142.798	-38.6495	-30.6043	-38.2591
4.5	0.375	2	2.06	7	-86.4035	-10.5298	-85.7595	-99.4857	-76.0239	-99.3409	-25.9817	-16.8941	-25.8454
5.5	0.458333	2	1.96	5	-46.5161	-4.05412	-46.3391	-73.1162	-56.6438	-73.0312	-17.9302	-10.2988	-17.8744
0.5	0.041666	3	2.74	18	-863.861	-266.946	-821.581	-870.576	-230.070	-958.156	-258.362	-690.178	-190.386
1.5	0.125	3	2.4	18	-347.139	-107.271	-330.149	-348.105	-217.812	-356.388	-149.623	-217.808	-144.755
2.5	0.208333	3	2.24	15	-197.706	-51.1699	-190.969	-190.042	-148.275	-191.062	-87.1231	-88.9644	-85.1514
3.5	0.291666	3	2.12	14	-117.494	-28.4244	-114.004	-123.095	-102.302	-123.216	-54.5093	-43.8435	-54.2004
4.5	0.375	3	2.02	14	-68.7331	-16.6279	-66.6914	-87.3258	-73.8224	-87.3040	-36.0486	-24.6073	-35.9258
5.5	0.458333	3	1.95	15	-43.2903	-11.2043	-41.8152	-65.4387	-55.5037	-65.3983	-24.8578	-15.1373	-24.8012
0.5	0.041666	4	2.65	41	-697.213	-457.411	-526.195	-471.409	-176.304	-655.881	-537.225	-705.182	-615.967
1.5	0.125	4	2.33	31	-275.332	-141.805	-236.006	-225.724	-184.619	-235.862	-193.714	-246.155	-195.727
2.5	0.208333	4	2.18	33	-154.454	-84.1217	-129.537	-138.716	-134.890	-140.200	-103.112	-107.911	-103.067
3.5	0.291666	4	2.08	35	-96.1408	-55.1439	-78.7541	-96.6499	-96.5507	-96.9427	-63.5127	-55.1714	-63.3991
4.5	0.375	4	1.99	23	-57.0004	-22.2717	-52.4692	-72.0100	-71.0525	-72.0593	-42.2153	-31.5787	-42.1422
5.5	0.458333	4	1.92	21	-34.3949	-12.3259	-32.1104	-55.9058	-54.0288	-55.8972	-29.4462	-19.6467	-29.4028
0.5	0.041666	5	2.3	76	-247.682	-240.325	-59.9216	-69.9272	-67.0889	-75.7137	-270.860	-402.503	-285.056
1.5	0.125	5	2.21	50	-175.267	-134.261	-112.660	-102.769	-113.252	-105.736	-161.065	-226.494	-163.515
2.5	0.208333	5	2.1	35	-106.499	-61.0853	-87.2395	-86.8026	-100.691	-87.643	-97.4639	-120.825	-97.8067
3.5	0.291666	5	2.02	35	-68.7331	-39.4235	-56.3029	-69.5666	-79.9154	-69.8032	-63.6003	-68.4966	-63.6191
4.5	0.375	5	1.95	31	-43.2903	-22.2960	-37.1071	-56.0640	-62.3959	-56.1238	-43.8464	-41.5959	-43.8187

## AR=5 ZI PLANE DH=0.21

Z	Z(FT)	I	VOLT	THETA	VEL	IVEL	ZVEL	TVZ	EVZ	FVZ	TVX	EVX	FVX
0.5	0.041666	0	2.7	0	-786.901	0	-786.501	-795.555	-622.913	-667.824	0	0	0
1.5	0.125	0	2.41	0	-358.263	0	-358.263	-365.381	-263.681	-352.425	0	0	0
2.5	0.208333	0	2.24	0	-197.706	0	-197.706	-205.657	-148.059	-207.155	0	0	0
3.5	0.291666	0	2.13	0	-123.236	0	-123.236	-135.207	-95.2970	-134.490	0.000025	0	0
4.5	0.375	0	2.03	0	-72.9298	0	-72.9298	-93.5547	-66.6069	-93.2907	-0.00001	0	0
5.5	0.458333	0	1.96	0	-46.5161	0	-46.5161	-68.0512	-49.2318	-67.9308	0	0	0
0.5	0.041666	1	2.71	0	-805.700	0	-805.700	-793.625	-440.023	-682.158	-40.7078	-440.002	-22.3414
1.5	0.125	1	2.39	4	-336.237	-23.4546	-325.418	-361.156	-250.063	-350.757	-33.5380	-83.3532	-30.2715
2.5	0.208333	1	2.23	5	-190.042	-16.5632	-189.319	-205.485	-145.074	-203.494	-24.3557	-29.0145	-23.6167
3.5	0.291666	1	2.11	0	-111.916	0	-111.916	-132.048	-94.2519	-131.469	-16.8415	-13.4644	-16.6154
4.5	0.375	1	2.03	0	-72.9298	0	-72.9298	-91.3955	-66.1445	-91.1721	-11.5314	-7.34935	-11.4548
5.5	0.458333	1	1.97	0	-49.8752	0	-49.8752	-66.6196	-48.9929	-66.5128	-7.99809	-4.45388	-7.96817
0.5	0.041666	2	2.7	2	-786.901	-27.4623	-786.422	-784.702	-278.058	-729.800	-98.7306	-556.089	-59.1806
1.5	0.125	2	2.39	7	-336.237	-40.9768	-333.731	-344.358	-219.080	-341.452	-74.4684	-146.051	-68.9481
2.5	0.208333	2	2.23	8	-190.042	-26.4486	-188.192	-191.189	-137.225	-190.588	-49.3623	-54.8896	-48.7907
3.5	0.291666	2	2.1	8	-106.499	-14.8217	-105.463	-122.170	-91.4618	-121.929	-93.0012	-26.1317	-32.6676
4.5	0.375	2	2.01	6	-64.6905	-6.76091	-64.3261	-84.9467	-64.5136	-64.6231	-22.1847	-14.4251	-22.0683
5.5	0.458333	2	1.95	6	-43.2903	-4.52504	-43.0531	-62.4309	-48.3658	-62.3583	-15.3099	-8.79375	-15.2622
0.5	0.041666	3	2.69	5	-768.393	-66.9695	-765.469	-743.348	-196.447	-818.13	-220.604	-599.314	-162.563
1.5	0.125	3	2.37	15	-315.085	-81.5496	-304.249	-297.232	-165.980	-304.305	-127.757	-185.977	-123.601
2.5	0.208333	3	2.19	7	-161.214	-19.6470	-160.013	-162.269	-126.606	-163.139	-74.3908	-75.9630	-73.5611
3.5	0.291666	3	2.09	6	-101.241	-10.5825	-100.686	-105.106	-87.3517	-105.209	-46.5433	-37.4362	-46.2794
4.5	0.375	3	2	4	-60.7702	-4.23509	-60.6222	-74.5639	-63.0339	-74.5453	-30.7804	-21.0112	-30.6755
5.5	0.458333	3	1.92	2	-34.3949	-1.20035	-34.3739	-55.8754	-47.3923	-55.8409	-21.2250	-12.9251	-21.1767
0.5	0.041666	4	2.59	40	-598.724	-384.857	-458.659	-402.516	-150.538	-560.030	-458.714	-502.125	-525.949
1.5	0.125	4	2.29	25	-238.867	-104.712	-214.693	-192.736	-157.639	-201.393	-165.404	-210.182	-167.123
2.5	0.208333	4	2.14	20	-129.142	-44.1690	-121.354	-118.444	-115.177	-119.711	-88.0435	-92.1412	-88.0051
3.5	0.291666	4	2.01	16	-64.5805	-17.8292	-62.1749	-32.5253	-82.4406	-82.7753	-54.2309	-47.1086	-54.1339
4.5	0.375	4	1.94	14	-40.1560	-9.72424	-39.0020	-61.4664	-60.6688	-61.5224	-36.0459	-26.9637	-35.9835
0.5	0.041666	5	2.28	60	-230.249	-199.401	-115.125	-59.7079	-57.2844	-64.6488	-231.276	-345.681	-243.397
1.5	0.125	5	2.17	41	-147.869	-97.0107	-111.598	-87.7502	-95.7011	-50.2835	-137.526	-193.394	-139.618
2.5	0.208333	5	2.08	20	-96.1408	-32.6819	-90.2429	-74.1171	-85.9765	-74.8347	-83.2204	-103.168	-83.5131
3.5	0.291666	5	1.98	21	-53.3694	-19.1257	-49.8246	-59.4000	-68.2364	-59.6020	-54.3056	-53.4864	-54.3217
4.5	0.375	5	1.92	21	-34.3949	-12.3259	-32.1104	-47.8707	-53.2772	-47.9218	-37.4387	-35.5170	-37.4150

ALL ZY PLANE The coordinates Z and Y are given in inches.  
 MEASUREMENT DATA The voltmeter reading is given under the VOLT column.  
 The displacement angle is given under the Theta column in degrees.  
 T stands for Tyaglo's predicted values.  
 E stands for Esman's predicted values.  
 F stands for Flynn's predicted values.

AR=1 COMPOSITE OF ALL ZY VALUES

AR=1 ZY PLANE DH=0.21

Z	Z(FT)	Y	VOLT	THETA	VEL	YVEL	ZVEL	TV2	EV2	FV2	TVY	EVY	Fy
0.5	0.041666	0	2.82	0	-1032.34	0	-1032.34	-989.412	-731.261	-775.314	0	0	
1.5	0.125	0	2.57	0	-568.043	0	-568.043	-515.390	-315.635	-483.441	0	0	
2.5	0.208333	0	2.35	0	-294.789	0	-294.789	-281.146	-173.986	-275.796	0	0	
3.5	0.291666	0	2.2	0	-168.151	0	-168.151	-168.959	-109.822	-167.732	0	0	
4.5	0.375	0	2.09	0	-101.241	0	-101.241	-110.556	-75.5156	-110.173	0	0	
5.5	0.458333	0	2	0	-60.7702	0	-60.7702	-77.2576	-55.0732	-77.1015	0	0	
0.5	0.041666	1	2.83	0	-1054.81	0	-1054.81	-909.188	-505.856	-857.250	-346.211	-505.832	-177.40
1.5	0.125	1	2.55	8	-530.388	-74.9289	-533.148	-451.352	-291.358	-444.615	-158.809	-97.1180	-139.42
2.5	0.208333	1	2.33	10	-275.332	-47.8106	-271.149	-253.292	-166.503	-251.191	-72.6881	-33.3003	-69.722
3.5	0.291666	1	2.19	8	-161.214	-22.4366	-159.646	-156.824	-106.468	-156.125	-36.7414	-15.2096	-36.132
4.5	0.375	1	2.06	5	-86.4035	-7.53052	-86.0747	-104.796	-73.7140	-104.524	-20.4469	-8.19040	-20.285
5.5	0.458333	1	1.99	4	-57.0004	-3.97613	-55.8616	-74.2662	-53.9946	-74.1395	-12.3264	-4.90858	-12.273
0.5	0.041666	2	2.69	60	-768.393	-665.446	-384.200	-343.837	-284.604	-472.621	-592.054	-640.308	-662.09
1.5	0.125	2	2.44	30	-392.977	-196.483	-340.329	-275.772	-239.838	-290.436	-236.282	-179.870	-233.75
2.5	0.208333	2	2.28	25	-230.249	-97.3071	-208.677	-184.751	-151.656	-186.391	-113.545	-68.2607	-112.03
3.5	0.291666	2	2.15	20	-135.215	-46.2460	-127.060	-126.378	-100.662	-126.477	-60.9184	-32.3544	-60.406
4.5	0.375	2	2.04	18	-77.2726	-23.8784	-73.4906	-89.8195	-70.9375	-89.7518	-35.5201	-17.7337	-35.344
5.5	0.458333	2	1.97	14	-49.8752	-12.0658	-48.3937	-66.2472	-52.4816	-65.1822	-22.1440	-10.7344	-22.072
0.5	0.041666	3	2.38	80	-325.553	-320.606	-56.5340	-71.5809	-157.385	-79.5285	-302.026	-668.845	-321.18
1.5	0.125	3	2.29	52	-238.867	-188.229	-147.062	-126.762	-169.174	-132.363	-193.681	-239.655	-197.26
2.5	0.208333	3	2.19	37	-161.214	-97.0211	-128.752	-114.514	-124.488	-116.075	-113.518	-105.812	-113.67
3.5	0.291666	3	2.09	36	-101.241	-59.5080	-81.9063	-91.1906	-89.0677	-91.5372	-68.2176	-54.0755	-68.068
4.5	0.375	3	2.05	24	-81.7632	-33.2559	-74.6945	-70.9552	-65.3269	-71.0060	-42.8293	-30.8481	-42.724
5.5	0.458333	3	1.95	20	-43.2903	-14.8060	-40.6796	-55.4962	-49.4659	-55.4808	-28.0938	-19.1114	-20.038
0.5	0.041666	4	2.12	74	-117.494	-112.943	-32.3867	-25.6136	-106.562	-26.5296	-168.617	-665.977	-172.30
1.5	0.125	4	2.16	62	-141.456	-124.898	-66.4107	-59.3441	-124.453	-60.6508	-133.625	-259.270	-135.20
2.5	0.208333	4	2.1	47	-105.499	-77.8885	-72.6328	-67.1732	-100.432	-67.8538	-93.8621	-125.537	-94.231
3.5	0.291666	4	2.04	41	-77.2726	-50.6951	-58.3185	-61.988	-76.7237	-62.2352	-63.7582	-68.5020	-63.704
4.5	0.375	4	1.97	34	-49.8752	-27.8897	-41.3485	-53.1445	-58.7128	-53.2126	-43.5274	-40.7721	-43.485

AR#1 ZY PLANE OH=0.29

Z	Z(FT)	Y	VOLT	THETA	VEL	YVEL	ZVEL	TVZ	EVZ	FVZ	TVY	EVY	FVY
0.5	0.041666	0	2.91	0	-1246.45	0	-1246.45	-1155.75	-356.430	-306.012	0	0	0
1.5	0.125	0	2.64	0	-680.119	0	-680.119	-603.601	-369.658	-556.184	0	0	0
2.5	0.208333	0	2.41	0	-359.262	0	-359.262	-329.262	-203.764	-323.600	0	0	0
3.5	0.291666	0	2.25	0	-205.556	0	-205.556	-197.677	-128.619	-196.440	0	0	0
4.5	0.375	0	2.13	0	-123.236	0	-123.236	-129.479	-88.4404	-129.030	0	0	0
5.5	0.458333	0	2.03	0	-72.9298	0	-72.9298	-90.4805	-64.4992	-90.2977	0	0	0
0.5	0.041666	1	2.89	0	-1196.53	0	-1196.53	-1064.8	-592.435	-1003.97	-405.467	-592.407	-207.769
1.5	0.125	1	2.6	32	-614.474	-325.620	-521.105	-528.603	-341.236	-520.712	-185.950	-113.740	-163.253
2.5	0.208333	1	2.4	13	-347.139	-78.0890	-338.242	-296.644	-155.000	-294.184	-85.1290	-38.9998	-81.6555
3.5	0.291666	1	2.24	15	-197.706	-51.1698	-190.969	-183.665	-124.650	-182.846	-43.0298	-17.9128	-42.3172
4.5	0.375	1	2.12	12	-117.454	-24.4284	-114.927	-122.732	-86.3305	-122.413	-23.5465	-9.59222	-23.759
5.5	0.458333	1	2.02	5	-68.7331	-7.18452	-68.3565	-66.9772	-63.2360	-66.8288	-14.4361	-5.74870	-14.3740
0.5	0.041666	2	2.76	72	-904.131	-659.877	-279.397	-402.685	-393.315	-553.512	-693.386	-749.899	-775.404
1.5	0.125	2	2.5	46	-468.661	-337.125	-325.560	-322.972	-260.887	-340.145	-276.723	-210.655	-273.762
2.5	0.208333	2	2.33	34	-275.332	-153.963	-229.261	-216.371	-177.650	-218.293	-132.978	-79.9438	-131.211
3.5	0.291666	2	2.2	26	-158.151	-73.7125	-151.133	-148.008	-117.850	-148.124	-71.3448	-37.8920	-70.7458
4.5	0.375	2	2.1	19	-105.499	-34.6725	-100.657	-105.192	-83.0768	-105.113	-41.5995	-20.7689	-41.3887
5.5	0.458333	2	2.02	18	-68.7331	-21.2395	-65.2691	-77.5857	-61.4640	-77.5056	-25.9340	-12.5717	-25.8507
0.5	0.041666	3	2.43	79	-381.179	-374.176	-72.7352	-83.8323	-184.322	-93.1401	-353.719	-783.321	-376.153
1.5	0.125	3	2.35	55	-294.789	-241.476	-169.065	-148.458	-198.126	-155.018	-226.831	-280.673	-231.024
2.5	0.208333	3	2.24	36	-197.706	-116.208	-159.948	-134.114	-145.795	-135.941	-132.947	-123.922	-133.133
3.5	0.291666	3	2.14	35	-129.142	-74.0725	-105.787	-106.798	-104.312	-107.204	-79.6933	-63.3308	-79.7154
4.5	0.375	3	2.05	27	-81.7632	-37.1155	-72.8516	-83.0994	-76.5079	-83.1590	-50.1597	-36.1279	-50.0373
5.5	0.458333	3	1.98	21	-53.3694	-19.1257	-49.8245	-64.9346	-57.9321	-64.9755	-32.9022	-22.3924	-32.6352
0.5	0.041666	4	2.23	79	-190.042	-185.899	-39.5133	-29.9974	-124.801	-31.0703	-197.477	-779.961	-201.855
1.5	0.125	4	2.23	65	-190.042	-172.236	-80.3164	-69.5011	-145.753	-71.0315	-156.495	-303.645	-159.372
2.5	0.208333	4	2.15	55	-125.215	-110.761	-77.5567	-78.6702	-117.621	-79.4673	-109.527	-147.024	-110.36
3.5	0.291666	4	2.09	59	-96.1408	-73.6478	-61.7984	-72.5975	-85.8653	-72.6870	-74.6707	-80.2264	-74.6366
4.5	0.375	4	2.01	36	-64.6805	-38.0180	-52.3277	-62.2404	-68.7617	-52.3202	-50.9773	-47.7504	-50.9330
5.5	0.458333	4	1.95	32	-43.2903	-22.9402	-36.7123	-52.0170	-53.5224	-52.0242	-55.4773	-30.4099	-35.4361

AR=1 ZY PLANE DH=0.345

Z	Z(FT)	Y	VOLT	THETA	VEL	YVEL	ZVEL	TVZ	EVZ	FNVZ	TVY	EVY	FVY
0.5	0.041666	0	2.94	0	-1323.92	0	-1323.92	-1261.56	-932.402	-988.572	0	0	0
1.5	0.125	0	2.64	0	-680.119	0	-680.119	-657.154	-402.454	-616.417	0	0	0
2.5	0.208333	0	2.42	0	-369.609	0	-369.609	-358.479	-221.843	-351.657	0	0	0
3.5	0.291666	0	2.26	0	-213.595	0	-213.595	-215.433	-140.030	-213.868	0	0	0
4.5	0.375	0	2.14	0	-129.142	0	-129.142	-140.966	-95.2870	-140.478	0	0	0
5.5	0.458333	0	2.07	0	-91.1954	0	-91.1954	-98.5082	-70.2217	-98.3091	0	0	0
0.5	0.041666	1	2.94	0	-1323.92	0	-1323.92	-1159.27	-644.997	-1093.04	-441.441	-644.966	-226.212
1.5	0.125	1	2.62	18	-646.755	-199.857	-615.101	-575.502	-371.500	-566.920	-202.492	-123.831	-177.792
2.5	0.208333	1	2.4	15	-347.139	-89.8459	-335.311	-322.963	-212.301	-320.288	-92.6817	-42.4599	-88.9055
3.5	0.291666	1	2.25	11	-205.556	-39.2218	-201.780	-199.960	-135.753	-199.071	-46.8475	-19.3932	-46.0741
4.5	0.375	1	2.14	16	-129.142	-35.5962	-124.139	-133.621	-93.9898	-133.276	-26.0711	-10.4432	-25.8671
5.5	0.458333	1	2.04	15	-77.2726	-19.9995	-74.6396	-94.694	-68.8464	-94.5332	-15.7169	-6.25873	-15.6501
0.5	0.041666	2	2.93	63	-1054.81	-939.847	-478.883	-438.413	-362.887	-602.583	-754.904	-816.431	-844.233
1.5	0.125	2	2.52	41	-495.807	-325.277	-374.191	-351.626	-305.808	-370.321	-301.274	-229.345	-298.060
2.5	0.208333	2	2.35	34	-294.789	-164.843	-244.391	-235.568	-193.422	-237.660	-144.777	-87.0366	-142.856
3.5	0.291666	2	2.22	26	-182.563	-80.0301	-164.087	-161.139	-128.350	-161.266	-77.6746	-41.2538	-77.0247
4.5	0.375	2	2.11	24	-111.916	-45.5203	-102.241	-114.525	-90.4496	-114.439	-45.2903	-22.6115	-45.0622
5.5	0.458333	2	2.02	16	-68.7331	-18.9453	-66.0705	-84.4692	-66.9172	-84.3867	-28.2349	-13.6871	-28.1450
0.5	0.041666	3	2.47	83	-429.757	-426.553	-52.3774	-91.2700	-200.676	-101.392	-385.101	-852.818	-409.519
1.5	0.125	3	2.38	56	-325.553	-269.894	-182.048	-161.630	-215.707	-168.766	-246.955	-305.574	-251.522
2.5	0.208333	3	2.26	43	-213.595	-145.671	-156.214	-146.013	-158.730	-148.001	-144.743	-134.917	-144.947
3.5	0.291666	3	2.17	40	-147.869	-95.0483	-113.275	-116.273	-113.566	-116.715	-86.9916	-68.9496	-86.7894
4.5	0.375	3	2.08	44	-96.1408	-66.7847	-69.1582	-90.4721	-83.2958	-90.5369	-54.6100	-39.3332	-54.4776
5.5	0.458333	3	2	23	-60.7702	-23.7447	-55.9393	-70.7610	-63.0720	-70.7415	-35.8213	-24.3682	-35.7491
0.5	0.041666	4	2.3	80	-247.682	-243.919	-43.0114	-32.6588	-135.873	-33.8236	-214.998	-849.160	-219.761
1.5	0.125	4	2.25	64	-205.556	-184.752	-90.1111	-75.6673	-158.685	-77.3306	-170.38	-330.585	-172.422
2.5	0.208333	4	2.17	50	-147.869	-113.274	-95.0492	-85.6499	-128.057	-86.5160	-119.68	-160.068	-120.151
3.5	0.291666	4	2.1	48	-106.499	-79.1442	-71.2624	-79.0384	-97.8273	-79.3528	-81.2956	-87.3442	-81.3245
4.5	0.375	4	2.04	33	-77.2726	-42.0854	-64.8064	-67.7624	-74.8624	-67.8490	-55.5000	-51.9869	-55.4525
5.5	0.458333	4	1.98	33	-53.3694	-29.0669	-44.7594	-56.6320	-58.271	-56.6397	-38.6249	-33.108	-38.5805

AR=2 ZY PLANE DH=0.21

Z	Z(FT)	Y	VOLT	THETA	VEL	YVEL	ZVEL	TVZ	EVZ	FNZ	TVY	EVY	FVY	
0.5	0.041666	0	2.86		0 -1124.19	0 -1124.19	-940.507	-704.454	-748.264	0	0	0	0	
1.5	0.125	0	2.58		0 -583.258	0 -583.258	-477.714	-303.649	-451.173	0	0	0	0	
2.5	0.208333	0	2.35		0 -294.789	0 -294.789	-264.547	-168.189	-259.905	0	0	0	0	
3.5	0.291666	0	2.2		0 -168.151	0 -168.151	-161.794	-105.647	-160.674	0	0	0	0	
4.5	0.375	0	2.09		0 -101.241	0 -101.241	-107.192	-73.6028	-106.631	-0.00001	0	0	0	
5.5	0.458333	0	2.01		0 -64.6805	0 -64.6805	-75.5256	-53.8363	-75.3754	0	0	0	0	
0.5	0.041666	1	2.87		49 -1147.97	49 -1147.97	-866.382	-753.141	-711.652	-489.735	-787.056	-518.956	-489.676	-374.597
1.5	0.125	1	2.53		26 -509.750	26 -509.750	-223.458	-458.161	-384.734	-281.980	-384.207	-182.925	-93.9897	-166.447
2.5	0.208333	1	2.33		14 -275.332	14 -275.332	-66.6085	-267.153	-231.524	-161.785	-230.067	-78.1365	-32.3562	-75.3668
3.5	0.291666	1	2.19		16 -161.214	16 -161.214	-44.4366	-154.969	-148.491	-103.831	-147.892	-38.3594	-14.8327	-37.7651
4.5	0.375	1	2.08		6 -96.1408	6 -96.1408	-10.0494	-95.6141	-101.098	-72.1028	-100.848	-21.0317	-8.01132	-20.8709
5.5	0.458333	1	1.97		5 -49.8752	5 -49.8752	-4.34688	-49.6854	-72.4198	-52.9411	-72.2993	-12.5719	-4.81277	-12.5183
0.5	0.041666	2	2.5		64 -468.661	64 -468.661	-421.228	-205.449	-151.237	-378.010	-179.237	-428.789	-566.902	-461.638
1.5	0.125	2	2.37		42 -315.085	42 -315.085	-210.832	-234.154	-205.112	-260.777	-214.262	-221.256	-130.372	-221.057
2.5	0.208333	2	2.27		34 -221.826	34 -221.826	-124.043	-183.902	-160.499	-155.416	-161.912	-112.686	-46.6199	-111.549
3.5	0.291666	2	2.16		38 -141.456	38 -141.456	-87.0892	-111.469	-116.993	-101.131	-117.110	-61.3897	-21.6688	-60.9289
4.5	0.375	2	2.05		25 -81.7632	25 -81.7632	-34.5544	-74.1027	-85.6905	-70.7188	-85.6352	-35.9071	-11.7853	-35.7339
5.5	0.458333	2	1.99		15 -57.0004	15 -57.0004	-14.7527	-55.0582	-64.2145	-52.1430	-64.1549	-22.3764	-7.10976	-22.3060
0.5	0.041666	3	2.3		70 -247.682	70 -247.682	-232.745	-84.7140	-45.4931	-184.323	-48.3369	-233.275	-645.033	-241.283
1.5	0.125	3	2.27		61 -221.826	61 -221.826	-194.012	-107.544	-95.7426	-186.422	-98.7929	-168.737	-217.477	-170.968
2.5	0.208333	3	2.19		48 -161.214	48 -161.214	-119.805	-107.874	-97.8204	-130.964	-98.9628	-106.956	-91.6697	-107.105
3.5	0.291666	3	2.09		35 -101.241	35 -101.241	-58.0695	-82.9324	-83.1983	-91.3806	-83.4975	-66.6546	-45.6879	-66.5265
4.5	0.375	3	2.03		35 -72.9298	35 -72.9298	-41.8306	-59.7407	-67.0373	-66.1413	-67.0874	-42.5193	-25.7204	-42.4220
5.5	0.458333	3	1.98		20 -53.3694	20 -53.3694	-18.2533	-50.1508	-53.4587	-49.7181	-53.4462	-28.0820	-15.8186	-28.0266
0.5	0.041666	4	2.2		82 -168.151	82 -168.151	-166.515	-23.4034	-19.5319	-118.244	-20.0139	-142.628	-650.254	-144.733
1.5	0.125	4	2.17		70 -147.869	70 -147.869	-138.951	-50.5752	-48.1318	-134.946	-48.9394	-118.409	-247.387	-119.455
2.5	0.208333	4	2.11		60 -111.916	60 -111.916	-96.9223	-55.9588	-58.3233	-105.091	-58.8239	-87.3595	-116.695	-87.6421
3.5	0.291666	4	2.04		40 -77.2726	40 -77.2726	-49.6696	-59.1944	-56.5362	-79.4561	-56.7429	-61.3296	-62.4274	-61.3483
4.5	0.375	4	1.99		35 -57.0004	35 -57.0004	-32.6939	-46.6921	-50.0107	-60.0072	-50.0733	-42.6715	-36.6697	-42.6367
5.5	0.458333	4	1.93		26 -37.2314	26 -37.2314	-16.3211	-33.4634	-42.6144	-46.3117	-42.6214	-30.0065	-23.1551	-29.3729

AR=2 ZY PLANE DH=0.29

Z	Z(FT)	Y	VOLT	THETA	VEL	YVEL	ZVEL	TVZ	EVZ	FNZ	TVY	EVY	FVY
0.5	0.041666	0	2.95		0 -1350.44	0 -1350.44	-1101.47	-825.024	-876.333	0	0	0	0
1.5	0.125	0	2.62		0 -646.755	0 -646.755	-559.477	-355.619	-528.393	0	0	0	0
2.5	0.208333	0	2.41		0 -358.263	0 -358.263	-309.825	-196.975	-304.389	0	0	0	0
3.5	0.291666	0	2.25		0 -205.556	0 -205.556	-189.486	-124.900	-168.175	0	0	0	0
4.5	0.375	0	2.14		0 -129.142	0 -129.142	-125.539	-86.2002	-125.115	-0.00001	0	0	0
5.5	0.458333	0	2.04		0 -77.2726	0 -77.2726	-88.4522	-63.0506	-88.2762	0	0	0	0
0.5	0.041666	1	2.94	37	-1323.92 -796.753	-1057.33 -833.454	-573.555	-921.754	-607.777	-573.486	-438.711		
1.5	0.125	1	2.59	25	-598.734 -253.035	-542.638 -450.583	-330.242	-449.956	-214.233	-110.076	-194.935		
2.5	0.208333	1	2.38	20	-325.553 -111.345	-305.920 -271.150	-189.475	-269.444	-91.5099	-37.8941	-88.2662		
3.5	0.291666	1	2.23	15	-190.042 -49.1863	-183.566 -173.906	-121.602	-173.205	-44.9247	-17.3714	-44.2288		
4.5	0.375	1	2.12	10	-117.494 -20.4026	-115.709 -118.402	-84.4435	-118.109	-24.6314	-9.38249	-24.4431		
5.5	0.458333	1	2.03	4	-72.9298 -5.08730	-72.7522 -84.8147	-62.0022	-84.6737	-14.7237	-5.63650	-14.6609		
0.5	0.041666	2	2.36	80	-304.831 -300.199	-52.9356 -177.122	-442.708	-209.915	-502.178	-663.930	-540.649		
1.5	0.125	2	2.3	51	-247.682 -192.485	-155.872 -240.218	-305.41	-250.934	-259.125	-152.686	-258.892		
2.5	0.208333	2	2.21	40	-175.267 -112.659	-134.262 -187.969	-182.016	-189.524	-131.973	-54.5991	-130.642		
3.5	0.291666	2	2.12	35	-117.494 -67.3919	-96.2463 -137.017	-118.440	-137.154	-71.8968	-25.3775	-71.3571		
4.5	0.375	2	2.05	34	-81.7632 -45.7212	-67.7849 -100.356	-82.8227	-100.292	-42.0527	-13.8024	-41.8499		
5.5	0.458333	2	1.99	25	-57.0004 -24.0893	-51.6600 -75.2050	-61.0675	-75.1352	-26.2063	-8.32663	-26.1238		
0.5	0.041666	3	2.35	75	-294.789 -284.743	-76.2990 -53.2794	-215.871	-56.61	-273.201	-755.433	-282.580		
1.5	0.125	3	2.29	60	-238.867 -206.854	-119.434 -112.129	-218.329	-115.701	-197.618	-254.699	-200.230		
2.5	0.208333	3	2.21	45	-175.267 -123.932	-123.933 -114.562	-153.379	-115.900	-125.262	-107.359	-125.437		
3.5	0.291666	3	2.13	35	-123.236 -70.6849	-100.949 -97.4380	-107.020	-97.7884	-78.0628	-53.5076	-77.9128		
4.5	0.375	3	2.05	35	-81.7632 -46.8972	-66.9766 -78.5110	-77.4617	-78.5697	-49.7966	-30.1225	-49.6827		
5.5	0.458333	3	1.99	25	-57.0004 -24.0893	-51.6600 -62.6084	-58.2276	-62.5937	-32.8884	-18.5261	-32.8235		
0.5	0.041666	4	2.22	74	-182.563 -175.490	-50.3225 -22.8749	-138.482	-23.4394	-167.039	-761.548	-169.505		
1.5	0.125	4	2.19	60	-161.214 -139.615	-80.6082 -56.3697	-158.043	-57.3156	-139.675	-289.728	-139.900		
2.5	0.208333	4	2.12	49	-117.494 -88.6741	-77.0839 -68.3056	-124.249	-68.8919	-102.311	-136.667	-102.642		
3.5	0.291666	4	2.05	44	-81.7632 -56.7972	-58.8157 -66.2127	-93.0554	-66.4546	-71.8254	-73.1121	-71.8483		
4.5	0.375	4	2	32	-60.7702 -32.2031	-51.5361 -58.5703	-70.2777	-58.6435	-49.9749	-42.9459	-49.9341		
5.5	0.458333	4	1.95	32	-43.2903 -22.9402	-36.7123 -49.9080	-54.2381	-49.9162	-35.1423	-27.1181	-35.1029		

AR=2 ZY PLANE OH=0.345

Z	Z(FT)	Y	VOLT	THETA	VEL	YVEL	ZVEL	TVZ	EVZ	FNVZ	TVY	EVY	FVY
0.5	0.041666	0	2.97	0	-1404.55	0	-1404.55	-1159.20	-898.221	-554.082	0	0	0
1.5	0.125	0	2.65	0	-697.213	0	-697.213	-609.115	-387.170	-575.273	0	0	0
2.5	0.208333	0	2.43	0	-381.179	0	-381.179	-337.313	-214.451	-331.394	0	0	0
3.5	0.291666	0	2.27	0	-221.826	0	-221.826	-206.298	-135.981	-204.870	0	0	0
4.5	0.375	0	2.15	0	-135.215	0	-135.215	-136.677	-93.8480	-136.216	-0.00002	0	0
5.5	0.458333	0	2.05	0	-81.7632	0	-81.7632	-96.2998	-68.6446	-96.1082	0	0	0
0.5	0.041666	1	2.99	25	-1460.10	-617.062	-1323.30	-907.399	-624.441	-1003.54	-661.700	-624.366	-477.635
1.5	0.125	1	2.61	20	-630.480	-215.636	-592.458	-490.560	-359.542	-489.888	-233.240	-119.842	-212.230
2.5	0.208333	1	2.4	9	-347.139	-54.3043	-342.866	-295.207	-206.285	-293.350	-99.6288	-41.2561	-96.0973
3.5	0.291666	1	2.25	7	-205.556	-25.0509	-204.024	-189.335	-132.391	-188.572	-49.9105	-18.9127	-48.1528
4.5	0.375	1	2.14	7	-129.142	-15.7383	-128.179	-128.907	-91.9355	-128.587	-26.8167	-10.2149	-26.6117
5.5	0.458333	1	2.04	5	-77.2726	-6.73471	-76.9785	-92.3396	-67.5031	-92.1860	-16.0300	-6.13658	-15.9617
0.5	0.041666	2	2.61	70	-630.480	-592.456	-215.641	-192.835	-491.986	-228.539	-546.732	-722.835	-588.616
1.5	0.125	2	2.47	40	-429.757	-276.241	-329.214	-261.530	-332.506	-273.197	-282.115	-166.233	-281.861
2.5	0.208333	2	2.33	30	-275.332	-137.665	-239.445	-204.646	-198.164	-206.448	-143.682	-59.4432	-142.232
3.5	0.291666	2	2.2	25	-168.151	-71.0636	-152.397	-149.173	-128.948	-149.322	-78.2756	-27.6291	-77.6880
4.5	0.375	2	2.1	20	-106.499	-36.4248	-100.076	-109.260	-90.1708	-109.190	-45.7837	-15.0270	-45.5629
5.5	0.458333	2	2.03	12	-72.9298	-15.1628	-71.3361	-81.8773	-66.4855	-81.8014	-28.5313	-9.06538	-28.4415
0.5	0.041666	3	2.38	74	-325.553	-312.941	-89.7367	-58.0064	-235.023	-61.6325	-297.440	-822.456	-307.651
1.5	0.125	3	2.31	51	-256.697	-199.490	-161.545	-122.077	-237.700	-125.967	-215.150	-277.296	-217.994
2.5	0.208333	3	2.23	45	-190.042	-134.379	-134.380	-124.727	-166.987	-126.183	-135.376	-116.884	-136.566
3.5	0.291666	3	2.15	37	-135.215	-81.3741	-107.987	-106.082	-116.515	-106.464	-84.9886	-58.2549	-84.8253
4.5	0.375	3	2.07	31	-91.1954	-46.9689	-78.1699	-85.4766	-84.3342	-85.5405	-54.2147	-32.7950	-54.0906
5.5	0.458333	3	2	25	-60.7702	-25.6824	-55.0766	-68.1631	-63.3936	-68.1471	-35.8063	-20.7697	-35.7356
0.5	0.041666	4	2.25	80	-205.556	-202.433	-35.6960	-24.9044	-150.769	-25.5190	-181.859	-829.113	-184.544
1.5	0.125	4	2.21	67	-175.267	-161.333	-68.4833	-61.3709	-172.065	-62.4007	-150.979	-315.433	-152.312
2.5	0.208333	4	2.13	58	-123.236	-104.509	-65.3057	-74.3658	-135.272	-75.0040	-111.388	-148.793	-111.749
3.5	0.291666	4	2.1	50	-106.499	-81.5830	-68.4569	-72.0871	-101.311	-72.3506	-78.1990	-79.5987	-78.2227
4.5	0.375	4	2.01	40	-64.6805	-41.5756	-49.5483	-63.7667	-76.5128	-63.8465	-54.4087	-46.7562	-54.3643
5.5	0.458333	4	1.96	35	-46.5161	-26.6804	-38.1038	-54.336	-59.0502	-54.3449	-38.2602	-29.5241	-38.2172

AR=5 ZY PLANE DH=0.21

Z	Z(FT)	Y	VOLT	THETA	VEL	YVEL	ZVEL	TVZ	EVZ	FVZ	TVY	EVY	FVY	
0.5	0.041666	0	2.83		0 -1054.81	0 -1054.81	-795.555	-622.813	-667.824	0	0	0	0	
1.5	0.125	0	2.47		0 -429.757	0 -429.757	-365.381	-263.881	-352.425	0.000026	0	0	0	
2.5	0.208333	0	2.27		0 -221.826	0 -221.826	-209.657	-148.099	-207.135	0	0	0	0	
3.5	0.291666	0	2.15		0 -135.215	0 -135.215	-135.207	-95.2970	-134.490	0	0	0	0	
4.5	0.375	0	2.05		0 -81.7632	0 -81.7632	-93.5547	-66.6069	-93.2907	-0.00001	0	0	0	
5.5	0.458333	0	1.97		0 -49.8752	0 -49.8752	-68.0512	-49.2318	-67.9308	0	0	0	0	
0.5	0.041666	1	2.64		60 -600.119	60 -600.119	-589.998	-340.062	-363.394	-276.457	-422.005	-478.923	552.9333	-461.581
1.5	0.125	1	2.42		31 -369.609	31 -369.609	-190.361	-316.817	-272.479	-217.521	-273.385	-157.778	145.0236	-150.024
2.5	0.208333	1	2.26		25 -213.595	25 -213.595	-90.2691	-193.583	-180.061	-136.328	-180.093	-67.5782	54.5351	-65.9596
3.5	0.291666	1	2.12		11 -117.494	11 -117.494	-22.4189	-115.336	-123.781	-90.9316	-123.388	-33.9778	25.98239	-33.5747
4.5	0.375	1	2.04		10 -77.2726	10 -77.2726	-13.4181	-76.0986	-88.2307	-64.5805	-88.0444	-19.0971	14.35233	-18.9749
5.5	0.458333	1	1.96		10 -46.5161	10 -46.5161	-8.07739	-45.8094	-65.2766	-48.1449	-65.1790	-11.6495	8.754289	-11.6053
0.5	0.041666	2	2.38		66 -325.553	66 -325.553	-297.406	-132.416	-79.6544	-613.707	-85.5968	-281.784	0.099423	-289.748
1.5	0.125	2	2.29		46 -238.867	46 -238.867	-171.826	-165.932	-139.201	-259.126	-142.606	-171.099	0.013993	-170.838
2.5	0.208333	2	2.19		35 -161.214	35 -161.214	-92.4686	-132.059	-124.162	-145.662	-124.833	-94.3889	0.004719	-93.6821
3.5	0.291666	2	2.1		27 -106.499	27 -106.499	-48.3495	-94.8919	-97.5170	-93.9149	-97.5650	-53.6801	0.002173	-53.5539
4.5	0.375	2	2.02		20 -68.7331	20 -68.7331	-23.5079	-64.5880	-74.9156	-65.7565	-74.8664	-32.5233	0.001183	-32.3881

AR=5 ZY PLANE DH=0.29

Z	Z(FT)	Y	VOLT	THETA	VEL	YVEL	ZVEL	TVZ	EVZ	FVZ	TVY	EVY	FVY	
0.5	0.041666	0	2.69		0 -1196.53	0 -1196.53	-931.717	-729.411	-782.125	0	0	0	0	
1.5	0.125	0	2.53		0 -509.750	0 -509.750	-427.918	-309.045	-412.745	0.000031	0	0	0	
2.5	0.208333	0	2.33		0 -275.332	0 -275.332	-245.540	-173.447	-242.587	0	0	0	0	
3.5	0.291666	0	2.2		0 -168.151	0 -168.151	-158.348	-111.607	-157.509	0	0	0	0	
4.5	0.375	0	2.09		0 -101.241	0 -101.241	-109.567	-78.0070	-109.257	-0.00001	0	0	0	
5.5	0.458333	0	2.01		0 -64.6805	0 -64.6805	-79.6984	-57.6580	-79.5574	0	0	0	0	
0.5	0.041666	1	2.74	55	-863.861 -707.630 -455.493	-425.591	-323.774	-494.233	-560.893	647.57	-540.583			
1.5	0.125	1	2.46	30	-417.264 -208.631 -361.362	-319.115	-254.750	-320.176	-184.782	169.845	-175.702			
2.5	0.208333	1	2.28	23	-230.249 -89.9651 -211.945	-211.816	-159.661	-210.917	-79.1445	63.86901	-77.2489			
3.5	0.291666	1	2.17	19	-147.869 -48.1413 -139.813	-144.967	-106.494	-144.507	-39.7933	30.42938	-39.3211			
4.5	0.375	1	2.07	14	-91.1954 -22.0620 -68.4866	-103.331	-75.6338	-103.113	-22.3556	16.80879	-22.2225			
5.5	0.458333	1	1.99	9	-57.0004 -8.91679	-56.2997	-76.4490	-56.3851	-76.3347	-13.6433	10.25262	-13.5916		
0.5	0.041666	2	2.44	70	-392.977 -369.277 -134.408	-93.2876	-718.745	-100.247	-330.013	0.116439	-339.339			
1.5	0.125	2	2.36	48	-304.831 -226.532 -203.972	-163.026	-303.477	-167.013	-200.383	0.016388	-200.078			
2.5	0.208333	2	2.22	41	-182.563 -119.771 -137.782	-145.413	-170.593	-146.198	-110.544	0.005527	-109.716			
3.5	0.291666	2	2.13	21	-123.236 -44.1636 -115.050	-114.207	-109.988	-114.263	-63.1019	0.002545	-62.7199			
4.5	0.375	2	2.06	21	-86.4035 -30.9541 -80.6547	-87.7377	-77.0109	-87.6801	-38.0899	0.001386	-37.9315			
5.5	0.458333	2	1.97	10	-49.8752 -8.66069	-49.1175	-67.9021	-57.0058	-67.8428	-24.2716	0.000839	-24.2024		
0.5	0.041666	3	2.24	73	-197.706 -189.066	-57.8049	-35.3742	-319.182	-36.4633	-200.198	-638.282	-203.187		
1.5	0.125	3	2.23	55	-190.042 -155.673	-109.004	-81.2919	-250.39	-82.7495	-154.958	-166.910	-155.902		
2.5	0.208333	3	2.16	41	-141.456 -92.8037	-106.759	-90.6619	-157.213	-91.3371	-104.938	-62.8796	-104.943		
3.5	0.291666	3	2.09	37	-101.241 -60.9284	-80.8553	-82.1180	-105.081	-82.3206	-68.5383	-30.0205	-68.4069		
4.5	0.375	3	2	25	-60.7702 -25.6824	-55.0766	-69.0801	-74.7638	-69.1132	-45.1468	-16.6127	-45.0513		
5.5	0.458333	3	1.94	24	-40.1960 -16.3491	-36.7209	-55.7557	-55.8188	-56.7402	-30.4914	-10.1480	-30.4351		

AR=5 ZY PLANE DH=0.345

Z	Z(FT)	Y	VOLT	THETA	VEL	YVEL	ZVEL	TVZ	EVZ	FNZ	TVY	EVY	FVY
0.5	0.041666	0	2.95	0	-1350.44	0	-1350.44	-1014.38	-794.125	-651.516	0	0	0
1.5	0.125	0	2.56	0	-553.087	0	-553.087	-465.883	-336.464	-449.364	0.000033	0	0
2.5	0.208333	0	2.35	0	-294.789	0	-294.789	-267.325	-188.935	-264.110	0	0	0
3.5	0.291666	0	2.23	0	-190.042	0	-190.042	-172.397	-121.509	-171.484	0	0	0
4.5	0.375	0	2.1	0	-106.499	0	-106.499	-119.287	-84.9279	-118.951	-0.00002	0	0
5.5	0.458333	0	2.02	0	-68.7331	0	-68.7331	-85.7694	-62.7735	-86.6159	0	0	0
0.5	0.041666	1	2.75	57	-883.844	-741.252	-481.390	-463.350	-352.5	-538.082	-610.657	705.0233	-588.544
1.5	0.125	1	2.48	28	-442.486	-207.733	-390.692	-347.427	-277.352	-348.582	-201.176	184.9138	-191.290
2.5	0.208333	1	2.31	15	-256.697	-66.4378	-247.950	-230.609	-173.826	-229.630	-86.1663	69.53555	-84.1025
3.5	0.291666	1	2.19	13	-161.214	-36.2652	-157.083	-157.828	-115.943	-157.328	-43.3238	33.12911	-42.8097
4.5	0.375	1	2.1	14	-106.499	-25.7644	-103.336	-112.499	-82.3441	-112.262	-24.3499	18.30009	-24.1942
5.5	0.458333	1	2.01	10	-64.6805	-11.2315	-63.6978	-83.2316	-61.3876	-83.1072	-14.8538	11.16225	-14.7975
0.5	0.041666	2	2.43	70	-381.179	-358.191	-130.373	-101.564	-782.514	-109.141	-359.292	0.126770	-369.446
1.5	0.125	2	2.36	41	-304.831	-199.986	-230.059	-177.490	-330.402	-181.831	-218.162	0.017842	-217.829
2.5	0.208333	2	2.25	35	-205.556	-117.901	-168.382	-158.314	-185.728	-159.169	-120.351	0.006017	-119.450
3.5	0.291666	2	2.15	27	-135.215	-61.3861	-120.477	-124.340	-119.747	-124.401	-68.7004	0.002771	-68.2845
4.5	0.375	2	2.07	21	-91.1954	-32.6813	-85.1383	-95.5220	-83.8435	-95.4592	-41.4692	0.001509	-41.2968
5.5	0.458333	2	2	13	-60.7702	-13.6702	-59.2127	-73.9264	-62.0634	-73.862	-26.4250	0.000914	-26.3497
0.5	0.041666	3	2.28	76	-230.249	-223.409	-55.7039	-38.5127	-347.500	-39.6984	-217.959	-694.911	-221.214
1.5	0.125	3	2.25	53	-205.556	-164.164	-123.707	-88.5042	-272.604	-90.0912	-168.706	-181.719	-169.734
2.5	0.208333	3	2.17	46	-147.869	-106.368	-102.719	-98.7055	-171.161	-99.4406	-114.249	-68.4584	-114.254
3.5	0.291666	3	2.1	31	-106.499	-54.8510	-91.2880	-89.4035	-114.404	-89.6242	-74.6191	-32.684	-74.4761
4.5	0.375	3	2.02	26	-68.7331	-30.1304	-61.7769	-75.2090	-81.3970	-75.2450	-49.1523	-18.0866	-49.0484
5.5	0.458333	3	1.97	21	-49.8752	-17.8735	-46.5625	-61.7912	-60.7711	-61.7742	-33.1966	-11.0483	-33.1354

**APPENDIX D**

```

1 REM FOR A GIVEN FLOWRATE (Q), LENGTH (L) AND WIDTH (W), THIS COMPUTER PROGRAM
  WILL GENERATE A GRID OF X, Y AND Z VELOCITY COMPONENT VALUES THAT FLOW
  INTO A FLANGED RECTANGULAR EXHAUST HOOD.
2 REM THIS MATHEMATICAL MODEL WAS DEVELOPED BY TYAGLO AND SHEPELEV.
  CLS
  OPEN "TYAGLO.PRN" FOR OUTPUT AS #1
  1 INPUT "WHAT IS THE SLOT LENGTH IN FT";L
40 INPUT "WHAT IS THE SLOT WIDTH IN FT";W
50 INPUT "WHAT IS THE FLOW IN CFM";Q
60 PI=3.1415927#
70 A=L/2
80 B=W/2
90 XINC = .0833
100 YINC = .0833
110 ZINC = .0833
120 DIM X(5,5,5)
130 DIM Y(5,5,5)
140 DIM Z(5,5,5)
150 DIM VX(5,5,5)
160 DIM VY(5,5,5)
170 DIM VZ(5,5,5)
180 COUNT = 0
190 CLS
200 PRINT "COMPUTING. PLEASE WAIT"
210 FOR I=0 TO 5
220 FOR J=0 TO 5
230 FOR K=0 TO 5
240 E=I-1
250 F=J-1
260 G=K-1
270 IF I=0 THEN X(I,J,K) = 0 ELSE X(I,J,K) = X(E,J,K) + XINC
280 IF J=0 THEN Y(I,J,K) = 0 ELSE Y(I,J,K) = Y(I,F,K) + YINC
290 IF K=0 THEN Z(I,J,K) = .041667 ELSE Z(I,J,G) = Z(I,J,G) + ZINC
300 P1 = (X(I,J,K) + A)
310 P2 = (X(I,J,K) - A)
320 P3 = (Y(I,J,K) + A)
330 P4 = (Y(I,J,K) - A)
340 P5 = (X(I,J,K) + B)
350 P6 = (X(I,J,K) - B)
360 P7 = (Y(I,J,K) + B)
370 P8 = (Y(I,J,K) - B)
380 N5 = SQR ((Z(I,J,K)^2 + P7^2 + P2^2))
390 N6 = SQR ((Z(I,J,K)^2 + P1^2 + P7^2))
400 N7 = SQR ((Z(I,J,K)^2 + P8^2 + P1^2))
410 N8 = SQR ((Z(I,J,K)^2 + P8^2 + P2^2))
420 N1 = Z(I,J,K) * N6
430 N2 = Z(I,J,K) * N7
440 N3 = Z(I,J,K) * N5
450 N4 = Z(I,J,K) * N8
460 T1 = ATN ((P7 * P1) / N1)
470 T2 = ATN ((P8 * P1) / N2)
480 T3 = ATN ((P7 * P2) / N3)
490 T4 = ATN ((P8 * P2) / N4)
500 COEF = -Q/ ( 8* PI * A * B)
510 VX(I,J,K) = COEF * ( LOG (((N5 + P7)/ (N6 + P7)) * ((N7 + P8)/ (N8 + P8))))
520 VY(I,J,K) = COEF * (LOG (((N7 + P1)/ (N6 + P1)) * ((N5 + P2)/ (N8 + P2))))
530 VZ(I,J,K) = COEF * ( T1 - T2 - T3 + T4)
540 WRITE #1, Q, L, W, X(I,J,K), Y(I,J,K), Z(I,J,K), VX(I,J,K), VY(I,J,K), VZ(I,J,K)
550 NEXT K,J,I
560 CLOSE #1
570 CLS
580 PRINT "PROGRAM COMPLETED"
590 END

```

1 REM FOR A GIVEN FLOWRATE (Q), HOOD LENGTH (L) AND HOOD WIDTH (W), THIS  
COMPUTER PROGRAM WILL GENERATE A GRID OF X, Y AND Z VELOCITY COMPONENT  
VALUES THAT FLOW INTO A FLANGED RECTANGULAR HOOD.

REM THIS MATHEMATICAL MODEL WAS DEVELOPED BY FLYNN AND ELLENBECKER.

10 CLS

15 OPEN "FLYNNI.PRN" FOR OUTPUT AS #1

20 INPUT "WHAT IS THE SLOT LENGTH IN FT";L

30 INPUT "WHAT IS THE SLOT WIDTH IN FT";W

40 INPUT "WHAT IS THE FLOW IN CFM";Q

50 PI=3.1415927#

60 A=L/2

70 B=W/2

80 XINC = .08333

90 YINC = .08333

100 ZINC = .08333

110 DIM X(5,5,5)

120 DIM Y(5,5,5)

130 DIM Z(5,5,5)

140 DIM VX(5,5,5)

150 DIM VY(5,5,5)

160 DIM VZ(5,5,5)

170 DIM COUNT = 0

180 COUNT = 0

190 CLS

200 PRINT "COMPUTING. PLEASE WAIT"

210 FOR I=0 TO 5

220 FOR J=0 TO 5

230 FOR K=0 TO 5

240 T=I-1

250 F=J-1

260 G=K-1

270 IF I=0 THEN X(I,J,K) = 0 ELSE X(I,J,K) = X(T,J,K) + XINC

280 IF J=0 THEN Y(I,J,K) = 0 ELSE Y(I,J,K) = Y(I,F,K) + YINC

290 IF K=0 THEN Z(I,J,K) = .041667 ELSE Z(I,J,G) = Z(I,J,G) + ZINC

300 QA = (A^2 \* B^2)

310 QB = (A^2 + B^2)

320 QC = (X(I,J,K)^2 \* B^2)

330 QD = (Y(I,J,K)^2 \* A^2)

340 Q1 = QA - QC - QD - (Z(I,J,K)^2 \* QB)

350 Q2 = QB - (X(I,J,K)^2) - (Y(I,J,K)^2) - (Z(I,J,K)^2)

360 AF = (1/3) \* ((3\*Q1)-(Q2^2))

370 R1 = -(Z(I,J,K)^2 \* A^2 \* B^2)

380 BF = ((1/27) \* (2\*Q2^3 - 9\*Q1\*Q2 + 27\*R1))

390 MM = 2\*SQR(-AF/3)

400 PRELM = (3\*BF) / (AF\*MM)

405 IF PRELM =>1 THEN LA = 0

410 LA = ((PI/2) - (ATN(PRELM/(SQR(1-PRELM^2))))) /3

420 LACOS = COS(LA)

430 LAMBDA = (2\*SQR(-AF/3) \* LACOS) - (Q2/3)

440 IF LAMBDA < 0 THEN LAMBDA = (2\*SQR(-AF/3)\*COS(LA + 2\*PI/3)) - (Q2/3)

450 E1 = (A^2 + LAMBDA)

460 E2 = (B^2 + LAMBDA)

470 E3 = (((X(I,J,K) \* LAMBDA)^2) \* (E2^2))

480 E4 = (((Y(I,J,K) \* LAMBDA)^2) \* (E1^2))

490 E5 = (Z(I,J,K)^2) \* (E1^2) \* (E2^2)

500 E = E3 + E4 + E5

510 COEF = -Q/(2 \* PI \* E)

520 VX(I,J,K) = (COEF \* X(I,J,K)) \* (E1^.5) \* (E2^1.5) \* LAMBDA^1.5

530 VY(I,J,K) = (COEF \* Y(I,J,K)) \* (E2^.5) \* (E1^1.5) \* LAMBDA^1.5

540 VZ(I,J,K) = (COEF \* Z(I,J,K)) \* (LAMBDA^.5) \* (E1^1.5) \* (E2^1.5)

550 WRITE #1, Q, L, W, X(I,J,K), Y(I,J,K), Z(I,J,K), VX(I,J,K), VY(I,J,K), VZ(I,J,K)

560 NEXT K,J,I

570 CLOSE #1

```

1 REM FOR A GIVEN FLOWRATE (Q), LENGTH (L), AND WIDTH (W), THIS COMPUTER PROGRAM
  WILL GENERATE A GRID OF X, Y AND Z VELOCITY COMPONENT VALUES THAT FLOW
  INTO A FLANGED RECTANGULAR HOOD.
2 REM THIS MATHEMATICAL MODEL WAS DEVELOPED BY ESMEN, WEYEL AND MCGUIGAN.
10 CLS
    OPEN "ESMEN.PRN" FOR OUTPUT AS #1
    INPUT "WHAT IS THE SLOT LENGTH IN FT"; L
40 INPUT "WHAT IS THE SLOT WIDTH IN FT"; W
50 INPUT "WHAT IS THE FLOW IN CFM"; Q
60 PI=3.1415927#
70 A=L/2
80 B=W/2
90 XINC = .08333
100 YINC = .08333
110 ZINC = .08333
120 DIM X(5,5,5)
130 DIM Y(5,5,5)
140 DIM Z(5,5,5)
150 DIM VX(5,5,5)
160 DIM VY(5,5,5)
170 DIM VZ(5,5,5)
180 COUNT = 0
190 CLS
200 PRINT "COMPUTING. PLEASE WAIT"
210 FOR I=0 TO 5
220 FOR J=0 TO 5
230 FOR K=0 TO 5
240 E=I-1
250 F=J-1
260 G=K-1
270 IF I=0 THEN X(I,J,K) = 0 ELSE X(I,J,K) = X(E,J,K) + XINC
280 IF J=0 THEN Y(I,J,K) = 0 ELSE Y(I,J,K) = Y(I,F,K) + YINC
290 IF K=0 THEN Z(I,J,K) = .0260416 ELSE Z(I,J,K) = Z(I,J,G) + ZINC
300 IF X(I,J,K) > A THEN KX=1 ELSE KX=0
310 IF Y(I,J,K) > B OR Y(I,J,K) = B THEN KY=1 ELSE KY=0
320 KK=16*(Z(I,J,K)^2)
330 H=(2*X(I,J,K)*(KX+1)) - (2*A*KX)
340 S=(2*Y(I,J,K) * (KY+1)) - (2*A*KY)
350 D=SQR(KK+H^2 + S^2)
360 R = SQR ((Z(I,J,K)^2) +(KX * ((X(I,J,K)-A)^2))+(KY * ((Y(I,J,K)-B)^2)))
370 ND = SQR (1+((Z(I,J,K) * X(I,J,K))+ (Y(I,J,K) * Z(I,J,K))/ (A^2 + B^2)))
380 FR = (.375 * PI * ((R/A) + (R/B))) + (PI * (R^2))/(2*A*B) + ND
390 BETA = ((2* X(I,J,K)) * (KX+1) - (2*A*KX)) / D
400 GAMMA = (2*Y(I,J,K)* (KY+1) - (2*A*KY)) / D
410 ALPHA = (4*Z(I,J,K))/D
420 VX(I,J,K)=- (Q*BETA) / (4*A*B*FR)
430 VY(I,J,K) =-(Q*GAMMA)/(4*A*B*FR)
440 VZ(I,J,K) =-(Q*ALPHA) / (4*A*B*FR)
450 WRITE #1, Q, L, W, X(I,J,K), Y(I,J,K), Z(I,J,K), VX(I,J,K), VY(I,J,K), VZ(I,J,K)
460 NEXT K,J,I
470 CLOSE #1
480 PRINT "PROGRAM COMPLETED"
490 END

```

**APPENDIX B**

## PERFORMANCE INDEX RESULTS

AR=1

	XZ PLANE Z VEL	X VEL	YZ PLANE Z VEL	Y VEL		
MODEL A						
P I	236.99	684.8391	4908.599	1359.985	1513.327	6660.024
Bias	-6.777	7.064407	-33.0004	-11.9203	9.65328	-9.61184
N	89	89	89	89	89	89
MODEL B						
P I	3137.769	3178.9	2039.213	5161.242	6452.229	2144.816
Bias	3.729177	12.92197	-29.1875	19.4244	15.51128	-5.79898
N	89	89	89	89	89	89
MODEL C						
P I	10371.87	17691.37	9740.46	34992.37	24633.58	30519.1
Bias	48.3171	67.5388	-29.5364	26.07652	59.79361	-45.6116
N	89	89	89	89	89	89

AR=2

	XZ PLANE Z VEL	X VEL	YZ PLANE Z VEL	Y VEL		
MODEL A						
P I	614.3149	1182.572	2361.232	6149.571	5263.231	2445.124
Bias	-0.00696	12.05851	-26.6493	21.8178	22.68456	1.564276
N	89	89	89	90	90	90 -
MODEL B						
P I	4562.798	4947.738	1475.888	11685.7	9215.16	5220.799
Bias	7.027916	17.46035	-21.2091	28.74939	26.68989	6.163674
N	89	89	89	90	90	90
MODEL C						
P I	13841.63	32057.19	15293.4	47681.01	27397.87	24002.05
Bias	56.99319	92.27943	-271.857	11.49662	35.46966	-26.8905
N	89	89	89	90	90	90

AR=5

	XZ PLANE Z VEL	X VEL	YZ PLANE Z VEL	Y VEL
MODEL A				
P I	495.5392 551.9623	1615.572	4712.006	4909.917 899.2789
Bias	-15.8391 -4.55691	-29.586	20.88961	23.23786 2.040203
N	105	105	105	72 72 72
MODEL B				
P I	3213.87 2578.236	1683.957	9010.236	10200.33 1167.867
Bias	-13.0044 -2.29307	-27.9545	26.14159	27.02797 2.954377
N	105	105	105	72 72 72
MODEL C				
P I	7119.162 34957.94	29957.78	29024.2	37217.78 108165.5
Bias	26.64213 86.29879	-85.9018	7.33447	0.544292 102.8959
N	105	105	105	72 72 72

## PAIRED T-TEST RESULTS

AR=1

	XZ VEL	Z VEL	X VEL	YZ VEL	Z VEL	Y VEL
<b>A vs. C</b>						
Mean Diff	-10134.8	-17006.5	-4831.86	-33632.3	-23120.2	-23859.0
SD Diff	23257.25	50945.16	31647.48	74533.86	69017.51	73765.29
T Value	4.111	3.149	1.44	4.257	3.16	3.051
df	88	88	88	88	88	88
Prob	0	0.002	0.153	0	0.002	0.003
 <b>A vs. B</b>						
Mean Diff	-2900.77	-2494.06	2869.386	-3801.25	-4938.89	4515.205
SD Diff	11118.59	11300.21	17615.10	18445.07	18604.31	21972.24
T Value	2.461	2.082	1.537	1.944	2.504	1.939
df	88	88	88	88	88	88
Prob	0.016	0.04	0.128	0.055	0.014	0.056
 <b>C vs. B</b>						
Mean Diff	7234.107	14512.47	7701.246	29831.12	18181.35	28374.27
SD Diff	17205.80	47323.36	48951.15	70709.88	62815.74	84845.66
T Value	3.966	2.893	1.484	3.98	2.731	3.155
df	88	88	88	88	88	88
Prob	0	0.005	0.141	0	0.008	0.002

AR=2

	XZ VEL	Z VEL	X VEL	YZ VEL	Z VEL	Y VEL
<b>A vs. C</b>						
Mean Diff	-13227.3	-30874.6	-12932.1	-41531.4	-22134.6	-21556.9
SD Diff	28304.54	86122.39	56988.79	84854.58	53654.15	70440.79
T Value	4.409	3.382	2.141	4.643	3.914	2.903
df	88	88	88	89	89	89
Prob	0	0.001	0.035	0	0	0.005
<b>A vs. B</b>						
Mean Diff	-3948.48	-3765.16	885.343	-5536.13	-3951.92	-2775.67
SD Diff	15406.67	15705.52	6626.302	26395.70	27793.99	16125.70
T Value	2.418	2.262	1.26	1.99	1.349	1.633
df	88	88	88	89	89	89
Prob	0.018	0.026	0.211	0.05	0.181	0.106
<b>C vs. B</b>						
Mean Diff	9278.838	27109.45	13817.51	35995.30	18182.70	18781.25
SD Diff	17506.47	80169.75	62213.01	79032.05	49975.05	72274.18
T Value	5	3.19	2.095	4.321	3.452	2.465
df	88	88	88	89	89	89
Prob	0	0.002	0.039	0	0.001	0.016

AR=5

	XZ VEL	Z VEL	X VEL	YZ VEL	Z VEL	Y VEL
<b>A vs. C</b>						
Mean Diff	-6623.62	-34405.9	-28342.2	-24312.1	-27358.1	-93704.6
SD Diff	14567.36	99657.44	83650.90	61777.74	74036.81	353021.8
T Value	4.659	3.538	3.472	3.339	3.135	2.252
df	104	104	104	71	71	71
Prob	0	0.001	0.001	0.001	0.002	0.027
<b>A vs. B</b>						
Mean Diff	-2718.33	-2026.27	-68.385	-4298.23	-4575.43	-241.148
SD Diff	8151.848	6303.772	3487.812	22025.12	21952.84	1149.174
T Value	3.417	3.294	0.201	1.656	1.769	1.781
df	104	104	104	71	71	71
Prob	0.001	0.001	0.841	0.102	0.081	0.079
<b>C vs. B</b>						
Mean Diff	3905.291	32379.70	28273.82	20013.96	22782.72	93463.45
SD Diff	12303.70	97049.82	84979.28	55260.61	69071.42	351890.9
T Value	3.252	3.419	3.409	3.073	2.799	2.254
df	104	104	104	71	71	71
Prob	0.002	0.001	0.001	0.003	0.007	0.027

**APPENDIX F**

TABLE OF LEAST-SQUARES  
FOR ALL ASPECT RATIOS

Z VELOCITY COMPONENT

MODEL A  $Y = 1.099525 X + 12.14823$   $R^2 = 0.983230$   
STD ERR OF Y EST = 36.97721  
STD ERR OF X COEF = 0.006225  
N = 534 df = 532

MODEL B  $Y = 1.179742 X + 25.11261$   $R^2 = 0.955055$   
STD ERR OF Y EST = 60.53566  
STD ERR OF X COEF = 0.011095  
N = 534 df = 532

MODEL C  $Y = 1.525846 X + 34.17274$   $R^2 = 0.790961$   
STD ERR OF Y EST = 130.5529  
STD ERR OF X COEF = 0.034  
N = 534 df = 532

Y VELOCITY COMPONENT

MODEL A  $Y = 1.067826 X + 9.107664$   $R^2 = 0.867913$   
STD ERR OF Y EST = 58.42394  
STD ERR OF X COEF = 0.026399  
N = 251 df = 249

MODEL B  $Y = 1.114082 X + 10.43671$   $R^2 = 0.894663$   
STD ERR OF Y EST = 52.1736  
STD ERR OF X COEF = 0.024225  
N = 251 df = 249

MODEL C  $Y = 0.302478 X + -73.8379$   $R^2 = 0.1889$   
STD ERR OF Y EST = 144.777  
STD ERR OF X COEF = 0.3025  
N = 251 df = 249

X VELOCITY COMPONENT

MODEL A  $Y = 0.883932 X + 18.42701$   $R^2 = 0.880307$   
STD ERR OF Y EST = 42.29473  
STD ERR OF X COEF = 0.019443  
N = 283 df = 281

MODEL B  $Y = 0.893246 X + 16.19453$   $R^2 = 0.943207$   
STD ERR OF Y EST = 29.13392  
STD ERR OF X COEF = 0.013075  
N = 283 df = 281

MODEL C  $Y = 0.4854 X + -7.85577$   $R^2 = 0.575612$   
STD ERR OF Y EST = 79.6404  
STD ERR OF X COEF = 0.485404  
N = 283 df = 281

YZ VELOCITY PLANE

MODEL A  $Y = 1.1838 X + 27.9095$   $R^2 = 0.984$   
STD ERR OF Y EST = 38.172  
STD ERR OF X COEF = 0.009374  
N = 259 df = 257

MODEL B  $Y = 1.2776 X + 42.8472$   $R^2 = 0.9601$   
STD ERR OF Y EST = 60.5119  
STD ERR OF X COEF = 0.0162  
N = 283 df = 281

MODEL C  $Y = 0.93895 X + -30.2245$   $R^2 = 0.6028$   
STD ERR OF Y EST = 191.0136  
STD ERR OF X COEF = 0.04754  
N = 283 df = 281

XZ VELOCITY PLANE

MODEL A  $Y = 1.0453 X + 20.9842$   $R^2 = 0.9974$   
STD ERR OF Y EST = 15.047  
STD ERR OF X COEF = 0.00318  
N = 283 df = 281

MODEL B  $Y = 1.09266 X + 28.3931$   $R^2 = 0.965341$   
STD ERR OF Y EST = 55.02442  
STD ERR OF X COEF = 0.01235  
N = 283 df = 281

MODEL C  $Y = 1.2781 X + 22.4373$   $R^2 = 0.94792$   
STD ERR OF Y EST = 67.417  
STD ERR OF X COEF = 0.01786  
N = 283 df = 281

TABLE OF LEAST SQUARES FOR EACH MODEL  
 TOTAL VELOCITIES OVER ALL PLANES AND ASPECT RATIOS

MODEL A

DEP VAR: MEAS N: 534 MULTIPLE R: .992 SQUARED MULTIPLE R: .985  
 ADJUSTED SQUARED MULTIPLE R: .985 STANDARD ERROR OF ESTIMATE: 37.155

VARIABLE	COEFFICIENT	STD ERROR	STD COEF TOLERANCE	T	P(2 TAIL)
CONSTANT	23.314	2.285	0.000 1.0000000	10.203	0.000
PRED	1.101	0.006	0.992 1.0000000	184.216	0.000

ANALYSIS OF VARIANCE

SOURCE	SUM-OF-SQUARES	DF	MEAN-SQUARE	F-RATIO	P
REGRESSION	.468476E+08	1	.468476E+08	33935.546	0.000
RESIDUAL	734419.330	532	1380.487		

$$Y = 1.101 X + 23.314 \quad R^2 = 0.985$$

MODEL B

DEP VAR: MEAS N: 534 MULTIPLE R: .977 SQUARED MULTIPLE R: .954  
 ADJUSTED SQUARED MULTIPLE R: .953 STANDARD ERROR OF ESTIMATE: 64.449

VARIABLE	COEFFICIENT	STD ERROR	STD COEF TOLERANCE	T	P(2 TAIL)
CONSTANT	33.603	4.067	0.000 1.0000000	8.263	0.000
PRED	1.166	0.011	0.977 1.0000000	104.515	0.000

ANALYSIS OF VARIANCE

SOURCE	SUM-OF-SQUARES	DF	MEAN-SQUARE	F-RATIO	P
REGRESSION	.453722E+08	1	.453722E+08	10923.326	0.000
RESIDUAL	2209769.569	532	4153.702		

$$Y = 1.166 X + 33.603 \quad R^2 = 0.954$$

## MODEL C

DEP VAR: MEAS N: 534 MULTIPLE R: .869 SQUARED MULTIPLE R: .755  
 ADJUSTED SQUARED MULTIPLE R: .755 STANDARD ERROR OF ESTIMATE: 147.925

VARIABLE	COEFFICIENT	STD ERROR	STD COEF TOLERANCE	T	P(2 TAIL)
CONSTANT	-6.556	9.225	0.000 1.0000000	-0.711	0.478
PRED	1.096	0.027	0.869 1.0000000	40.528	0.000

## ANALYSIS OF VARIANCE

SOURCE	SUM-OF-SQUARES	DF	MEAN-SQUARE	F-RATIO	P
REGRESSION	.359410E+08	1	.359410E+08	1642.514	0.000
RESIDUAL	.116411E+08	532	21881.678		

$$Y = 1.096 X - 6.556 \quad R^2 = 0.755$$

**APPENDIX G**

## ANOVA TEST - MEASURED VELOCITY

DEP VAR: HP N: 534 MULTIPLE R: .066 SQUARED MULTIPLE R: .00

## ANALYSIS OF VARIANCE

SOURCE	SUM-OF-SQUARES	DF	MEAN-SQUARE	F-RATIO	P
PLANES	9430.300	1	9430.300	0.105	0.746
HOODS	152602.926	2	76301.463	0.850	0.428
PLANES* HOODS	52815.908	2	26407.954	0.294	0.745
ERROR	.473763E+08	528	89727.752		-

## ANOVA TEST - MODEL A

DEP VAR: VEL. N: 534 MULTIPLE R: .092 SQUARED MULTIPLE R: .00

## ANALYSIS OF VARIANCE

SOURCE	SUM-OF-SQUARES	DF	MEAN-SQUARE	F-RATIO	P
PLANE	154331.839	1	154331.839	2.128	0.145:
AR	126318.577	2	63159.288	0.871	0.419
PLANE*					
AR	77671.796	2	38835.898	0.536	0.586
ERROR	.382893E+08	528	72517.566		

## ANOVA TEST - MODEL B

DEP VAR: VEL N: 534 MULTIPLE R: .097 SQUARED MULTIPLE R: .00

## ANALYSIS OF VARIANCE

SOURCE	SUM-OF-SQUARES	DF	MEAN-SQUARE	F-RATIO	P
PLANE	161372.173	1	161372.173	2.575	0.109
AR	102950.289	2	51475.145	0.822	0.440
PLANE*					
AR	81499.168	2	40749.584	0.650	0.522
ERROR	.330830E+08	528	62657.108		

## ANOVA TEST - MODEL C

DEP VAR: VEL N: 534 MULTIPLE R: .065 SQUARED MULTIPLE R: .00

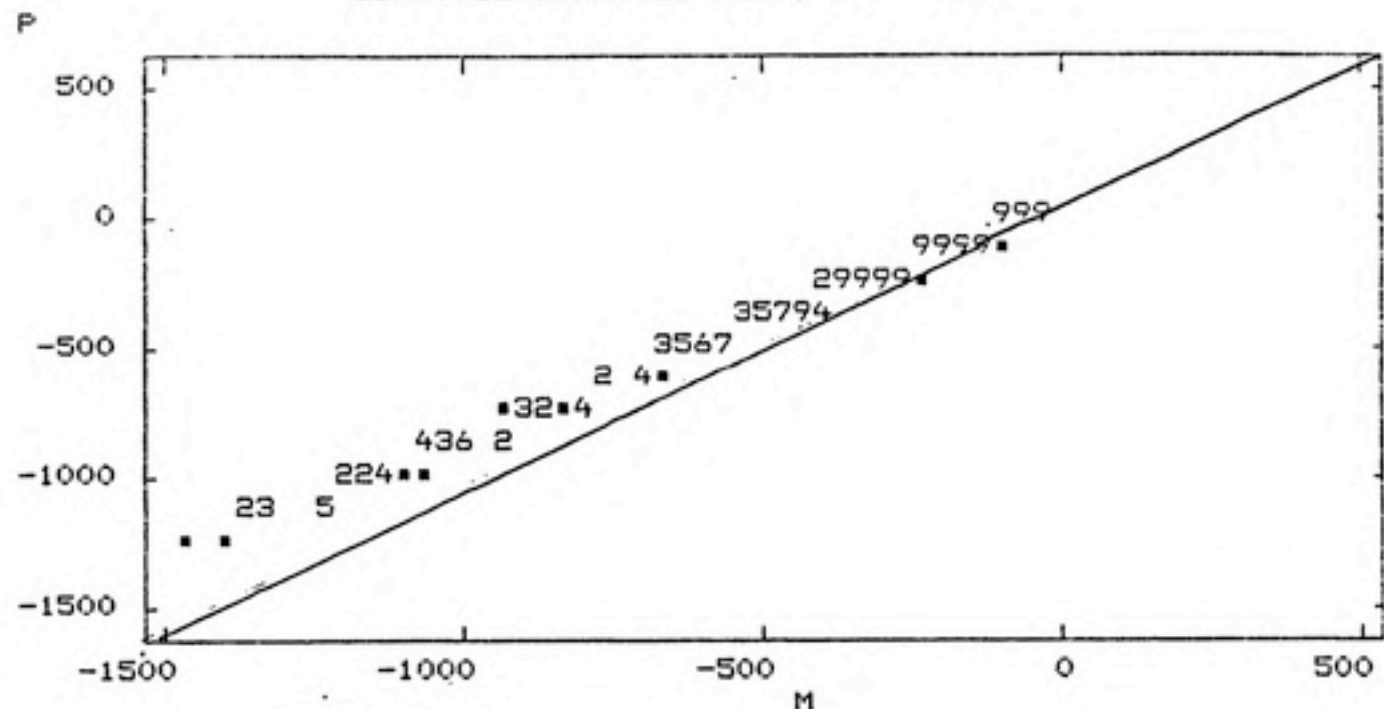
## ANALYSIS OF VARIANCE

SOURCE	SUM-OF-SQUARES	DF	MEAN-SQUARE	F-RATIO	P
PLANE	55754.465	1	55754.465	0.988	0.321
AR	36309.828	2	18154.914	0.322	0.725
PLANE* AR	31244.040	2	15622.020	0.277	0.758
ERROR	.298110E+08	528	56460.202		

**APPENDIX H**

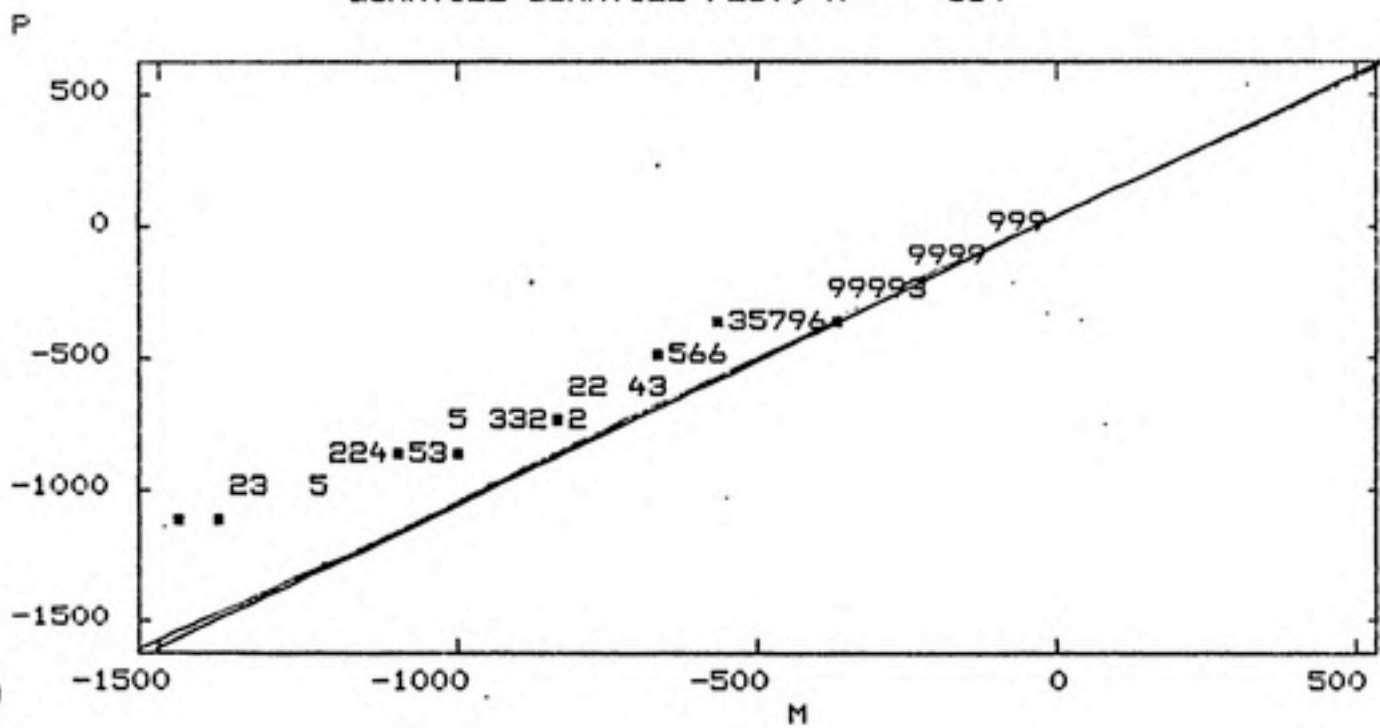
## MODEL A

QUANTILE-QUANTILE PLOT, N = 534



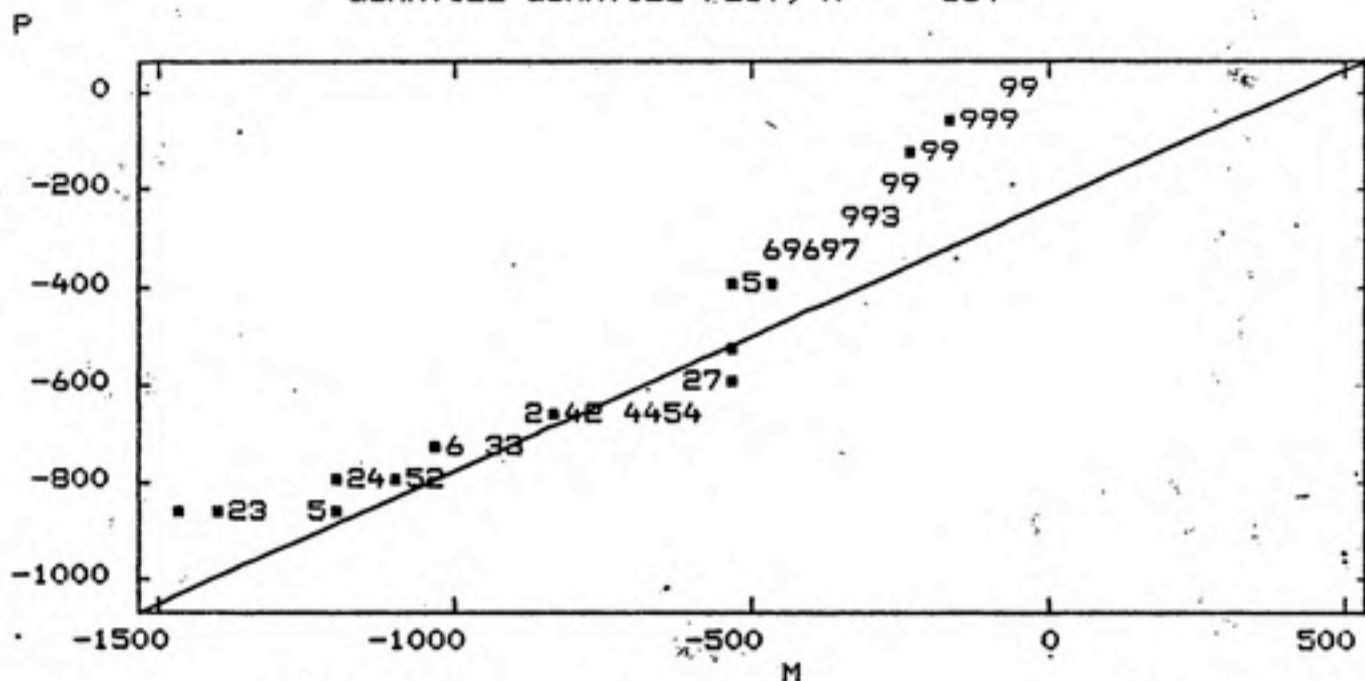
## MODEL B

QUANTILE-QUANTILE PLOT, N = 534



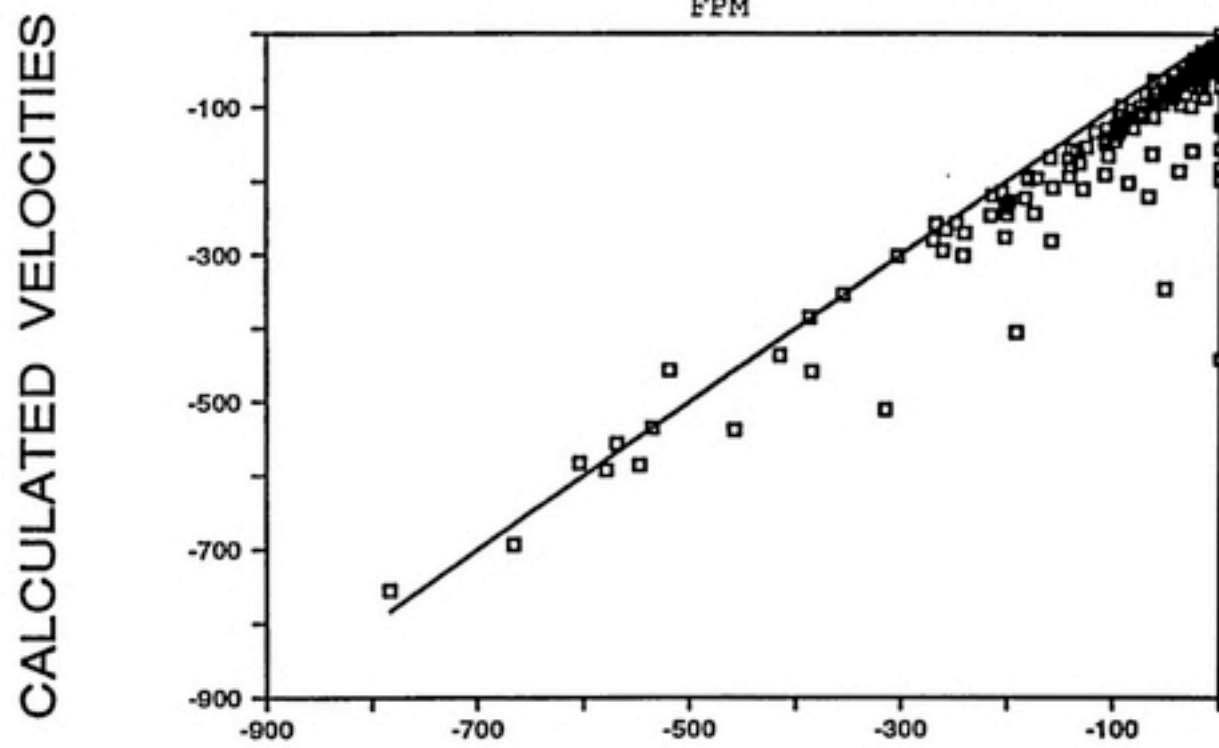
MODEL C

QUANTILE-QUANTILE PLOT, N = 534



**APPENDIX I**

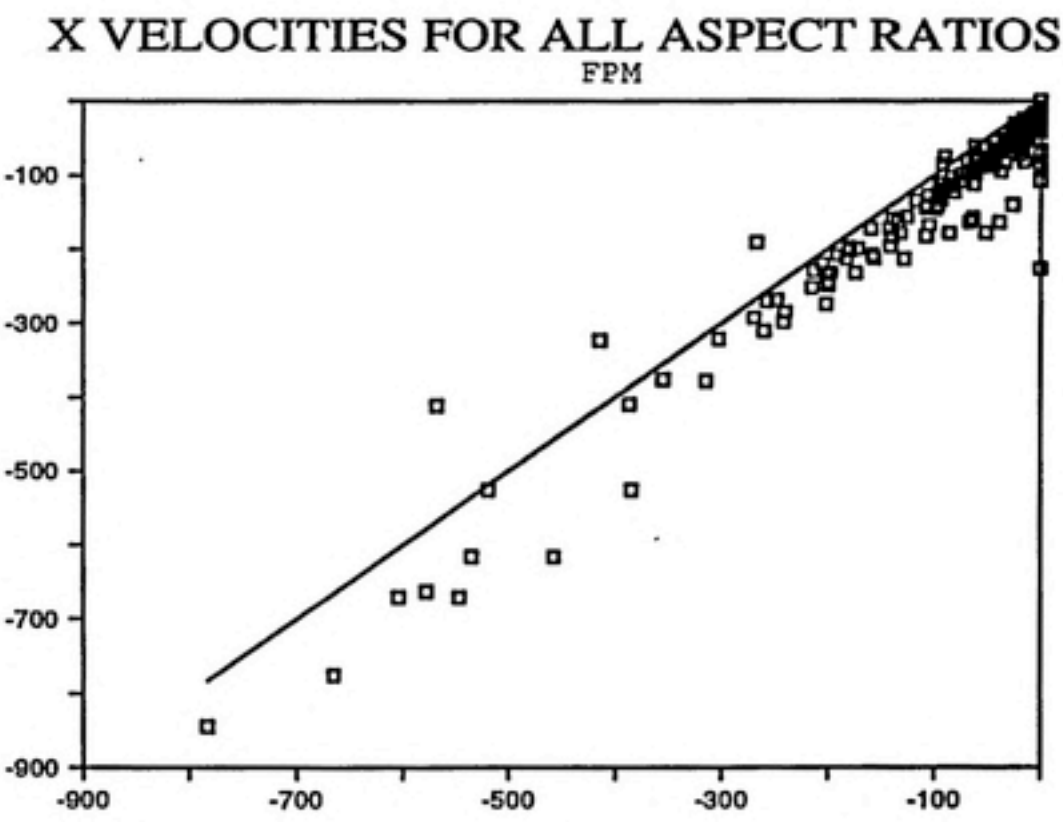
### X VELOCITIES FOR ALL ASPECT RATIOS FPM



EXPERIMENTAL VELOCITIES

□ MODEL A

CALCULATED VELOCITIES

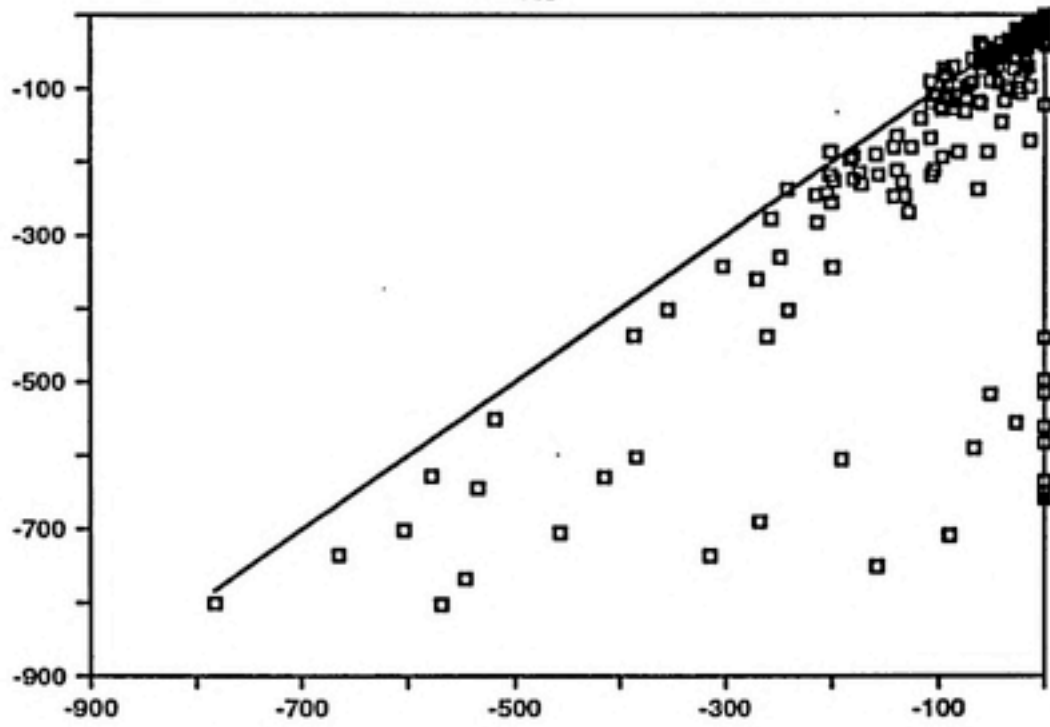


EXPERIMENTAL VELOCITIES

□ MODEL B

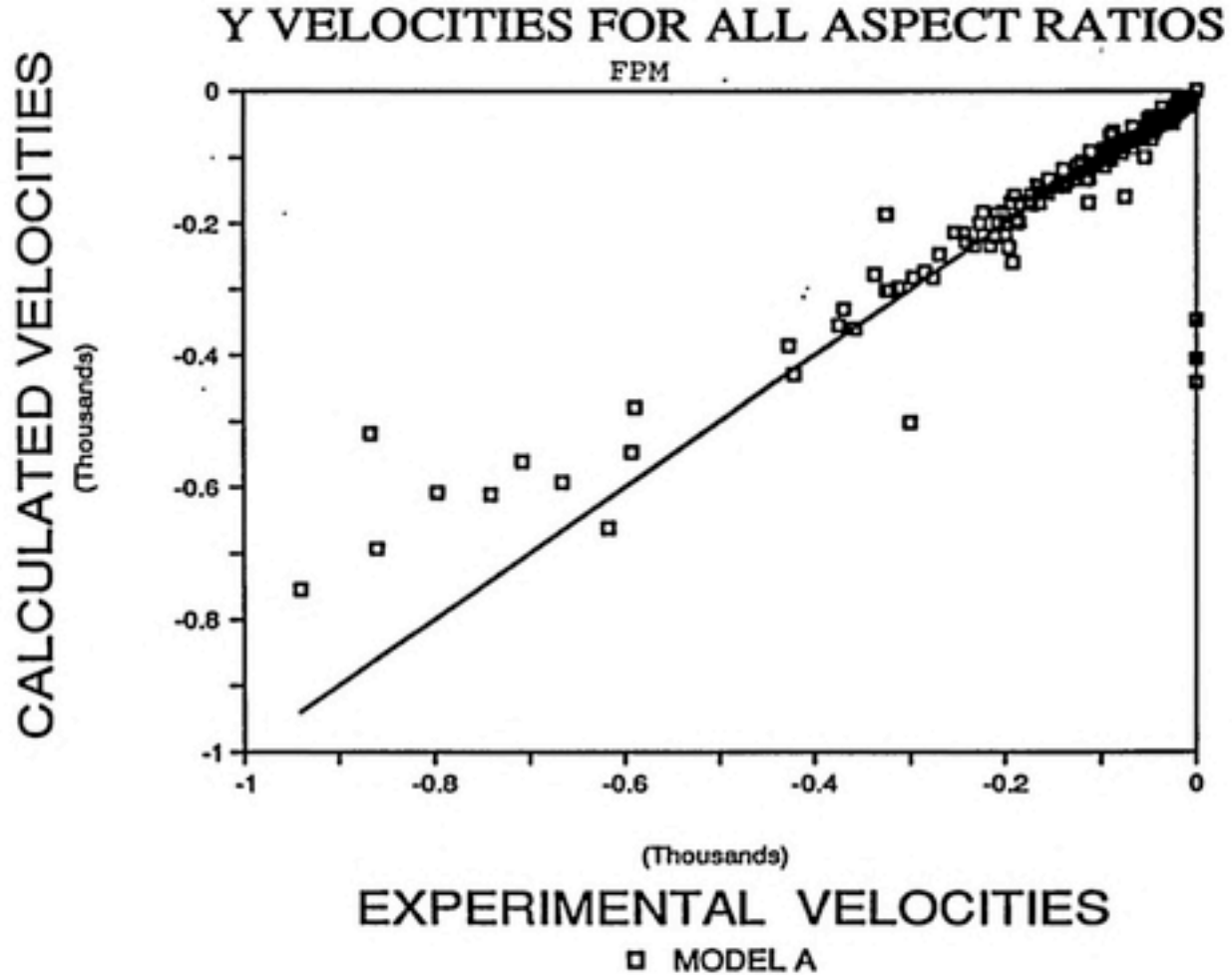
CALCULATED VELOCITIES

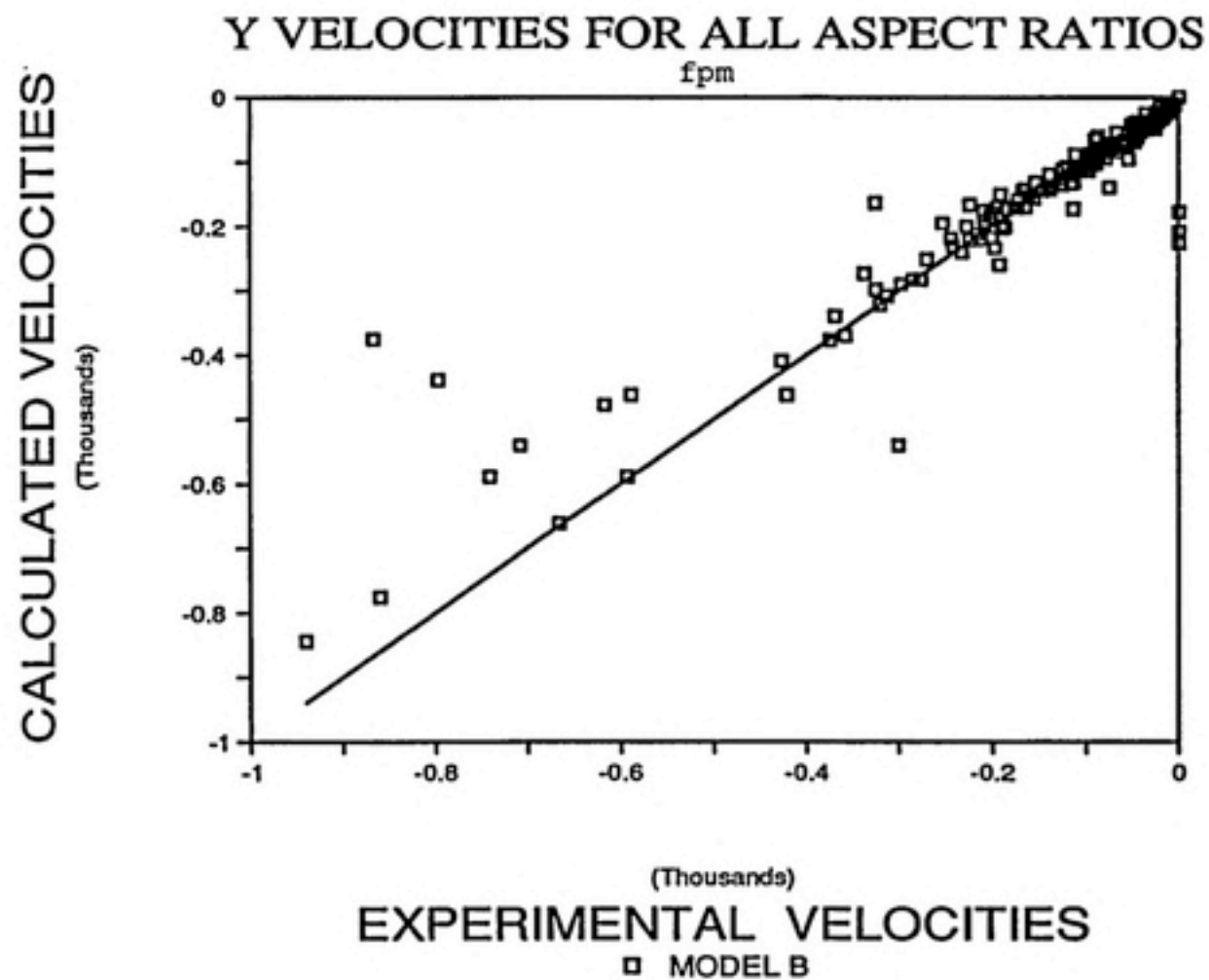
X VELOCITIES FOR ALL ASPECT RATIOS  
FPM

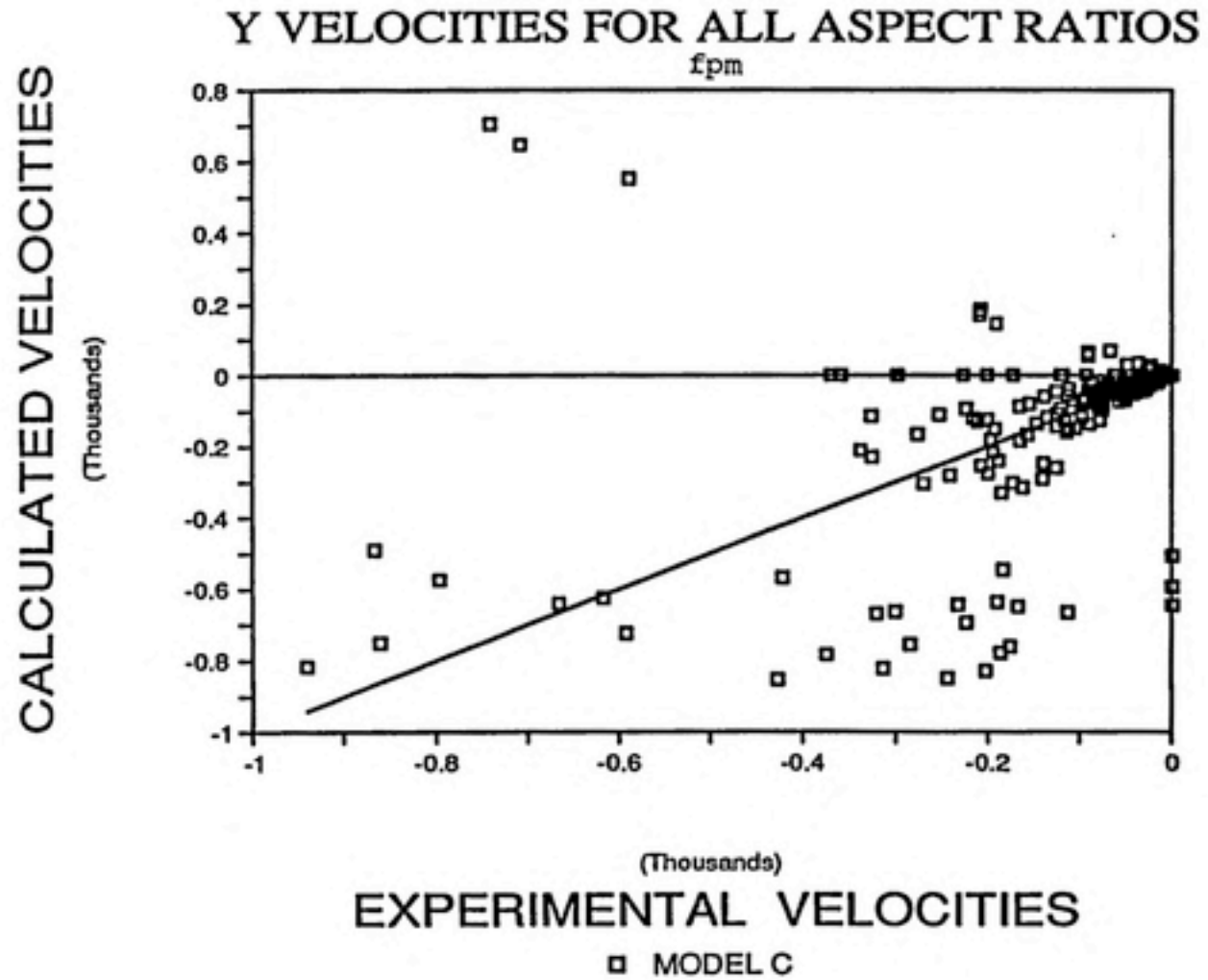


EXPERIMENTAL VELOCITIES

□ MODEL C

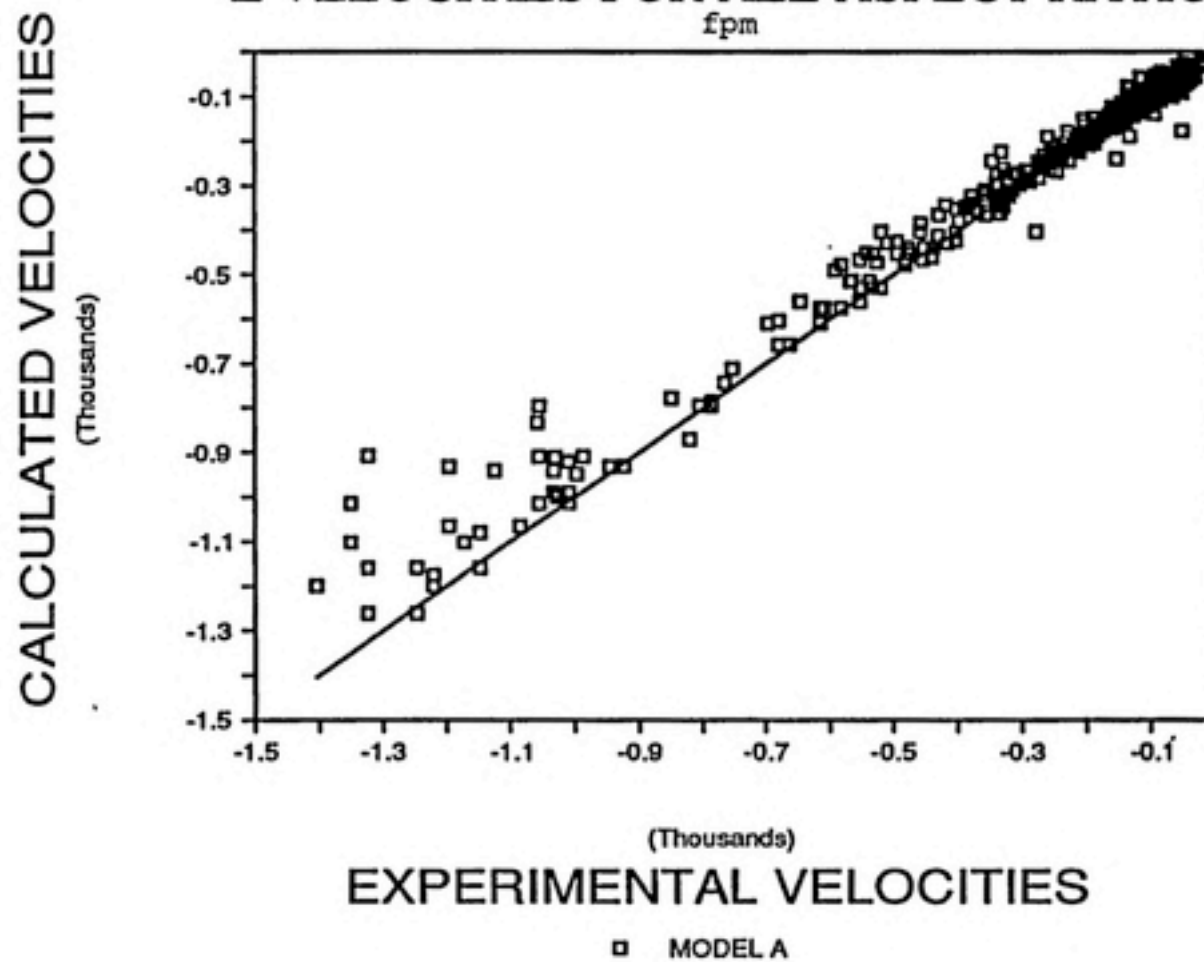




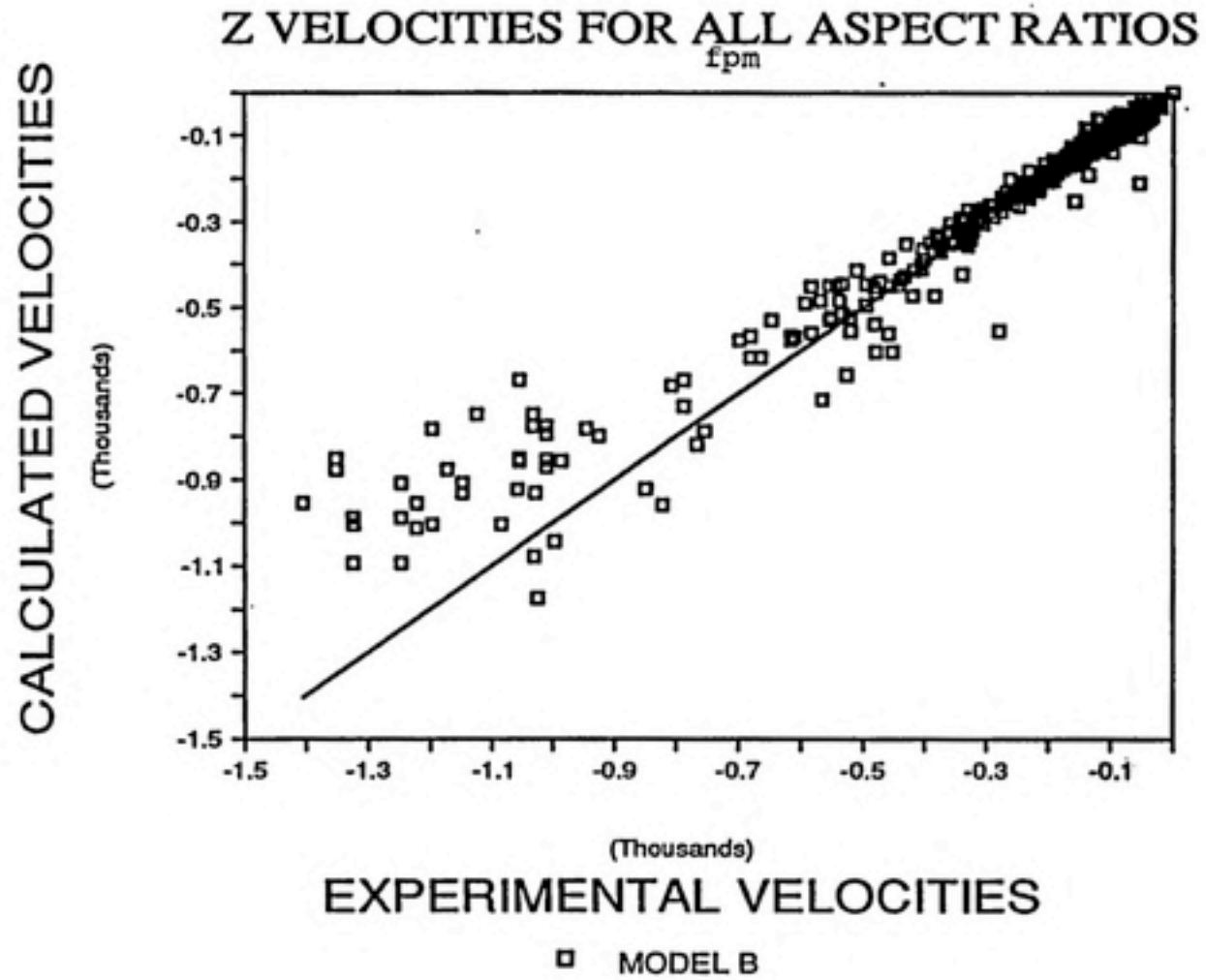


### Z VELOCITIES FOR ALL ASPECT RATIOS

fpm



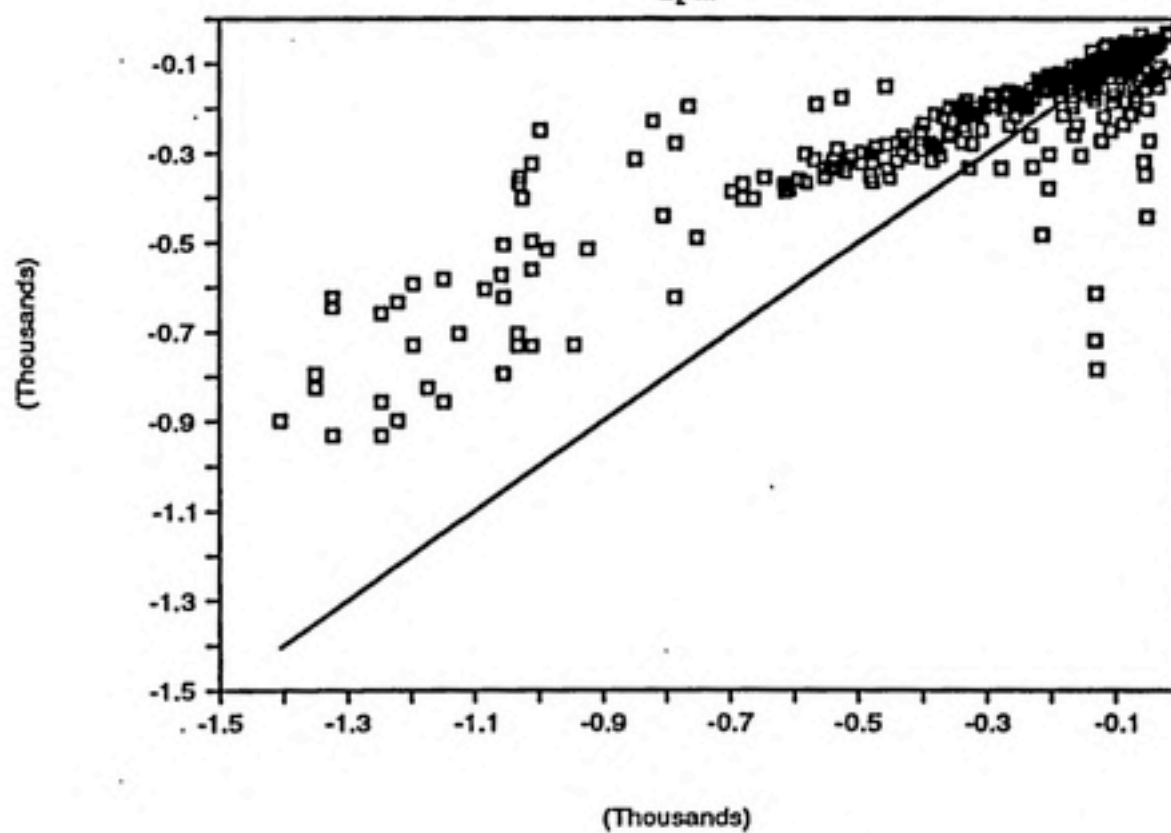
□ MODEL A



CALCULATED VELOCITIES

### Z VELOCITIES FOR ALL ASPECT RATIOS

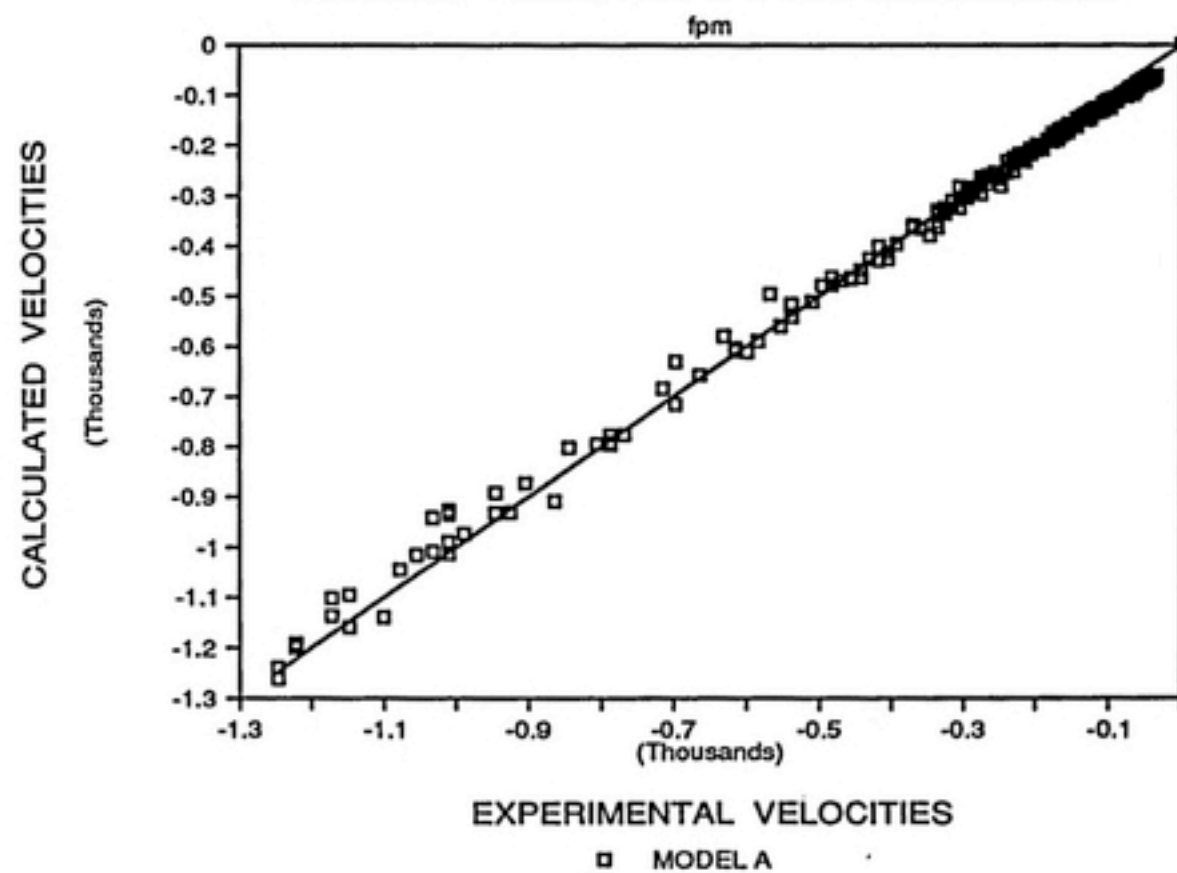
fpm



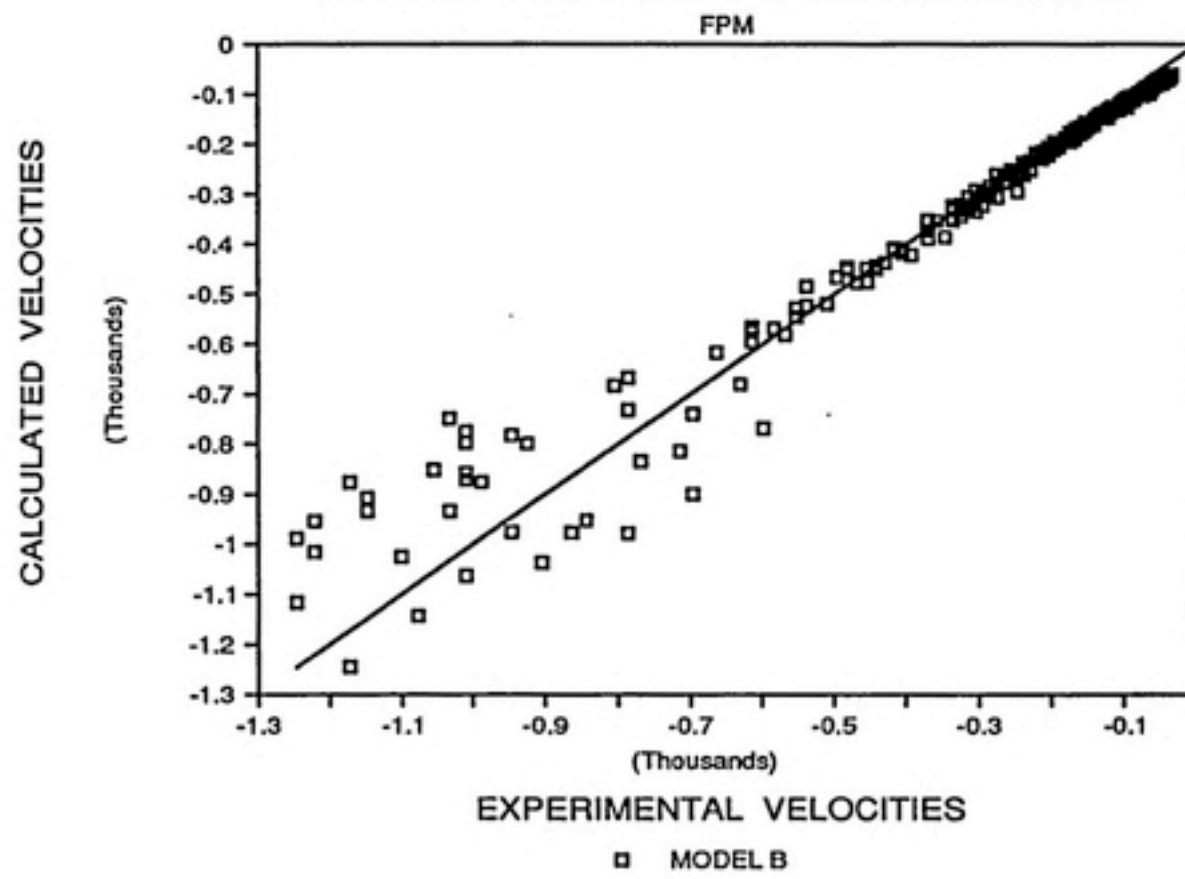
EXPERIMENTAL VELOCITIES

□ MODEL C

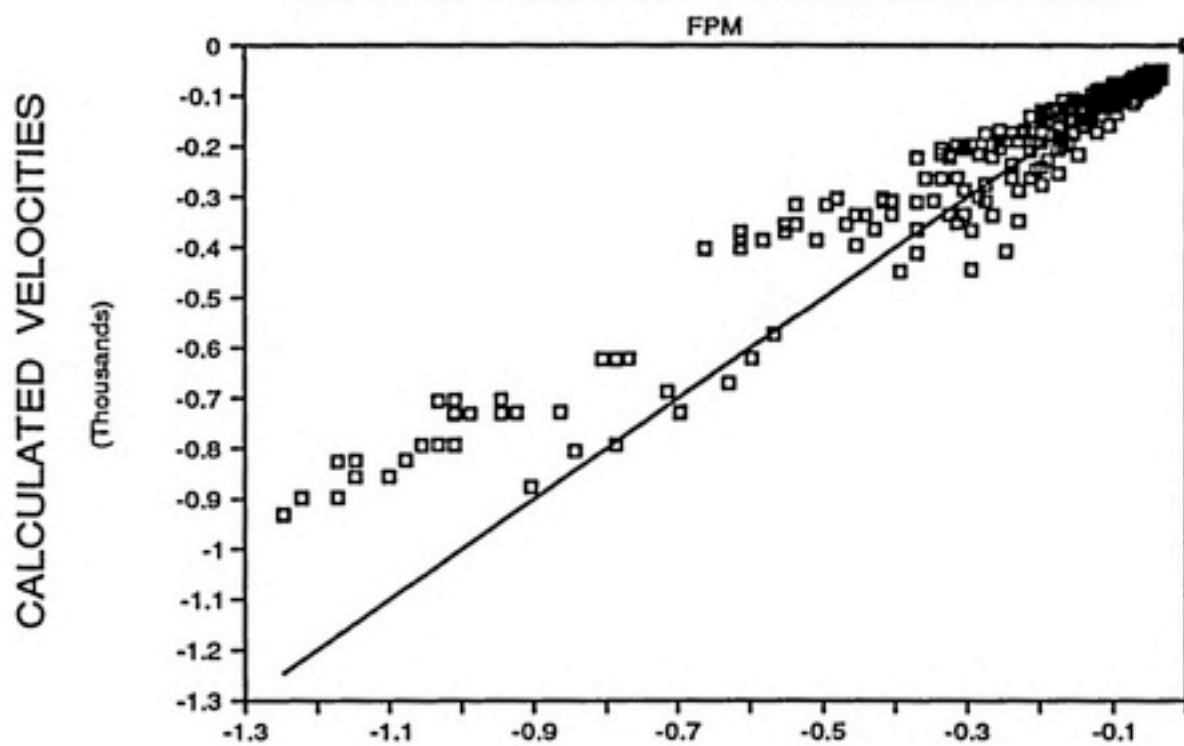
### TOTAL VELOCITY FOR XZ PLANE



### TOTAL VELOCITY FOR XZ PLANE



### TOTAL VELOCITY FOR XZ PLANE

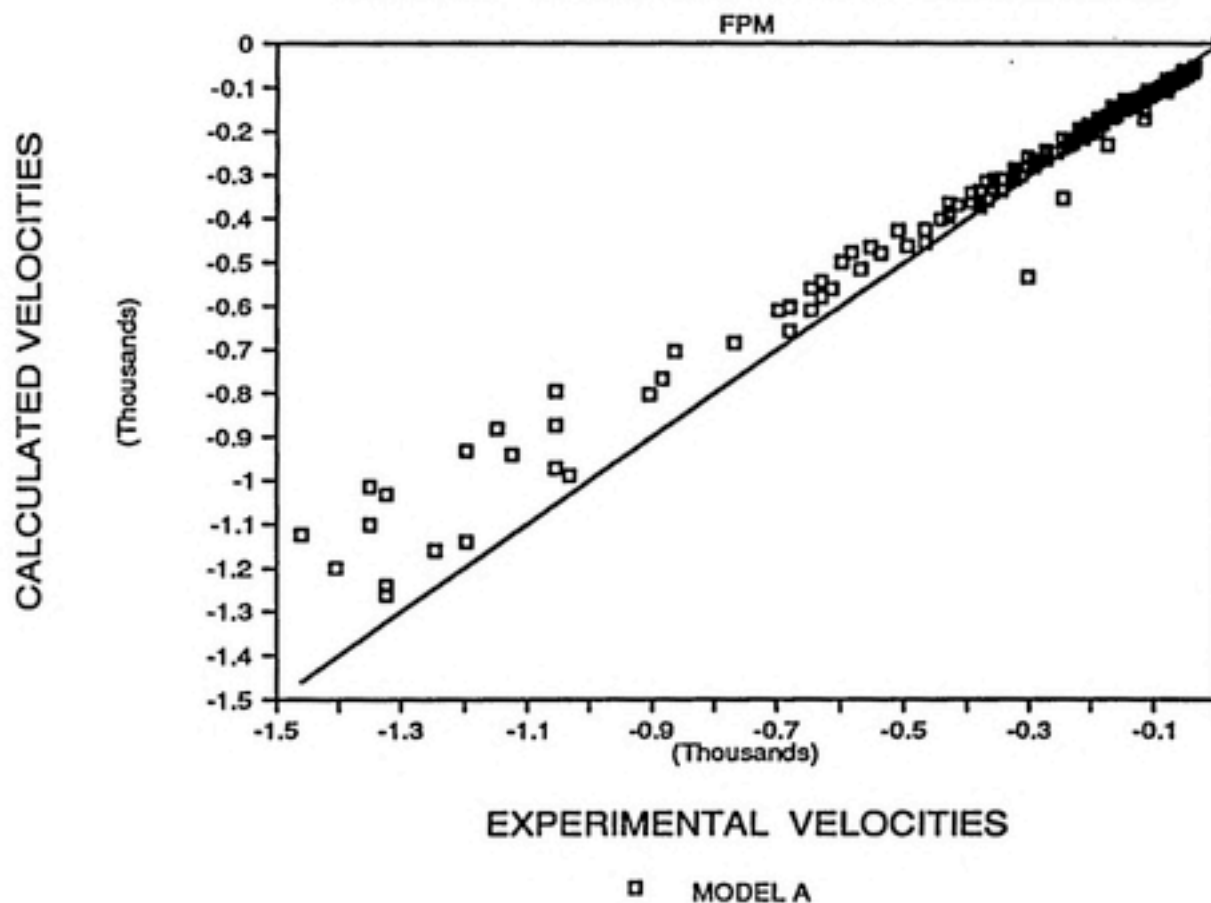


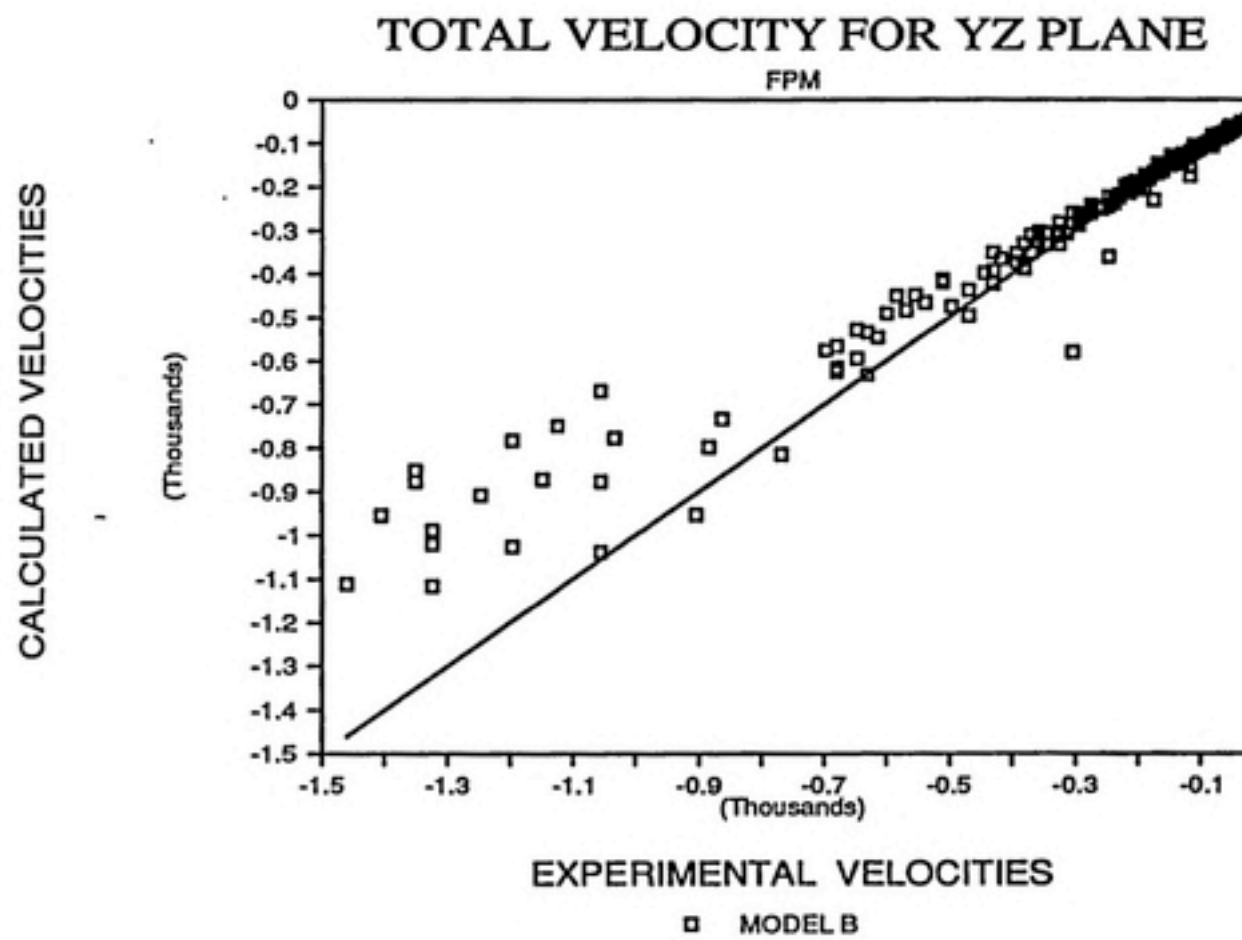
### EXPERIMENTAL VELOCITIES

(Thousands)

□ MODEL C

### TOTAL VELOCITY FOR YZ PLANE





### TOTAL VELOCITY FOR YZ PLANE

